Consiglio Nazionale delle Ricerche

Study Commission for the Drafting and Analysis of Technical Standards for Construction

CNR-DT 203 R1/2026

Guidelines for the Design, Execution and Inspection of Reinforced Concrete Structures with Fiber-Reinforced Polymer (FRP) Bars

All literary rights reserved

by the

National Research Council of Italy (Consiglio Nazionale delle Ricerche)

TABLE OF CONTENTS

1 INTRODUCTION TO THE PRESENT REVISION (DT 203 R1) OF THE CNR DT 203 GUIDELINES

This document provides design provisions for the use of fiber-reinforced polymer (FRP) composite bars as internal reinforcement in reinforced concrete (RC) elements intended for structural use.

The use of fiber-reinforced composites as a replacement for steel in the construction of concrete structural elements is now a reality in many countries. These materials make it possible to combine significantly greater durability of structures compared to similar structures with traditional steel reinforcement, greater sustainability in the sourcing and processing of raw materials, a much lower weight, which facilitates transportation and installation operations. The use of non-metallic reinforcement allows, in principle, the use of seawater in the concrete mix; however, this requires a carefully designed mix to counteract the aggressive action of marine ions, which are potentially harmful not only to traditional reinforcement but also to the cement matrix. This possibility is particularly important from the perspective of sustainability of RC construction.

In light of this growing interest, several international standards and Guidelines have been introduced in recent years, and others have been updated. A list of the most recent Guidelines is provided at the end of this Introduction. Even regulatory documents traditionally dedicated to RC with steel reinforcement, such as the Model Code and Eurocode 2 (EC2), now include sections on the use of non-metallic reinforcement.

This document, in particular, is an update of the Guidelines published in 2006 by the CNR, which issued a series of documents on the structural use of FRP materials, including *DT 200/2004* (updated in 2026, version R2) for the design of strengthening interventions on RC and masonry structures using FRP materials, *DT 201/2005* for the design of strengthening interventions on timber structures using FRP materials, *DT 202/2005* for the design of strengthening interventions on steel structures using FRP materials.

These Guidelines have been prepared based on the current state of knowledge, incorporating the results and experience gained from theoretical and experimental studies carried out within several research projects on composite materials, funded at both national and international levels. Italian researchers have been involved in these projects since the early 2000s, and many of them are members of the Working Group responsible for drafting these Guidelines.

2 INTRODUCTION

2.1 CONTENTS AND PURPOSES OF THESE GUIDELINS

These Guidelines provide the principles and rules for design of new RC structures with FRP (Fiber Reinforced Polymer) bars, as well as for strengthening existing structural elements in which the bars are used as passive reinforcement within appropriate enlargements of the original concrete section.

Although research and the first applications date back more than twenty years, these are still innovative materials and technologies. Therefore, this Document sets out design criteria and fields of application that have been widely validated through theoretical and experimental studies. In this regard, although studies in the field exist, the principles and application rules contained in this Document are not directly applicable to prestressed concrete structures with prestressing tendons made of FRP materials. However, for this Document, FRP bars may be used in pre-stressed structural elements, but only as secondary (passive) reinforcement.

Over the past 10–15 years, technological development has consolidated pultrusion techniques for the production of FRP bars. In particular, glass fiber-reinforced polymer (GFRP) is by far the most widely used, both in terms of the number of manufacturers and the quantity of qualified products and volumes produced. However, bars made of carbon fiber-reinforced polymer (CFRP), basalt fiber-reinforced polymer (BFRP), and aramid fiber-reinforced polymer (AFRP) are also available on the market.

Although carbon fiber-reinforced polymer (CFRP) bars offer superior performance in both strength and stiffness, their significantly higher cost limits their use to specific applications, such as strengthening existing structures in the form of circular or rectangular section bars. It should also be noted that the available experimental studies mainly concern GFRP bars, although many tests on elements reinforced with CFRP bars are already available. Finally, for basalt (BFRP) and aramid (AFRP) fiber bars, no certified products are currently available (and thus it is not possible at present to compile statistics on material properties), and experimental research is either absent or very limited.

It should further be noted that, in this field, technology is continuously evolving thanks to the development of new materials and manufacturing techniques, which inevitably pose challenges for drafting design Guidelines. On the one hand, limiting the Guidelines solely to bars for which all experimental aspects have been fully explored could hinder the development of new materials and technologies. On the other hand, it is impossible to predict the properties of materials still in development, as well as the potential emergence of critical issues not yet encountered with the materials currently most in use.

Representative examples, in addition to the types of FRP bars described above, include bidirectional glass fiber meshes and FRP bars with thermoplastic resins. The latter would have the advantage of allowing the bars to be bent in the factory after the production process (an operation that is certainly not possible with thermosetting resin bars). However, at present, the costs of these materials are not comparable to those of more common bars. As for FRP meshes, no European Assessment Document (EAD) currently exists that would allow their qualification, nor are they included in the "*Linea guida per l'identificazione, la qualificazione e l'accettazione di barre e staffe in composito fibrorinforzato per uso strutturale*" issued by the (Italian) Consiglio Superiore dei Lavori Pubblici (CSLLPP) in December 2021.

Therefore, considering the above, these Guidelines provide design provisions exclusively for FRP bars with circular cross-sections made of glass and carbon fibers that bear:

- the CE mark on the basis of a *European Technical Assessment* (ETA) issued in accordance with EAD 260023-00-0301 and with the intended use therein declared (i.e., FRP bars as internal reinforcement of construction works and elements made of RC - beams, columns,

panels, slabs, and other structural elements - and as post-re-bars) and referred to the mandatory geometric and mechanical characteristics specified in this Document, or

- a CVT (*Technical Assessment Certificate*) in accordance with the Guideline issued by the Consiglio Superiore dei Lavori Pubblici (CSLLPP) and above cited.

These Guidelines also specify the minimum required values for specific geometric and mechanical characteristics deemed essential to the design. As noted earlier, FRP bars made of basalt and aramid fibers are not included within the scope of these Guidelines, even though their qualification is provided for both by EAD 260023-00-0301 and for basalt fibers only by the CSLLPP Guidelines. This exclusion applies at least until a statistically significant number of qualified products is available on the market, along with adequate experimental research concerning concrete elements reinforced with these types of bars.

From a theoretical point of view, the main difference compared to the traditional theory of RC with steel bars concerns the mechanical behavior of FRP, which exhibits an essentially linear-elastic stress–strain relationship up to failure and therefore lacks appreciable ductility reserves. Structural analysis methods that assume plastic redistribution capacity in the element are therefore not applicable. Consequently, particular attention is required for applications in seismic zones, where the almost complete absence of ductility in structures reinforced with FRP bars shall be considered. For this purpose, a specific chapter of these Guidelines is dedicated to the design criteria for elements in seismic areas, which may vary depending on the type of structure and whether the system design is based on the requirement of dissipative capacity. In this case, performance requirements in terms of ductility necessarily call for the use of “hybrid” reinforcement — that is, reinforcement in which FRP bars are coupled with steel reinforcement in critical regions where plastic hinges may form. If, on the contrary, design does not require energy dissipation during the earthquake, only FRP reinforcement can be used. A third case of great importance in many applications such as the structural elements of bridge decks is where combinations of non-seismic actions are more significant than seismic ones; in this case too, it is possible to envisage the use of only FRP reinforcement.

It should be emphasized that, in the behavior of RC members with FRP bars, serviceability limit-state checks can also be of great importance, particularly for deformation and cracking. Serviceability limit state checks are particularly relevant for structures reinforced with (GFRP) bars, due to their higher tensile strength, but lower elastic modulus compared to steel bars.

Finally, regarding the bond between FRP bars and concrete, experimental tests evidenced that current surface preparation techniques for the bars can, in some cases, provide bond properties comparable or higher than those of steel bars. However, a careful assessment of bond quality is required, based on the qualification tests prescribed by both EAD 260023-00-0301 and the CSLLPP Guideline.

The present Guidelines have considered and critically evaluated the criteria and rules contained in international codes and guidelines. On certain aspects, specific research and in-depth studies have been carried out, leading to innovative design criteria — for example: the definition of the partial safety factor for the strength of GFRP bars, derived from an extensive experimental database; the evaluation of strength reduction due to long-term loading effects (creep rupture); the definition of bond classes; the criteria for assessing serviceability performance; and the design criteria for seismic areas. Some of these studies are presented extensively in the Appendices.

The approach adopted in the Guidelines is the semi-probabilistic limit-state method, following a framework similar to that of European normative documents (Eurocodes). However, most of the general concepts can also be applied, with appropriate adjustments, in other regulatory contexts.

Finally, the last chapter of the Document provides an overview of emerging application areas in which the use of FRP bars has proven particularly promising. In addition to their well-known durability, lightweight characteristics open up interesting possibilities for the use of such bars — for example,

in temporary works, tunnel linings, retaining walls in marine environments, temporary works in excavations, pavement reinforcement, and as soil-retaining anchors. Also of great interest is the use of FRP bars for strengthening existing structures using the NSM (Near-Surface Mounted) technique, both in masonry in seismic zones and in deteriorated RC structures (such as infrastructure). In the latter case, the combined use with high-performance concretes or mortars could minimize cover thickness, with clear benefits in terms of reduced impact of construction activities and control of added weight. Finally, mention should also be made of the use of FRP bars to improve connections in masonry elements. It should be noted that even for these applications, the Document does not provide specific design provisions. However, for these applications, the latest version of DT 200 (revision R2 of 2026) contains design indications for strengthening interventions in RC and masonry elements made with FRP bars applied using the NSM technique.

The Codes and the Guidelines currently available at the international level include:

- ACI 440.1R (2015). *Design and construction of structural concrete reinforced with FRP bars*, American Concrete Institute, Farmington Hills, MI, USA.
- ACI CODE-440.11-22 (2022). *Building Code requirements for structural concrete reinforced with Glass Fiber-Reinforced Polymer (GFRP) Bars—Code and commentary*, American Concrete Institute, Farmington Hills MI;
- AFGC (2023). *Recommendations for the use of FRP (Fibre Reinforced Polymer) rebars for reinforced concrete structures*, Association Francaise de Genie Civil;
- CEN (2023). *Eurocode 2: Design of concrete structures - Part 1-1: General rules and rules for buildings*, Annex R, EN 1992-1-1:2004;
- *fib* Model Code 2020 (2024). *fib Model Code for concrete structures* 2020, federation international du beton, Lausanne, Switzerland;
- *fib* bulletin n.40 (2007). *FRP Reinforcement for RC structures*, Task Group 9.3 *(Fibre Reinforced Polymer)* Reinforcement for Concrete Structures, federation international du beton, Lausanne, Switzerland;
- CAN/CSA S806-2017, (2021). *Design and construction of building structures with fibre-reinforced polymers*, Canadian Standard Association (CSA) International, Toronto, Ontario, Canada.
- CAN/CSA-S6-19, (2019). *Canadian high bridge design code*, Canadian Standard Association (CSA) International, Toronto, Ontario, Canada.
- Japan Society of Civil Engineers (JSCE), 2023, *Recommendation for design and construction of concrete structures using continuous fiber reinforcing materials*.

2.2 SYMBOLS

The meaning of the main symbols used in this Document is given below.

Roman upper-case Letters

Symbol	Definition
A_b	nominal area of the FRP bar
$A_{b,eff}$	effective area of the FRP bar
$A_{b,min}$	minimum admissible area of the FRP bar with respect to the nominal area
$A_{b,max}$	maximum admissible area of the FRP bar with respect to the nominal area
A_c	area of the concrete section
$A_{c,ef}$	effective tensile area of concrete

A_f	area of longitudinal FRP reinforcement
A_{fc}	area of longitudinal FRP reinforcement in compression
A_{fw}	area of FRP bars used as transverse reinforcement
B_s	width of the FRP stirrup arm
D_{max}	Maximum diameter of aggregates in concrete
E_c	instantaneous longitudinal modulus of elasticity of concrete
$E_{c,eff}$	effective longitudinal modulus of elasticity of concrete
E_{fc}	compressive longitudinal modulus of elasticity of the FRP bar
E_f	tensile longitudinal modulus of elasticity of the FRP bar
E_s	tensile longitudinal modulus of elasticity of steel
I_1	moment of inertia of the RC section reinforced with FRP bars in the uncracked state
I_2	moment of inertia of the RC section reinforced with FRP bars in the cracked state
L_t	length of the FRP stirrup beyond the bend
M_{max}	bending moment acting at the most stressed section of the member
M_{cr}	cracking moment of the RC section with FRP bars
M_{Rd}	design value of the resistant bending moment
$M_{Rd,fi,t}$	design value of bending moment in case of absence of fire protection and of esposure on the tension side
M_{Ed}	design value of the applied internal bending moment
N_{Rd}	design value of the resistant axial force
N_{Ed}	design value of the applied axial force
P_{fib}	fiber weight fraction
$R_{et,t}{}^{1000}$	tensile capacity retention rate after 1000 hours under alkaline environment and sustained loads
$R_{et,t}{}^{3000}$	tensile capacity retention rate after 3000 hours under alkaline environment
T_{pm}	melting temperature of FRP bar
T_g	glass transition temperature of FRP bar
T_{max}	maximum service temperature of the FRP bar
V_{fib}	fiber volume fraction
V_{Ed}	design value of the applied shear force
V_{Rd}	design shear resistance of the reinforced concrete member
$V_{Rd,ct}$	design shear resistance related to concrete mechanisms
$V_{Rd,f}$	design shear resistance of FRP transverse reinforcement
$V_{Rd,c}$	design shear resistance of the compressed concrete strut
V_{Sd}	design value of the applied shear force
Y_t	relaxation rate at time t, with t = 10, 120, or 1000 hours
$Y_{million}$	relaxation rate at 1 million hours

Lower-case Roman Letters

Symbol	**Definition**
b	width of the concrete section
b_w	minimum width of the concrete section
c	distance from the centroid of FRP bars to the section edge (mechanical cover)
c_{geom}	distance from the lower edge of FRP bars to the section edge (geometric cover)
d	distance from the centroid of FRP bars to the compressed edge (effective depth)
d_b	nominal diameter of the FRP bar
d_{bs}	nominal diameter of the steel bar
d_{bs}	nominal diameter of the FRP stirrup
d_{eff}	effective diameter of the FRP bar

d_s	distance from the centroid of the steel bars to the compressed edge
f	deflection of the structural element
f_1	deflection calculated assuming uncracked sections
f_2	deflection calculated assuming cracked sections
f_{cm}	mean value of cylindrical compressive strength of concrete
f_{cd}	design value of cylindrical compressive strength of concrete
f_{ck}	characteristic value of cylindrical compressive strength of concrete
f_{ctd}	design value of tensile strength of concrete
$f_{fatigue}$	tensile fatigue strength of the FRP bar
f_{fc}	mean value of compressive strength of FRP bar
f_{fck}	characteristic value of compressive strength of FRP bar
f_{ftd}	design value of tensile strength of the FRP bar
f_{ftk0}	characteristic value of tensile strength of the FRP bar
$f_{ftk,c}$	characteristic value of tensile strength for long-term static fatigue (creep) at 100 years
$f_{ftk,ca}$	characteristic value of tensile strength for long-term static fatigue (creep) at 100 years under alkaline environment
$f_{ftk,st}$	characteristic value of tensile strength of the straight portion of the FRP stirrup arm
f_{ubk}	characteristic value of tensile strength of the bent portion of the FRP stirrup
$f_{ubk,a}$	characteristic value tensile strength of the bent portion of the FRP stirrup after exposure under alkaline environment
f_{yd}	design value of yield stress of steel bars
$f_{c,FRP}$	compressive value of strength of the FRP bar
h	height of the concrete section
$h_{c,ef}$	effective concrete height in tension
$k_{1/r}$	geometric factor accounting for the effect of beam curvature on crack width
$k_{\phi/r}$	factor depending on the distribution of shear stresses along the bars
k_b	factor accounting for the effect of the position of FRP bars during casting
k_{fl}	factor accounting for the distribution of stresses prior to cracking
k_t	coefficient depending on the duration and the nature of the applied load
ℓ_a	anchorage length of FRP bars
ℓ_{ad}	design value of anchorage length of FRP bars
ℓ_b	bonded length of FRP bars
$\ell_{ad,fi,t}$	anchorage length of FRP bars at time t under fire conditions
$\ell_{ad,tot}$	length of the zone that must not be directly exposed to fire in order to ensure proper anchorage of the bars
m	coefficient in the simplified tension-stiffening model for calculation of deflection
q	behavior factor of the structure
s	spacing between FRP stirrups
s	slip at FRP bar-concrete interface
$s_{r,max}$	maximum crack spacing
x	distance from neutral axis to compressed edge at ULS
x_1	distance from neutral axis to compressed edge in the uncracked state (State 1) at SLE
x_2	distance from neutral axis to compressed edge in cracked state (State 2) at SLE
r_t	bend radius of bent bars or FRP stirrups
w_k	characteristic value of crack width

Lower-case Greek Letters

Symbol	Definition
α_f	homogenization coefficient for FRP bars–concrete
α_s	homogenization coefficient for steel bars–concrete
α_R	sensitivity factor (FORM)
$\alpha_{sp,L}$	longitudinal thermal expansion coefficient
$\alpha_{sp,T}$	transverse thermal expansion coefficient
β	target reliability index
β_1	dimensionless coefficient accounting for the quality of the bond of the bars
β_2	dimensionaless coefficient accounting for the duration of the loads
β_w	coefficient determining the maximum crack spacing starting from the mean value
γ	tension-stiffening coefficient
γ_c	partial factor for concrete
γ_f	partial factor for FRP bars
γ_m	partial factor for a material property
γ_{Rd}	partial factor for the resistance model and geometric deviations
$\gamma_{Rd,geo}$	partial factor accounting for geometric deviations
$\gamma_{Rd,mod}$	partial factor accounting for resistance model
$\varphi(t,t_0)$	creep coefficient for concrete
ε_c	current strain of concrete at the compressed edge
ε_{cu}	ultimate strain of concrete
ε_f	current strain in FRP tensile bars
ε_{ftd}	design value of the ultimate tensile strain of the FRP bar
ε_{ftk}	characteristic value of the ultimate tensile strain of the FRP bar
ε_s	current strain in steel tensile bars
$\varepsilon_{fu,T}$	design value of the ultimate strain of the FRP bar calculated as a function of the bar temperature under fire conditions
ε_{yd}	design value of yield strain of steel bars
ε_{fm}	mean strain in FRP bars between two successive cracks
ε_{cm}	mean value of the tensile strain in concrete between two successive cracks
η_a	environmental conversion factor
η_T	conversion factor for temperature effects
$\eta_{c,l}$	conversion factor for long-term static fatigue effects
η_c	conversion factor for static fatigue effects at 100 years
η_{ca}	conversion factor for static fatigue at 100 years, accounting for environmental effects
$\rho_E(T)$	reduction factor of the tensile modulus of elasticity at the temperature T reached by the FRP bar at time *t*
ρ_l	ratio of longitudinal tensile reinforcement to the concrete section area A_c
$\rho_{l,ef}$	ratio of longitudinal tensile reinforcement to the effective concrete area in tension, $A_{c,ef}$
$\rho_f(T)$	reduction factor of the tensile strength of the FRP bar at the temperature T reached by the bar at time *t*
ρ_s	percentage of FRP transverse reinforcement
σ_c	current normal compressive stress in concrete
σ_f	current normal tensile stress in FRP bars
$\sigma_{f,qp}$	normal tensile stress in FRP bars under the quasi-permanent load combination
σ_s	current normal tensile stress in steel bars
τ_b	bond strength at FRP bar–concrete interface (from pull-out tests on concrete

	element class C20/25)
$\tau_{b,a}$	bond strength at FRP bar–concrete interface after alkaline exposure (from pull-out tests on concrete element class C20/25)
$\tau_{b,C50/60}$	bond strength at FRP bar–concrete interface in high-strength concrete (from pull-out tests on concrete element class C50/60)
$\tau_{b,cb}$	bond strength at FRP bar–concrete interface under eccentric load (from pull-out tests on concrete element class C20/25 and cover c_b)
$\tau_{b,Tmax}$	bond strength at FRP bar–concrete interface at maximum service temperature (from pull-out tests on concrete element class C20/25)
τ_i	interlaminar shear strength of the FRP bar
τ_{mf}	mean bond strength at FRP-bar-concrete interface between two cracks at serviceability loads (SLE)
τ_s	transverse shear strength of the FRP bar
χ	Reduction factor of the characteristic tensile strength of the bent portion compared to the straight portion
χ_a	Reduction factor of the characteristic tensile strength of the bent portion compared to the straight portion after exposure to alkaline environment

2.3 ACRONYMS

Acronym	**Definitions**
CPR	Construction Product Regulation
CVT	Technical Assessment Certificate
DoPC	Declaration of Performance and Conformity
CCPC	Certificate of Constancy of Product Performance and Conformity
EAD	European Assessment Document
ETA	European Technical Assessment
FPC	Factory Production Control
FRP	Fiber Reinforced Polymer
NSM	Near-Surface Mounted bars
SLC	Collapse Limit State
SLS	Serviceability Limit State
ULS	Ultimate Limit State
LSLS	Life Safety Limit State
RC	Reinforced Concrete

3 MATERIALS

3.1 INTRODUCTION

(1) The scope of these Guidelines includes straight bars, bent bars in the form of stirrups, and bars with a 90° bend at one end, provided that they contain a fiber weight fraction not less than 70% or a fiber volume fraction not less than 50%. These bars shall be made of continuous glass or carbon fibers, produced with thermosetting or thermoplastic resins, and shall possess certain mandatory characteristics, qualified and above threshold values as specified in this chapter, including with reference to durability. Although FRP bars made with continuous basalt or aramid fibers are manufactured, the experimental data currently available are insufficient to allow their use within the scope of this Document.

(2) Carbon and glass FRP bars with non-circular cross-sections, as well as prefabricated meshes made with FRP bars, are not included within the scope of these Guidelines. In the future, it will be possible to extend the scope of application to bars with cross-sections different from the circular ones only following adequate testing and updating of these Guidelines.

(3) All products shall be qualified by means of CE marking issued on the basis of a European Technical Assessment (ETA) according to the intended use specified in EAD 260023-00-0301 and subsequent revisions (FRP bars as internal reinforcement for beams, columns, walls, slabs, and other possible concrete structural elements, or as post-installed reinforcement for strengthening interventions), hereinafter referred to as *EAD-FRP bars*. Alternatively, qualification tests may be provided through Technical Assessment Certificates (CVT) issued in accordance with the *Linea guida per l'identificazione, la qualificazione e l'accettazione di barre e staffe in composito fibrorinforzato per uso strutturale* published by the Consiglio Superiore dei Lavori Pubblici (CSLLPP) in December 2021 and subsequent updates, hereinafter referred to as *LG-FRP bars*.

3.2 REQUIRED CHARACTERISTICS

(1) The minimum values of the geometric and mechanical characteristics, the determination of which is mandatory for this document (hereinafter referred to as "mandatory characteristics"), are provided in Table 3-1. In Appendix A other characteristics useful for the qualification of FRP bars are listed.

(2) Regarding the tests conducted to verify the durability of FRP bars, it is worth noting that the minimum values indicated in Table 3-1 represent threshold levels of acceptability following accelerated aging procedures and are not necessarily representative of the actual exposure conditions of FRP bars.

(3) Products with CE marking are considered qualified under this document if accompanied by a DoPC declaring the performance values corresponding to the characteristics listed in Table 3-1.

Table 3-1 - Mandatory characteristics for FRP bars and acceptance limits

Mandatory characteristic	**Symbol [unit]**	**Reference standard**	**Acceptance limit**
Effective area	$A_{b,eff}$ [mm^2]	*EAD-FRP bars* §2.2.1 / *LG-FRP bars* – Tab. 1	Table 3-2
Effective diameter (circular bars)	$d_{b,eff}$ [mm]	*EAD-FRP bars* §2.2.1 / *LG-FRP bars* – Tab. 1	Table 3-2
Fiber volume fraction Fiber weight fraction[1]	V_{fib} [%] P_{fib} [%]	*LG-FRP bars* – Tab. 1	≥ 70% (by volume), ≥ 50% (by weigth)
Characteristic tensile strength	f_{ftk0} [MPa]	*EAD-FRP bars* §2.2.2 / *LG-FRP bars* – Tab. 2	Classes in Table 3-3
Mean longitudinal modulus of elasticity	E_f [GPa]	*EAD-FRP bars* §2.2.2 / *LG-FRP bars* – Tab. 2	Classes in Table 3-3
Glass transition temperature	T_g [°C]	*EAD-FRP bars* §2.2.11 / *LG-FRP bars* – Tab. 1	≥ 100 °C
Maximum service temperature	T_{max} [°C]	*EAD-FRP bars* §2.2.13 / *LG-FRP bars* – Tab. 1	See (5) of §4.1.
Transverse shear strength[2] (characteristic value)	τ_s [MPa]	*EAD-FRP bars* §2.2.5 / *LG-FRP bars* – Tab. 2	≥ 115
Interlaminar shear strength (mean value)	τ_i [MPa]	*EAD-FRP bars* §2.2.6 / *LG-FRP bars* – Tab. 2	≥ 38
Mean pull-out strength from concrete support (centered bar, C20/25 concrete)	τ_{bm} [MPa]	*EAD-FRP bars* §2.2.4 / *LG-FRP bars* – Tab. 2	≥ 7.0
Residual mean tensile strength in alkaline environment after 3000 hours at 60 °C	$R_{et,t}^{3000}$ [%]	*EAD-FRP bars* §2.2.16 *LG-FRP bars* – Tab. 2	GFRP bars: ≥ 60%[3] ≥ 80%[4] CFRP bars: ≥ 85%[3] ≥ 95%[4]
For shaped FRP bars (stirrups or bent bars): - Bend radius	r_t [mm]	*LG-FRP bars* – Tab. 1	$2r_t \geq 7\ d_b$
- Characteristic tensile strength of the straight portion	$f_{ftk,st}$ [MPa]	*EAD-FRP bars* §2.2.15 / *LG-FRP bars* – Tab. 2	Classes in Table 3-3 of this document
- Characteristic tensile strength of the bent portion[5]	f_{ubk} [MPa]	*EAD-FRP bars* §2.2.15 / *LG-FRP bars* – Tab. 2	≥ 40% $f_{ftk,st}$
- Reduction factor of bent portion strength after 3000 hours at 60 °C in alkaline environment	χ_a [%][6]	*EAD-FRP bars* §2.2.15	GFRP bars: ≥ 60%[3] ≥ 80%[4] CFRP bars: ≥ 85%[3] ≥ 95%[4]

[1] This characteristic is not declared in the DoPC, but the Manufacturer shall report its value in a signed declaration.

[2]Transverse shear strength is evaluated with reference to the effective diameter of the bar.

[3] This acceptance threshold applies if the test is conducted according to the methods specified in the *EAD-FRP bars*, adopting, as required by ISO 10406-1:2015, a solution with initial pH > 13 consisting of 8.0 g NaOH and 22.4 g KOH per liter of deionized water.

[4] This acceptance threshold applies if the test is conducted according to the methods specified in the *EAD-FRP bars*, adopting a solution with an initial pH between 12.6 and 13.0 consisting of 118.5 g $Ca(OH)_2$, 0.9 g NaOH, and 4.2 g KOH per liter of deionized water.

[5] The failure mode observed in the test must not be pull-out, as this would indicate that the bend radius r_t, or the length of bar beyond the bend, is inadequate. For stirrups, the length shall be at least equal to the stirrup width, B_s, and the two straight segments beyond the bends shall overlap. For bent anchorage bars, the length shall be at least 10 times the nominal bar diameter, d_b.

[6] The reduction factor $\chi_a = f_{ubk,a} / f_{ubk}$, where $f_{ubk,}$ is the characteristic tensile strength of the bent portion after 3000 hours of alkaline exposure at 60 °C, and f_{ubk} is the characteristic tensile strength of the bent portion under standard conditions.

(3) The standardized methods and procedures to be followed for the qualification of FRP bars, aimed at determining the geometric and mechanical properties of the FRP bars mentioned above, are provided in Appendix A.

(4) The bond properties of FRP bars with concrete depend on the production process and the characteristics of the surface treatment applied. Based on the results of bond tests and, in particular, on the value of the essential characteristic, the bond strength τ_b, it is possible to define, for a specific type of FRP bar, the quality of the bond according to the provisions of §5.3.

3.3 PROPERTIES OF FRP BARS

(1) The mechanical properties of FRP composite materials depend primarily on the type of resin and the nature of the fibers, as well as on the fiber volume fraction or weight fraction.

(2) All mechanical properties, and in particular the strength and modulus of elasticity values, shall be referred to the effective area of the bar.

(3) FRP bars shall be identified solely on the basis of their class, defined by the type of fiber, the elastic modulus, and the tensile strength at failure (evaluated with respect to the effective area), and by their size, defined by the nominal diameter. The dimensional tolerance of the bars is evaluated based on cross-sectional area and is given in §3.3.1. In calculations, the strength and modulus values corresponding to the class and the nominal area of the bar shall be used.

(4) For FRP bars shaped as stirrups or with a 90° bend at one end, produced using the same manufacturing process as straight bars of the same nominal diameter, classification may refer to the latter, provided that the characteristics of the bent portion are also assessed. If shaped bars are produced using a different process than that used for straight bars of the same nominal diameter, they shall be considered a different product and therefore require their own qualification process. The characteristics listed in Table 3-1 shall in this case refer to the mechanical properties of the straight portion of the element. For bars made with thermoplastic resins, bending after the production process cannot be performed on site; it shall be done under controlled conditions at the production facility by heating.

3.3.1 Definition of nominal diameter and area of FRP bars

(1) The procedures for evaluating the diameter and the effective area of FRP bars are provided in the *EAD-FRP bars* and in the *LG-FRP bars* documents. Accordingly, the nominal diameter of circular sections ranges from 5 mm to 32 mm, inclusive of the lower and upper limits.

(2) Given the considerable variety of bars available on the market, during the design stage, the calculation of the resisting area shall be based on the nominal diameter, d_b, of circular-section FRP bars. It is possible to associate a given nominal diameter and its corresponding nominal area, A_b, with an FRP bar if its effective area $A_{b,eff}$ falls within the intervals reported in Table 3-2 ($A_{b,min} \leq A_{b,eff} < A_{b,max}$), with the effective area measured according to the methods indicated in the current

qualification documents. The tolerances reported in Table 3-2 were established based on a statistical analysis of effective areas measured in an extensive sample of glass-fiber bars available on the market. For carbon-fiber bars, in the absence of an equivalent statistical sample, the same tolerances are assumed.

Table 3-2 - Minimum and maximum permissible tolerances in terms of cross-sectional area for bars with nominal diameters ranging from 5 to 32 mm

Nominal diameter d_b [mm]	**Nominal area A_b [mm^2]**	**Minimum area $A_{b,min}$ [mm^2]**	**Maximum area $A_{b,max}$ [mm^2]**
5	19.6	18	26
6	28.3	26	35
7	38.5	35	47
8	50.2	47	59
9	63.6	59	73
10	78.5	73	89
11	95.0	89	103
12	113.0	103	123
13	132.7	123	144
14	153.9	144	165
15	176.6	165	190
16	201.0	190	212
17	226.9	212	239
18	254.3	239	265
19	283.4	265	293
20	314.0	293	324
21	346.2	324	357
22	379.9	357	392
23	415.3	392	429
24	452.2	429	467
25	490.6	467	506
26	530.7	506	547
27	572.3	547	590
28	615.4	590	635
29	660.2	635	681
30	706.5	681	729
31	754.4	729	778
32	803.8	778	861

(3) The Manufacturer, once having defined the range of diameters to be placed on the market, may group 2 or 3 of consecutive diameters and consider the union of the ranges indicated for these diameters. In this case, the nominal diameter shall be taken as the smallest value among the chosen grouped diameters. In the technical datasheet, however, the Manufacturer shall also report the mean effective diameter, enabling an accurate evaluation of the reinforcement area, when necessary, such as when applying capacity design criteria in seismic design.

3.3.2 Tensile strength and modulus of elasticity in the longitudinal direction

(1) In order to reliably evaluate the mechanical properties of an FRP bar, adequate testing shall be carried out to obtain statistically significant values, also taking into account the consistency of

mechanical properties ensured by the production technology. For testing methods and production consistency control, reference should be made to the procedures specified in the *EAD-FRP bar* or in the *LG-FRP bars* documents. In particular, the tensile strength and modulus of elasticity of the bars shall be obtained from direct tensile tests. Further details are provided in Appendix A.

(2) FRP bars that may be used in accordance with these Guidelines are classified on the basis of the following mechanical characteristics:

- mean value of the modulus of elasticity, E_f;
- characteristic tensile strength at failure, f_{ftk0}, evaluated under standard environmental conditions.

The Manufacturer shall assess these characteristics on the basis of the results of the qualification procedures described in §3.2 and shall refer to the effective cross-sectional area of the bar.

(3) Table 3-3 lists the classes of FRP bars and the corresponding values of the above mechanical characteristics. Belonging to a class requires that the determined mean modulus of elasticity and characteristic tensile strength values of the bars are greater than or equal to those indicated in Table 3-3.

(4) For a specific product, all FRP bars with different nominal diameters shall fall within the same class. If, within the same product, bars with different nominal diameters show, during the qualification phase, modulus of elasticity and tensile strength values belonging to different classes, the product classification shall be based on the class with the lower characteristics.

(5) If an FRP bar exhibits mechanical characteristics lower than those of the minimum class indicated in Table 3-3, it may not be used in accordance with these Guidelines.

Table 3-3 - Classes of FRP bars made by glass and carbon fibers

Class E_f/f_{ftk0}	**Fiber type**	**Mean elastic tensile modulus, E_f [GPa]**	**Characteristic tensile strength, f_{ftk0} [MPa]**
E45/850	Glass	45	850 750 for diameters $d_b \geq 24$ mm
E50/1000	Glass	50	1000 900 for diameters $d_b \geq 24$ mm
E60/1100	Glass	60	1100 1000 for diameters $d_b \geq 24$ mm
C130/1000	Carbon	130	1000

3.4 COEFFICIENTS OF THERMAL EXPANSION

(1) The coefficients of thermal expansion of FRP bars in the longitudinal direction, α_l, and in the transverse direction, α_t, are closely related to those of the individual phases (fibers and matrix) that make up the composite material and to the volume fractions of the two phases: in general, the transverse coefficient is governed by the resin acting as the matrix, whereas the fibers govern the longitudinal coefficient. As the fiber volume fraction increases, the value of the coefficient α_l tends more and more toward that of the fiber.

(2) Typical values of the longitudinal and transverse coefficients of thermal expansion, α_l and α_t, respectively, are given in Table 3-4 for composite bars with a fiber volume fraction between 50% and 70%. It is recommended to use bars with a transverse coefficient of thermal expansion $\alpha_t < 40.0\ 10^{-6}$ $°C^{-1}$. Different transverse thermal expansion coefficients between FRP bars and concrete can, in fact, cause splitting cracks in the concrete as temperature increases, if no adequate concrete cover is provided to ensure sufficient confinement.

Table 3-4 - Coefficients of Thermal Expansion

Fiber type	α_l [10^{-6} °C^{-1}]	α_t [10^{-6} °C^{-1}]
Carbon	-9.0 ÷ 0.0	74.0 ÷ 104.0
Glass	6.0 ÷ 10.0	21.0 ÷ 23.0

3.5 CREEP RUPTURE

(1) FRP bars are sensitive to the phenomenon of static fatigue (or "*creep rupture*"), which consists of a progressive reduction of some mechanical properties (tensile strength, ultimate tensile strain, longitudinal elastic modulus) over time under sustained loads. This phenomenon, due to stress re-distribution between fibers and resin caused by the viscous deformations in the resin, is also strongly influenced by environmental factors such as temperature and humidity. Generally, thermosetting matrices (vinyl esters, epoxy and phenolic resins) are less viscous than thermoplastic ones (polypropylenes, nylons, polycarbonates, etc.) Because fibres reduce the viscosity of the matrix, these phenomena are more relevant when the FRP bars have a low volume percentage of fibres. FRP bars made of carbon fibers are less subjected to creep rupture in comparison to the ones made of glass fibrers.

(2) To mitigate the effects of creep and prevent bar failure due to creep failure, the levels of tensile stress under long-terms loads shall be appropriately limited. Provisions for this effect apply both to checks at the ultimate limit states and at the serviceability limit states (§ 4.6.2).

3.6 FRP MESHES

(1) Within the scope of these Guidelines are FRP meshes made as assemblies of FRP bars with circular cross-section, in carbon or glass fibers, in both directions, provided that the assembly does not alter any of the geometric or mechanical properties of the individual bars, which shall be qualified according to the procedures specified in the current qualification documents (*EAD-FRP bars* and *LG-FRP bars*).

(2) These Guidelines currently do not cover the use of other types of FRP meshes. With the availability of standardized qualification procedures and adequate experimental validation, the scope of application may also be extended to other types of meshes, subject to an update of these Guidelines and, if necessary, to the use of "*Design by Testing*" for the definition of specific capacity models.

3.7 FACTORY PRODUCTION CONTROL (FPC)

(1) FRP bars to be used as reinforcement in concrete structures shall be subject to a series of controls that ensure an adequate level of consistency in their geometric, mechanical, and physical properties. More specifically:

- The *Factory Production Control* (FPC) system shall include the evaluation of the geometric, physical, and mechanical properties of the finished products.
- The Manufacturer of bars shall use base components (fibers and resins) certified by their suppliers, which shall themselves be subject to regular production controls.

(2) For bars certified by means of a CVT, the sampling and testing of product specimens shall be carried out regularly on production batches of predefined quantities. Mechanical and physical tests shall be performed by qualified personnel with proven experience in characterizing composite materials, using appropriate and properly calibrated testing equipment. If the Manufacturer does not have an internal laboratory, they shall rely on laboratories qualified in the characterization of composite materials. The mechanical characteristics reported in the product technical datasheets shall be derived

from statistical analysis of measurements and test results. Production control records shall report all statistical data, such as the number of samples tested, mean values, standard deviations, and any other significant information. More specific indications regarding the tests to be carried out for factory production control are provided in the *LG-FRP bars*.

(3) For bars qualified through CE marking, Factory Production Control is regulated by §3.2 of the European qualification document *EAD-FRP bars*.

3.8 SITE ACCEPTANCE PROCEDURES

(1) The procedures for site acceptance are detailed in the current *LG-FRP bars* Guidelines. In the case of products qualified by means of a CVT, site acceptance inspections of the bars:

- Are mandatory and under the responsibility of the Field Engineer;
- Shall be carried out for each shipment batch when the production batch number differs among the various shipment batches, and shall cover all types of products supplied; if the production batch is the same for all shipment batches, it will be at the discretion of the Field Engineer to carry out one or more samples for testing;
- Shall consist of three samples taken on site, from each product (straight bars, stirrups, or bent FRP bars), for each shipment batch, provided that the marking and accompanying documentation prove that they originate from the same production facility. Otherwise, the controls shall also be extended to batches coming from all facilities.

(2) For products qualified through a CVT, the samples taken according to the methods and quantities indicated at point (1) in accordance with *LG-FRP bars* shall undergo the geometric and mechanical tests listed in Table 3-5.

Table 3-5 - Geometric and mechanical characteristics to be verified on samples taken on site according to the *LG-FRP bars*, and acceptance limits

	Characteristic	**Symbol [unit]**	**Acceptance Limit**
Geometric	- Effective area of the bar	$A_{b,eff}$ [mm^2]	Within the tolerances given in Table 3-1 relative to the nominal value declared by the Manufacturer for that diameter
	- Raggio di sagomatura delle staffe	r_t [mm]	$2r_t \geq 7\ d_b$
Mechanical	Tensile strength[1]	f_{ft} [MPa]	≥ 95% of the certified characteristic value, f_{ftk0}
	Mean longitudinal elastic modulus[2]	E_f [GPa]	≥ 95% of the certified mean value, E_f
	Ultimate strain[1]	ε_{ft} [mm/mm]	≥ 95% of the certified characteristic value, ε_{ftk0}
	Tensile strength of the straight portion of the stirrup[1]	$f_{ft,st}$ [MPa]	≥ 95% of the certified characteristic value, $f_{ftk,st}$

[1] The inequality shall be satisfied for the result of each specimen.

[2] The inequality shall be satisfied for the mean value of the three specimens.

(3) The tests listed in Table 3-5 shall be carried out by a certified Laboratory referred to in Article 59 of (Italian) DPR 380/2001, with proven experience and equipped with suitable instrumentation for

testing composite materials, within a timeframe deemed appropriate by the field engineer for verifying the quality and compliance of the supplied products with the project specifications, and in any case no later than 30 days from the delivery on site of the shipment batch to which said products belong.

The Field Engineer shall sign the request for testing to the Laboratory and shall include at least:

- the unambiguous indication of the commercial name of the product;
- the identification of the construction site and the location of product installation;
- the batch of the supplied material and the date of installation;
- the reference CVT.

(4) It is not permitted to perform any processing on site aimed at modifying the preformed products delivered by the Manufacturer, such as bending or other modifications that could affect the mechanical or durability characteristics of the supplied product. The only operations permitted on site are the cutting of bars, carried out with suitable tools under the Manufacturer's guidance, and the assembly of bars to create a bidirectional mesh, in both cases performed in such a way that the behavior of the individual bars is not altered. For FRP bars made with thermoplastic resins, bending operations may be performed only at the manufacturing plant after production.

(5) If the product is qualified through CE marking, the Field Engineer shall ensure that the corresponding *Certificate of Constancy of Performance and Product Conformity* (CCPC), issued by a qualified notified body, is valid and that the product arrives on site accompanied by the *Declaration of Performance and Conformity* (DoPC). In this case, the procedures referred to in points (1)–(3) are not required, and it remains at the discretion of the Field Engineer to decide whether to carry out additional acceptance tests on site according to Table 3-5, also considering that improper storage during the various phases of material supply could affect the mechanical characteristics of the bars.

(6) Appendix C details the duties and responsibilities of the different parties involved in design, realization and check of structures reinforced with FRP bars.

4 BASIC DESIGN CONCEPTS

4.1 INTRODUCTION

(1) The design of RC structures with FRP bars shall satisfy the checks at the Ultimate Limit States (ULS, essentially strength requirements) and Serviceability Limit States (SLS, functionality requirements), as defined in current Standards. Specific guidance on performing these checks for RC elements with FRP reinforcement is provided in this document.

(2) In all checks, no reliance shall be placed on the strength and stiffness contributions provided by FRP bars in compression or by the segments of bars subjected to compressive stresses. However, it is permitted not to deduct the area of concrete corresponding to the bars in the compression zone.

(3) Particular attention is required in structural analysis, since the almost total absence of ductility in RC structures with FRP bars must be duly considered. In particular, it is not permissible to adopt either elasto-plastic structural analyses or elastic analyses with redistribution. Seismic design checks must also duly account for the absence of ductility.

(4) These Guidelines also allow for the possible combined use of steel reinforcement and FRP reinforcement in the same structural element: in such cases, the sections are referred to as hybrid steel–FRP reinforcement.

(5) The service temperature of the RC element with FRP bars, estimated in accordance with current standards, shall be compatible with the service temperature of the FRP bars declared by the Manufacturer, T_{max}, particularly for elements exposed to significant thermal variations.

(6) FRP bars exhibit significant vulnerability to high temperatures, a condition that limits their use in structures where the risk of fire is considerable. Specific fire resistance checks of structural elements reinforced with FRP bars shall be performed in accordance with current fire safety regulations. These checks shall account for the glass transition temperature, T_g, of the FRP bars. Since concrete provides intrinsic thermal protection for FRP bars, increasing the concrete cover thickness and using aggregates with lower thermal conductivity can reduce bar temperatures and improve the fire resistance of structural elements. Furthermore, if a passive protection system is specifically designed to ensure that, under fire conditions, the bars do not exceed the value of T_g, the checks at the Ultimate Limit State can be carried out under ordinary conditions. In any case, FRP bars in tension, if made of continuous filaments and properly anchored in end zones of structural elements not directly exposed to thermal action, can prevent failure of the element and thus be accounted for in the calculation of flexural resistance. Appendix F provides simplified design and verification methods applicable, under certain conditions, to warrant the fire safety of structural elements.

4.2 BASIC REQUIREMENTS

(1) The fundamental requirements for the design of concrete structures reinforced with FRP bars can be considered satisfied if the following are ensured:

- the selection of appropriate materials;
- careful detailing of design features;
- the definition of suitable procedures for control during production of materials, execution of structures, and their use and maintenance.

4.3 DESIGN SERVICE LIFE OF STRUCTURE AND DURABILITY

(1) For the purposes of verifying the safety of structural concrete elements reinforced with FRP bars, reference should be made to the design service life of the structure and to the corresponding design values of actions established in the current National Standards.

(2) The structure shall be designed with due consideration of both environmental conditions and the maintenance program.

(3) To ensure the durability of the RC structure with FRP bars, the following factors shall be appropriately taken into account:

- the intended use;
- the expected environmental conditions;
- the composition, properties, and performance of the materials used.

(4) The reference service life of FRP bars qualified on the basis of a European Technical Assessment (ETA), according to the intended use specified in *EAD- FRP bars* (where is defined as '*working life'* of the product) and subsequent revisions, and properly installed, is considered to be 100 years, based on the current state of the art, available knowledge, and experience.

(5) Special design issues (environmental actions, loading conditions, etc.) shall be identified at the earliest stage so that their importance can be assessed appropriately with respect to the durability of FRP reinforcement considering their effective terms of use.

4.4 GENERAL DESIGN PRINCIPLES

4.4.1 General Provisions

(1) Using the partial factor method, it shall be verified that, in all design situations and by adopting the design values of actions and resistances, no limit state is violated, whether related to ultimate (ULS) or serviceability (SLS) conditions. The following limitation must be set $E_d \le R_d$, where E_d and R_d are, respectively, the design values of the generic effect of the applied actions (force, deformation, etc.) under consideration and of the corresponding capacity (in terms of resistance or maximum deformation) for the relevant limit state.

(2) The design values are derived from the characteristic values by applying appropriate partial factors. For ordinary materials, these values are specified in the current standards; for FRP reinforcement, they are provided in this document.

4.4.2 Design values of actions

(1) The design values of actions to be adopted in structural design are those prescribed by the applicable standards.

4.4.3 Design values of strength

(1) With reference to the condition $E_d \le R_d$ for a generic action E_d under a given limit state, the design strength, R_d can be expressed as:

$$R_d = R\left\{X_{d,i}; a_{d,i}\right\} = R\left\{\eta \frac{X_{k,i}}{\gamma_m \cdot \gamma_{Rd}}; a_{d,i}\right\} \tag{4.1a}$$

In Eq. (4.1a), $\mathrm{R}\{\cdot\}$ is an appropriate function corresponding to the specific strength model considered (for example, for bending, shear, etc.); the arguments of the function $\mathrm{R}\{\cdot\}$ are generally mechanical $\mathrm{X_i}$ and geometrical parameters $a_{,\mathrm{i}}$, of which $\mathrm{X_{d,i}}$ and $a_{\mathrm{d,i}}$ respectively, are the design values (EN 1992-1-1:2023). Moreover, in Equation (4.1a), γ_m is the partial factor related to the material properties uncertainties, γ_{Rd} is the partial factor related to strength model and geometry uncertainties, and η is the conversion factor taking into account the reduction of the mechanical properties due to the exposure to not standard environmental conditions, mainly related to humidity and temperature, and due to aging, scale effects or whatever other relevant parameter.

Eq. (4.1a) can be written as:

$$\mathrm{R_d} = \mathrm{R}\left\{\eta \frac{\mathrm{X}_{k,i}}{\gamma_\mathrm{f}}; a_{d,i}\right\} \tag{4.1b}$$

(2) In Eq. (4.1b), the simplified approach proposed in Eurocode 0 (EN 1990:2023), is assumed:

$$\gamma_\mathrm{f} = \gamma_\mathrm{m} \cdot \gamma_{\mathrm{Rd}} \tag{4.2}$$

where the partial factors γ_m and γ_{Rd} are combined in only one factor γ_f, indicated as partial factor of the FRP bars.

(3) The factor γ_{Rd}, and, thus, also γ_f, can be different depending on the type of actions applied to the FRP bars (bending moment, shear, confinement). Details about assessment of factors γ_{Rd}, γ_m and γ_f are reported in Appendix B.

4.4.4 Geometric and material properties

(1) The values of the geometric and mechanical characteristics of FRP bars shall be determined through measurements and laboratory tests carried out according to standardized procedures, as indicated in Appendix A. The design rules outlined in this document apply exclusively to products that meet the characteristics listed in Table 3-1, with diameters and corresponding effective areas specified in Table 3-2, and which fall within the classes defined in Table 3-3.

(2) The corresponding characteristic values shall quantify the mechanical properties related to the strength and deformation of FRP bars. Only stiffness parameters (as example, the elastic moduli) are to be evaluated by their corresponding mean values. In the absence of specific technical data for FRP bars, the values of strength and modulus of elasticity corresponding to one of the classes listed in Table 3-3 shall be used for the verifications in these Guidelines. Where the mandatory mechanical characteristics listed in Table 3-1 are known for a given product, or where the chosen product has mechanical characteristics exceeding the threshold values of the classes, and provided that the mandatory characteristics have been obtained through qualification carried out in accordance with the *EAD-FRP bars* or the *LG-FRP bars*, the actual strengths supplied by the Manufacturer may be used.

(3) The design value of the tensile strength or of the corresponding strain of the FRP bar (in all cases denoted by the symbol $\mathrm{X_d}$) can be expressed in general form by the following relation:

$$\mathrm{X_d} = \eta_\mathrm{T} \cdot \eta_\mathrm{a} \cdot \eta_{\mathrm{c},l} \frac{\mathrm{X_k}}{\gamma_\mathrm{f}} \tag{4.3}$$

where:

- $\mathrm{X_k}$ is the characteristic value of strength or strain parameter. If $\mathrm{X_k}$ represents the tensile

strength f_{ftk0}, it corresponds to the value that defines the class as given in Table 3-3;

- γ_f is the partial factor for FRP bars defined by Eq. (4.2) and to be evaluated as described in §4.5;
- η_T is a conversion factor accounting for temperature effects, to be evaluated as described in § 4.6.1 depending on the exposure conditions of the structure;
- η_a is an environmental conversion factor accounting for the durability of the bars as a function of the exposure conditions of the structure, to be evaluated as described in § 4.6.1;
- $\eta_{c,l}$ is a conversion factor accounting for static fatigue effects (*creep rupture*) under long-term loads, to be evaluated as described in § 4.6.2.

(4) In Eq. (4.3), it is possible to adopt $\eta_T = 1$, $\eta_a = 1$, $\eta_{c,l} = 1$ under whatever exposure condition in case of: 1) temporary structures having a design service life not exceeding 5 years (being the design service life defined in accordance with the current Standard), 2) verification of structural elements during the construction phases of the work, provided that such phases have a duration of less than 2 years.

4.5 PARTIAL FACTORS FOR MATERIALS

(1) For ultimate limit states (ULS), in case of flexural verifications, the value to be assigned to the partial factor for FRP bars, γ_f is equal to 1.25 for permanent and variable actions and equal to 1.10 for accidental actions. Details on the procedure followed to define the value of the partial factor γ_f are provided in Appendix B.

(2) For ultimate limit states (ULS), in case of shear stress and for assessing the effect of confinement induced by FRP stirrups on concrete elements under axial and bending forces or under mainly axial stresses, the value to be assigned to the partial factor for FRP bars, γ_f, is 1.40 for permanent and variable actions and 1.25 for accidental actions. Details on the procedure followed to define the value of the partial factor γ_f are provided in Appendix B.

(3) For all serviceability limit state (SLS) verifications, the value to be assigned to the partial factor is $\gamma_f = 1$.

(4) For concrete and steel reinforcement (in the case of hybrid reinforcement structures), the partial factors prescribed by the current Standards shall be adopted.

4.6 SPECIAL DESIGN ISSUES

4.6.1 Conversion factors for environmental and temperature actions

(1) The mechanical properties (for example, tensile strength, ultimate strain, and normal modulus of elasticity) of FRP bars can degrade under certain environmental conditions, such as alkaline environments and moisture (water and saline solutions) or in case of exposure to solar radiation.

(2) About the effects of an alkaline environment, water in the concrete's pores can degrade the polymer resin in the FRP bar. Damage to the resin from alkali attack is generally more severe than that from moisture. The main effects of moisture (due to exposure to water and/or saline solutions) regard the resin and include plasticization, a decrease in the glass transition temperature, a reduction in strength and stiffness (the latter less pronounced). Moisture absorption depends on the type of polymer resin, the fiber–matrix interface, and the composition and quality of the bars.

(3) The overall effect of the environment on the strength of the material is accounted for through the environmental conversion factor η_a.

(4) The effect of temperature on the tensile strength of the FRP bars is considered by means the conversion factor η_T. The effects of temperature can be significant in case of structural elements of bridges and should be considered for elements directly exposure to solar radiation.

(5) Table 4-1 provides, for glass fiber bars (GFRP) and carbon fiber bars (CFRP), the values to be assigned to the environmental conversion factor η_a and the factor η_T to be used in Eq. (4.2) for different exposure conditions of RC elements with FRP bars. The exposure classes reported in Table 4-1 are defined in EN 1992-1-1 (2023). It should be noted that, in the second column of Table 4-1, for completeness, the same nomenclature of exposure classes adopted for RC structures with steel reinforcement has been used.

Table 4-1 - Values of the factors η_T and η_a under different exposure conditions of the structure

Exposure condition	Exposure class*	η_T	η_a
1 (indoor dry environment)	X0, XC1 dry	1.0	GFRP: 0.85 CFRP: 0.95
2 (outdoor dry environment)	XS1	1.0: for elements not directly exposed to solar radiation 0.9: for elements directly exposed to solar radiation	GFRP: 0.85 CFRP: 0.95
3 (permanently or cyclically humid environment)	XC1 humid, XC2, XC3, XC4 XD1, XD2, XD3 XF1, XF2, XF3, XF4 XS2, XS3 XA1, XA2, XA3	1.0: for elements not directly exposed to solar radiation 0.9: for elements directly exposed to solar radiation	GFRP: 0.70 CFRP: 0.85

*The exposure classes are defined in EN 1992-1-1 (2023). For completeness, the same nomenclature used for RC structures with steel reinforcement has been adopted

4.6.2 Conversion factor for long-term effects $\eta_{c,l}$

(1) The effects of static fatigue (*creep rupture*) in FRP bars under long-term loads have to be considered both at SLE verifications, limiting the tensile stress in the bars under the quasi-permanent load combination, and at the SLU, adopting a reduced value of the tensile strength in the FRP bars that depends on the stresses in the bars under quasi-permanent load combination.

(2) For verifications at the Ultimate Limit State (ULS), the effects of static fatigue produced by long-term loads are accounted for by defining the conversion factor for long-term loads $\eta_{c,l}$, reported in Equation (4.3) and defined as follows:

$$\eta_{c,l} = 1 - \left(1 - \eta_c\right) \cdot \frac{\sigma_{f,qp}}{f_{ftk,c}} = 1 - \left(\frac{1}{\eta_c} - 1\right) \cdot \frac{\sigma_{f,qp}}{f_{ftk0}} \tag{4.4}$$

where

- $\sigma_{f,qp}$ is the current stress acting in the FRP bar under the long-term loads, , calculated with reference to the quasi-permanent combination of actions;

- $f_{ftk,c}$ is the characteristic value of the tensile strength of the FRP bar due to creep rupture at a time corresponding to the reference service life of the bars, conventionally taken as 100 years according to the definition given in *EAD-FRP bars*;
- $\eta_c = \frac{f_{ftk,c}}{f_{ftk0}}$ is the conversion factor for static fatigue (*creep rupture*) at 100 years, where f_{ftk0} is the characteristic value of the tensile strength of the FRP bar in the absence of environmental, temperature, or long-term load effects.

Equation (4.4) shows that, in the combination of actions at ULS, and in the case of relevant long-term stresses, the tensile strength of FRP bars is reduced compared to the characteristic strength f_{ftk0}. In particular, the conversion factor $\eta_{c,l}$ lies between η_c and 1. It is generally greater than η_c and coincides with it only if the level of quasi-permanent stress $\sigma_{f,qp}$ is precisely equal to the creep rupture strength $f_{ftk,c}$. For safety, it is possible to assume $\eta_{c,l} = \eta_c$ in the checks regarding ULS load combinations.

(3) The *EAD-FRP bars* indicates how to experimentally obtain the strength $f_{ftk,c}$ to be introduced in equation (4.4). In the absence of specific experimental indications for the strength $f_{ftk,c}$, the conversion factor for *creep rupture* at 100 years, η_c, may be assumed as the values given in Table 4-2, and consequently, $f_{ftk,c} = \eta_c \cdot f_{ftk0}$.

Table 4-2 - Conversion factor for static fatigue (*creep rupture*) at 100 years, η_c, for FRP bars

Loading mode	Fiber type	η_c
Quasi-permanent	Glass	0.50
	Carbon	0.80

(4) It should be noted that equation (4.4) requires evaluating the level of quasi-permanent stress, $\sigma_{f,qp}$, responsible for the reduction in strength of the FRP bar. This stress may be estimated using the methodology reported in § 7.2, which concerns stress checks in service, or with simplified procedures depending on the type of structural element being verified.

(5) For the stress limitation checks at SLS, in order to avoid nonlinear behavior of FRP bars and reduce the effects of static fatigue, under quasi-permanent combination of actions, the stress in the FRP bars shall be properly limited as a function of the static fatigue strength of the FRP bar, $f_{ftk,c}$, as indicated in point (1) of § 7.2.

(6) With regard to the effect of repeated cyclic loads, which for number of cycles and amplitude of the stress variation may cause fatigue phenomena in the materials, the performance of FRP bars is generally excellent. Among the different types, glass fiber bars are the most susceptible to the effects of cyclic loads. Lacking experimental data on the tensile strength of the FRP bars under fatigue loads (i.e., the mechanical characteristic $f_{fatigue}$ defined in E*AD-barre FRP* at §2.2.7 and in *LG-barre FRP* in Tab. 3), it is possible to carry out the verifications at ULS under cyclic actions that produce fatigue effects adopting the Eq. (4.3) for calculating the tensile strength in the FRP bars and assuming, on safety side, that $\eta_{c,l}$ is substituted by η_c that have the value listed Table 4-2.

4.6.3 Behavior of FRP bars under high temperatures

(1) The vulnerability of organic polymers to high temperatures can represent an essential critical issue for FRP bars when designing civil and industrial structures, where fire is an event that must be considered. The deterioration of the mechanical properties of FRP materials (especially strength and

Young's modulus) and of bond properties begins when temperatures approach the glass transition temperature (T_g). The T_g of products supplied by major FRP manufacturers typically ranges from 100°C to 175°C, depending on the resin type.

(2) The deterioration of mechanical properties depends on the type of fiber, the type of surface treatment of the bars, and, of course, the temperature reached in the material. Temperatures in FRP bars embedded in concrete remain limited for a specific period due to the concrete's low thermal conductivity. Therefore, the performance of RC elements with FRP bars in the event of fire can be satisfactory, even in the absence of specific fire protection systems (such as passive protection systems, consisting of conventional coatings or special insulating materials, or active protection systems), provided that the concrete cover is sufficient. Moreover, the phenomenon of concrete spalling, i.e., the detachment of the cover that protects the bar from direct fire exposure, is less likely in zones where the bars are in tension, where the role of the FRP bar is crucial for the element's strength.

(3) Fire resistance verification for RC elements (EN 1992-1-2, 2023) requires that the design effect in fire conditions at time t of fire exposure, $E_{fi,d,t}$, be calculated by combining mechanical actions for accidental design situations, and that the design capacity under the same conditions, $R_{fi,d,t}$, be calculated by adopting $\gamma_c = 1.0$ for concrete and $\gamma_f = 1.1$ for the FPR bars.

(4) The development and distribution of temperature inside structural elements exposed to fire (i.e., the thermal field) may be evaluated by decoupling the thermal and mechanical response models in accordance with recognized code provisions (EN 1992-1-2, 2023). The thermal field should be determined by solving the heat transfer problem due to radiation and convection from combustion gases to the external surface of the element, while accounting for the possible presence of protective materials. The thermal properties of concrete shall be evaluated in accordance with recognized code provisions (EN 1992-1-2, 2023). However, the presence of FRP bars can be neglected in the thermal model due to their small dimensions.

(5) The effect of high temperatures on the strength and stiffness of concrete may be evaluated in accordance with recognized code provisions (EN 1992-1-2, 2023). Appendix F provides, as an example, a simplified procedure for flexural verification of a concrete section reinforced with FRP bars under fire conditions.

(6) Portions of concrete exceeding 500 °C shall not be considered. To account only for the effective contribution of the concrete at temperatures below 500 °C, the values of b and d shall be appropriately reduced based on the temperature field evaluated through a thermal analysis of the structural element.

Essential References

1. EN 1990:2023, *Eurocode 0 - Basis of structural and geotechnical design*. European Committee for Standardization (CEN), Brussels, Belgium.
2. EN 1992-1-1:2023, *Eurocode 2: Design of concrete structures - Part 1-1: General rules and rules for buildings, bridges and civil engineering structures*. European Committee for Standardization (CEN), Brussels, Belgium.
3. EN 1992-1-2:2023, *Eurocode 2 - Design of concrete structures - Part 1-2: Structural fire design*. European Committee for Standardization (CEN), Brussels, Belgium.
4. EAD 260023-00-0301. *Carbon, glass, basalt and aramid Fibre Reinforced Polymer bars as reinforcement of structural elements.* Adopted January 2019, EOTA. OJ Publication: Decision (EU) 2024/1944.
5. LG (2021), *Linea guida per l'identificazione, la qualificazione e l'accettazione di barre e staffe in composito fibrorinforzato per uso strutturale*, Consiglio Superiore dei Lavori Pubblici, Dicembre 2021.

5 BOND BEHAVIOR

5.1 BOND OF FRP BARS IN CONCRETE

(1) The bond between concrete and FRP bars is a fundamental aspect for the behavior of the reinforced section, both at ultimate and service limit states. The proper cooperation between the FRP bar and the concrete is ensured by the bond mechanism that develops between them through shear stresses along the FRP bar–concrete interface.

(2) For design purposes, bond quality influences, at the Ultimate Limit State, the value of the minimum anchorage length that the FRP bar shall provide to ensure that it can develop a prescribed design stress. At the same time, at the Serviceability Limit State, it affects the checks for cracking (control of crack width) and deformability (control of maximum flexural displacements of the element) through coefficients that account for bond quality.

(3) The bond behavior of bars embedded as reinforcement within concrete elements generally depends on the geometry and mechanical properties of the bar, the physic-chemical properties of its surface, the strength of the concrete, the thickness of the concrete cover, and, to a lesser extent, the position of the bar relative to the casting direction. In the specific case of FRP bars, the bond behavior is influenced mainly by their mechanical properties (elastic and shear moduli, Poisson's ratio) and geometric characteristics (shape, diameter, or dimensions), as well as by their surface treatment (sand coating, presence of grooves, or surface deformations produced by different manufacturing technologies). Depending on the type of surface treatment, relevant factors include the geometric characteristics of the surface (size and spacing of ribs or protrusions), the stiffness and shear strength of any protrusions present, and the roughness of the sand coating.

(4) Bond failure, i.e., the slip of the FRP bar from the concrete, can occur either at the bar–concrete interface or through the formation of compressed concrete struts around the bar, depending on the surface finish of the bar. The compressive strength of concrete has less influence on the bond mechanism than that of steel bars. In fact, the action of the compressed concrete struts formed between the ribs of the bars ("mechanical interlocking") is effectively mobilized in the case of steel bars. In contrast, for FRP bars, it is activated only if they have a sufficiently stiff and strong surface indentation capable of inducing circumferential cracking of the surrounding concrete. Experimental evidence has nevertheless demonstrated good bond capacity of FRP bars, as a consequence of the physic-chemical adhesion that develops at the bar–concrete interface and of a frictional mechanism. The latter typically reaches its maximum resistance once significant damage occurs on the bar surface and limited damage develops in the surrounding concrete. The frictional mechanism is influenced both by the surface treatment and by the elastic modulus and Poisson's ratio of the bars, which affect the bar's contraction; this phenomenon is more pronounced in FRP bars than in steel bars due to their lower elastic modulus and, therefore, greater longitudinal and transverse deformations. Since the elastic modulus and Poisson's ratio of FRP bars depend on the type and volumetric percentage of resin and fibers, these parameters can also have a significant influence on the bond mechanism.

(5) The most common surface treatments of commercially available FRP bars can be classified into the following categories:

1. *Sand-coated bars*: a thin layer of sand and/or fine abrasive particles is bonded to the bar surface to increase roughness (Figure 5-1a) and improve physic-chemical adhesion.
2. *Ribbed bars*: ribs are present along the entire length of the bar, generally formed by resin protrusions (Figure 5-1b). The purpose here is to enhance the interlocking mechanism by locally modifying the bar shape.

3. *Indented bars*: the surface is indented along the entire length with a series of notches and protrusions, generally formed by fibers and resin (Figure 5-1c), sometimes combined with sand-coating (Figure 5-1d). The goal here is to improve the interlocking mechanism not only by modifying the bar shape but also by increasing the adhesion area between the concrete and the bar.
4. *Helically wrapped bars:* fibers of different types are helically wound around the bar (Figure 5-1e), sometimes combined with sand-coating (Figure 5-1f). In this case, the objective is to increase surface roughness, improve interlocking, and enlarge the concrete–bar contact area.

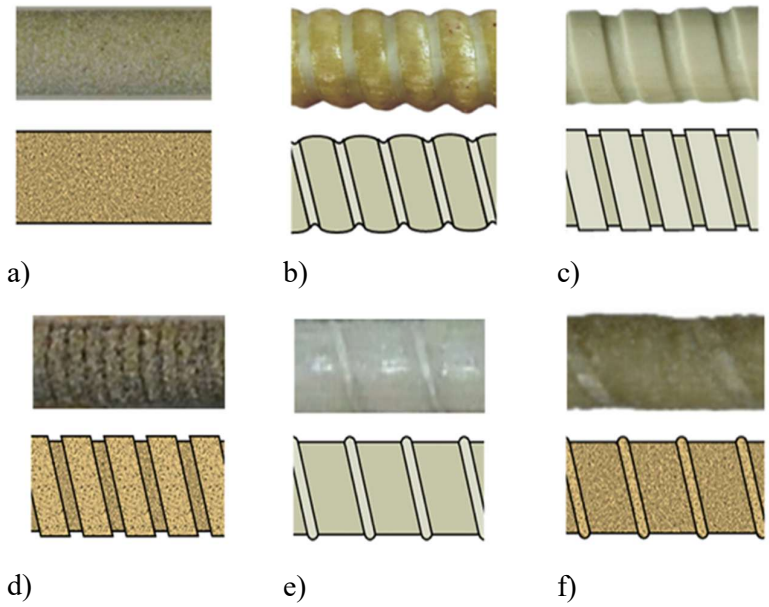

Figure 5-1 - Examples of the most common surface treatments of FRP bars: a) sand-coated bars; b) ribbed bars; c) indented bars; d) indented bars with sand-coating; e) helically wrapped bars; f) helically wrapped bars with sand-coating.

It should be noted that there are also bars without any surface treatment (smooth bars). For these, the level of adhesive and frictional mechanisms developing at the bar–concrete interface may render FRP bars unsuitable for use under this document unless the minimum threshold of bond strength is reached, to be verified by experimental bond tests (see §5.3). Therefore, it is strongly recommended to use bars with a minimal surface treatment that ensures the adequate transfer of bond stresses between the FRP bar and the surrounding concrete.

5.2 MODELING OF THE BOND BEHAVIOR

(1) The bond mechanism can be modeled at different levels of detail. In general, for conducting structural analyses, a macro-level bond model is adopted, which establishes a relationship between shear stresses and slips that develop at the FRP bar–concrete interface. This model can be obtained experimentally, as indicated in §5.3.

(2) The bond model must reflect the physic-chemical-mechanical characteristics of the different types of surface treatments applied to FRP bars, also considering the strength class of the surrounding concrete. The interlocking mechanism depends both on the strength and stiffness of the bar's surface protrusions (in ribbed or indented bars, for example) and on the tensile strength of the concrete. The same FRP bar, capable of developing good interlocking, may or may not cause cracking and shearing

of the concrete struts, depending on the concrete's strength.

(3) The bond model can be experimentally evaluated for the specific type of bar under consideration (see § 5.3), but, by way of example, two types of models can be considered depending on the prevailing mechanism:

a) a bond model based mainly on the physical-chemical adhesion at the bar–concrete interface;
b) a bond model based both on physical-chemical adhesion and on mechanical interlocking at the bar–concrete interface, which may be more or less significant depending on the type of surface treatment.

In the case of a bond mechanism based primarily on physical-chemical adhesion, the bond model typically follows the trend shown in Figure 5-2a: initially, shear stress increases with no slip until it reaches a maximum. Beyond the peak, the curve shows a rapid drop in bond strength until the shear stress vanishes or reaches a residual level, due to friction between the bar and the concrete, which remains constant as slip increases.

In the case of a bond mechanism also based on mechanical interlocking, the bond model typically follows the trend shown in Figure 5-2b. Here, the phase of chemical adhesion is followed by a second ascending branch in which the interface stress increases with slip, dominated by the interlocking of concrete aggregates into the bar's ribs. Again, once peak shear stress is reached—higher than in the adhesion-only case—a descending branch develops, characterized by a residual frictional mechanism up to the pull-out of the bar.

(4) For FRP bars capable of activating significant mechanical interlocking, the bond model must also account for the possibility of a "splitting" failure of the concrete, either complete or partial, occurring before the pull-out of the bar when the concrete cover is insufficient. For more details on the definition of minimum cover values, see §6.8.1.

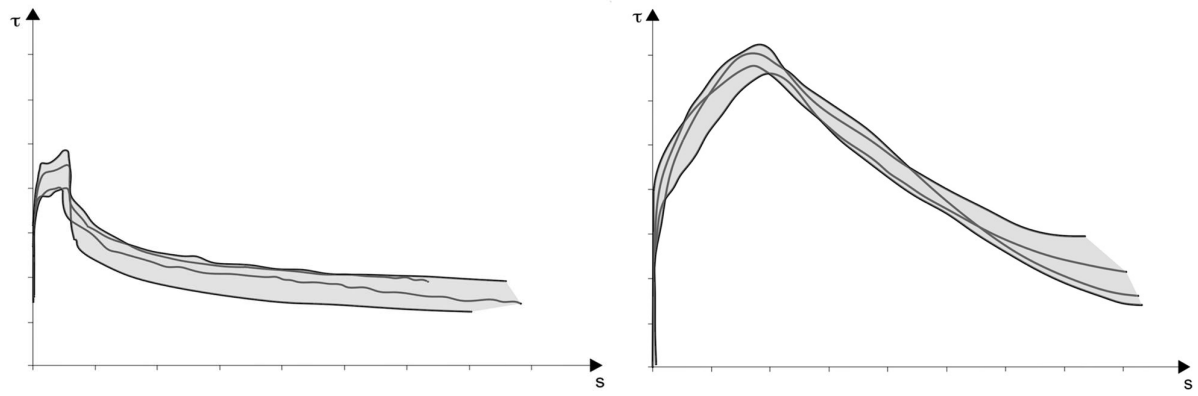

a) b)

Figure 5-2 - Examples of bond–slip relationship for FRP bars: a) mechanism based on physical-chemical adhesion; b) mechanism based on physical-chemical adhesion combined with mechanical interlocking.

5.3 EXPERIMENTAL CHARACTERIZATION OF THE BOND BEHAVIOR

(1) Complete characterization of the bond model requires the execution of specific experimental tests. The pull-out test (see Figure 5-3) is the most frequently used method to obtain an experimental relationship between the bond shear stress (assumed constant along the bonded length of the bar) and the

slip between the concrete and the FRP bars (τ_b-s relationship). Since the bond shear stress varies along the bar, the pull-out test is conducted with a limited bonded length between the bar and the concrete, so that the assumption of constant shear stresses along the bar can be considered acceptable.

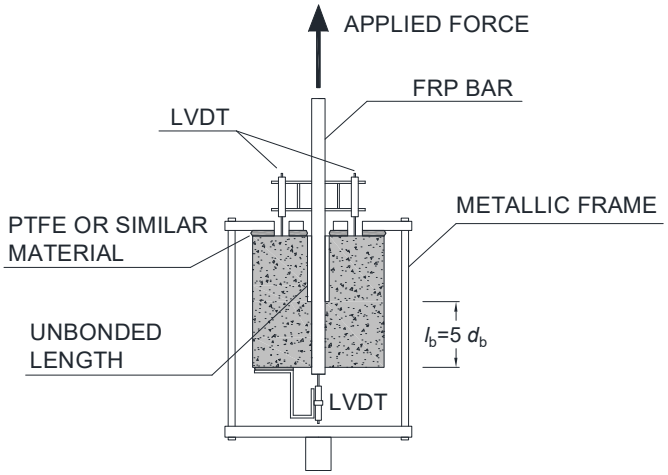

Figure 5-3 – Scheme of a pull-out test for the experimental characterization of the bond model of FRP bars.

(2) The bond quality of FRP bars shall be verified through pull-out tests on at least 5 specimens. For this purpose, pull-out tests shall be conducted on FRP bars embedded in concrete blocks of strength class C20/25, with a bonded length, ℓ_b, equal to 5 times the effective diameter of the FRP bar, $d_{b,eff}$, following the procedures set out in the current qualification guidelines (*EAD-FRP bars* or *LG-FRP bars*).

Assuming a constant distribution of bond shear stresses over the bonded length, ℓ_b, the peak bond shear stress, τ_b, is calculated from the maximum load, F_{max}, obtained in each pull-out test, provided that failure occurs at the FRP bar–concrete interface, as follows:

$$\tau_b = \frac{F_{max}}{\pi d_{b,eff} \cdot \ell_b} \qquad \text{with } \ell_b = 5 d_{b,eff} \tag{5.1}$$

For qualification purposes, the mean peak value shall be calculated based on the results of at least 5 pull-out tests.

The bond quality of FRP bars in concrete can be classified into the following classes:

- Bond class 1: $\tau_b > 15.0$ MPa
- Bond class 2: $7.0 \text{ MPa} \le \tau_b \le 15.0$ MPa

The design provisions given in these Guidelines are not valid for FRP bars for which bond tests show $\tau_b < 7.0$ MPa.

5.4 ANCHORAGE LENGTH

(1) The typical design criterion for anchorage of metallic bars requires the anchorage length be sufficiently long to assure yielding of the bar when subject to traction test. On the contrary, since FRP

bars have particularly high tensile strength, it is often unnecessary to ensure that they can be anchored up to their full tensile capacity. This is especially evident when bars are anchored in regions subjected to low stress (such as the ends of simply supported beams). On the contrary, particular attention shall be paid to the anchorage of bars in beams and columns of frame structures designed in seismic zones, since maximum stresses often occur at the ends of structural members.

(2) For straight FRP bars in tension zones, indicating with σ_{fd} the stress level in the bars under the ULS load combination, the anchorage length may be calculated using the following expressions, depending on the bond class defined in §5.3:

- For FRP bars in Bond class 1:

$$\ell_a = k_{cp} \cdot k_\ell \cdot d_b \cdot \left(\frac{\sigma_{fd}}{500}\right)^2 \cdot \left(\frac{25}{f_{ck}}\right)^{4/5} \cdot \left(\frac{d_b}{20}\right)^{2/5} \cdot \left(\frac{1.5d_b}{c_d}\right)^{1/2} \qquad k_\ell = 30 \qquad (5.2a)$$

- For FRP bars in Bond class 2:

$$\ell_a = k_{cp} \cdot k_\ell \cdot d_b \cdot \left(\frac{\sigma_{fd}}{500}\right)^{3/2} \cdot \left(\frac{25}{f_{ck}}\right)^{3/5} \cdot \left(\frac{d_b}{20}\right)^{3/10} \cdot \left(\frac{1.5d_b}{c_d}\right)^{1/2} \qquad k_\ell = 65 \qquad (5.2b)$$

where:

- k_{cp} is a coefficient accounting for the position of the bar during casting and its effect on bond (equal to 1.0 or 1.2 for good or poor bond conditions, respectively, as specified in EN 1992-1-1:2023);
- $c_d = \min(c_{geom,x}, c_{geom,y}, 0.5c_i, 3.75d_b)$, where $c_{geom,x}$ and $c_{geom,y}$ are the geometrical cover measured in the horizontal and vertical direction, respectively, c_i is the spacing between adjacent FRP bars, and d_b is the nominal diameter of the FRP bars.

The term $\left(\frac{1.5d_b}{c_d}\right)^{1/2}$ is considered in (5.2) only if it is greater than 1.

The exponents and the coefficient k_ℓ of these expressions were obtained through statistical analyses and regression of experimental results.

(3) To ensure that anchorage is provided for an FRP bar subjected to a tensile stress level σ_{fd}, the anchorage length, given by (5.2a, b) and measured from the section beyond which the bar is no longer considered effective but only anchored, shall not be less than the greater of 300 mm or 20 d_b, regardless of bar diameter or bond quality class. Therefore, the design value of anchorage length, ℓ_{ad} shall be taken as:

$$\ell_{ad} = \max\left(\ell_a, 300\,\text{mm}, 20d_b\right) \qquad (5.3a)$$

(4) For exposure condition 3, the design value of anchorage length, ℓ_{ad}, in Eq. (5.3a) shall be increased considering the environmental reduction factor η_a from Table 4-1, as follows:

$$\ell_{ad} = \frac{1}{\eta_a}\max\left(\ell_a, 300\,\text{mm}, 20d_b\right) \qquad (5.3b)$$

(5) For the evaluation of σ_{fd} in zones mainly subjected to shear stresses, the bending moment diagram shall be appropriately shifted, as required by current Codes for RC elements with steel reinforcement.

(6) If it is not possible to assure the design anchorage length ℓ_{ad} required by (5.3), anchorage of straight bars may be achieved by overlapping with additional FRP bars of the same nominal diameter, bent at 90° at their ends (Figure 5-4). The lap length of the straight portion of the additional bent bar shall be:

$$\ell_s = 1.25 \cdot \ell_{ad} \tag{5.4}$$

This anchorage method, often used to simplify reinforcement detailing (since it allows the main reinforcement bars to remain straight), shall be carefully considered in heavily reinforced sections, as significant reinforcement congestion may result. After bending at 90°, the hooked bar shall have a straight extension at least equal to 10 times the nominal bar diameter d_b: $L_t \geq 10 d_b$ (Figure 5-4).

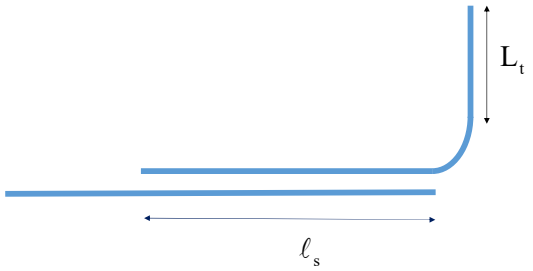

Figure 5-4 – Anchorage of FRP bars by overlapping with 90° bent bars

(7) Eqs. (5.2) may also be used to calculate, at sections located at a distance $\ell_b < \ell_{ad}$ from the end of an FRP bar, the maximum design stress, σ_{fd}, that can be developed in the bar, depending on the bond quality class. Inverting (5.2) gives the following equations:

- For FRP bars in bond quality class 1:

$$\sigma_{fd} = k \cdot \left(\frac{\ell_b}{d_b}\right)^{1/2} \cdot \left(\frac{f_{ck}}{25}\right)^{2/5} \cdot \left(\frac{20}{d_b}\right)^{1/5} \cdot \left(\frac{c_d}{1.5 d_b}\right)^{1/4} \leq f_{ftd} \qquad k = 92 \tag{5.5a}$$

- For FRP bars in bond quality class 2:

$$\sigma_{fd} = k \cdot \left(\frac{\ell_b}{d_b}\right)^{2/3} \cdot \left(\frac{f_{ck}}{25}\right)^{2/5} \cdot \left(\frac{20}{d_b}\right)^{1/5} \cdot \left(\frac{c_d}{1.5 d_b}\right)^{1/3} \leq f_{ftd} \qquad k = 31 \tag{5.5b}$$

In equation (5.5), the term that is a function of $\left(\frac{c_d}{1.5 d_b}\right)$, it is considered only if it is less than 1.

6 ULTIMATE LIMIT STATES (ULS)

6.1 ULTIMATE MOMENT RESISTANCE WITHOUT AND WITH AXIAL FORCE

6.1.1 Basic assumptions

(1) The ultimate limit state design for flexural actions requires that the structural element be sized so that the design moment resistance, M_{Rd}, is greater than or equal to the design value of applied bending moment, M_{Ed}, resulting from the design loads acting on the structure:

$$M_{Ed} \leq M_{Rd} \tag{6.1}$$

In the case of combined axial force and bending, the design value of applied axial force, N_{Ed}, shall be considered in the evaluation of M_{Rd}.

(2) The fundamental assumptions underlying the calculation of the design flexural resistance M_{Rd} at the ultimate limit state for a RC section with FRP bars are as follows:

- sections remain plain up to failure, with a linear distribution of normal strains in both compressed concrete and FRP tensile reinforcement;
- the tensile strength of concrete is neglected;
- the contribution of FRP bars in compression is neglected;
- the constitutive law for concrete is taken according to the current Code;
- the constitutive law for FRP bars is assumed to be linear-elastic up to failure.

Although the contribution of FRP bars in the compression zone is neglected, it is permitted not to deduct the area of concrete corresponding to them.

(3) Flexural failure occurs when one of the following conditions is reached:

- the ultimate compressive strain in concrete, ε_{cu}, is reached (concrete-side failure);
- the ultimate tensile strain in FRP bars, ε_{ftd}, is reached (FRP-side failure), calculated as a function of the design tensile strength:

$$\varepsilon_{ftd} = \frac{f_{ftd}}{E_f} = \eta_T \cdot \eta_a \cdot \eta_{c,l} \cdot \frac{f_{ftk0}}{\gamma_f \cdot E_f} \tag{6.2}$$

where γ_f is the partial factor for FRP bars defined in § 4.5 and η_T, η_a, and $\eta_{c,l}$ are the conversion factors defined in §4.6.1 and §4.6.2 depending on the exposure conditions of the structure. In Equation (6.2), bars are assumed to be fully anchored.

6.1.2 Design moment resistance

(1) The design flexural resistance of the section is calculated in accordance with the assumptions reported in § 6.1.1.

(2) Since FRP bars behave linear-elastic up to failure, the stresses in the FRP reinforcement are determined as the product of the strains and the longitudinal elastic modulus.

(3) When failure of the section occurs due to reaching the ultimate compressive strain in the concrete, ε_{cu}, a simplified constant distribution of normal stresses in the concrete (so called “stress-block”) may be adopted.

(4) In the case of pure bending, with reference to Figure 6-1, two failure regions can be identified

depending on the position of the strain diagram at failure: 1) failure region 1: when the ultimate tensile strain in the FRP reinforcement, ε_{ftd} is reached; 2) failure region 2: when the ultimate compressive strain in concrete, $\varepsilon_{cu,}$ is reached while the reinforcement remains in the elastic range. In Figure 6-1, *b, d* and *h* are the section width, effective depth, and total depth of the concrete section, respectively; *x* is the distance from the neutral axis to the compressed edge; A_f is the total area of the FRP tensile reinforcement; *c* is the distance from the centroid of the FRP reinforcement to the tension face of the section (mechanical cover). In Figure 6-1, the position of neutral axis *x* refers to a strain distribution corresponding to failure region 1. The two failure regions are separated by the line that connect the values of ultimate strains in the two materials, ε_{cu} and ε_{ftd}.

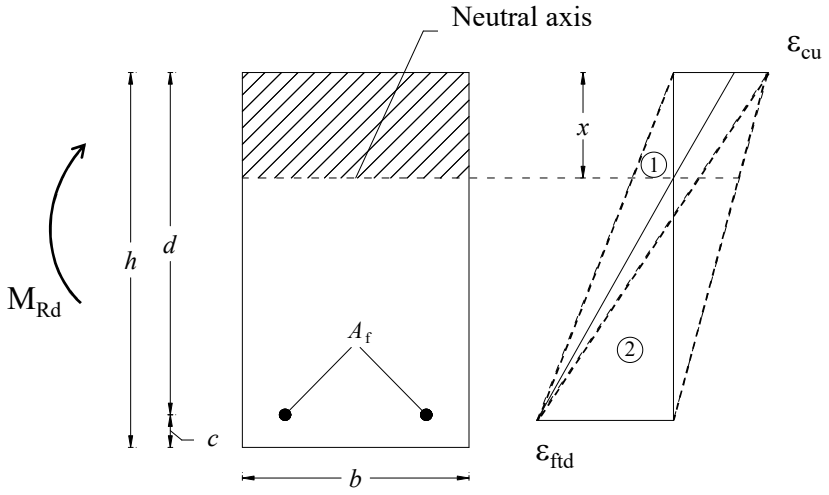

Figure 6-1 – Flexural failure modes of a concrete section reinforced with FRP bars under pure bending moment.

(5) In failure region 1, failure occurs when the FRP reinforcement reaches its ultimate strain; therefore, any strain diagram corresponding to this failure mode has as a fixed point the limiting strain value of the reinforcement ε_{ftd}. For reinforcement arranged in multiple layers, this value refers to the centroid of the outermost FRP bars.

The strains within the section can be determined based on the linear strain distribution using the following relationships (see Figure 6-1):

- Strain at the compressed edge of concrete: $\varepsilon_c = \varepsilon_{ftd} \cdot \dfrac{x}{(d-x)} \le \varepsilon_{cu}$ (6.3)
- Strain in the FRP bars: $\varepsilon_f = \varepsilon_{ftd}$ (6.4)

where *x* represents the distance from the neutral axis to the top (compressed) fiber.

The ultimate strain in the FRP bars, ε_{ftd}, is defined by Eq. (6.2) if the section under verification is located at a distance from the bar end greater than or equal to the anchorage length defined by Eqs. (5.3) and calculated assuming $\sigma_{fd} = f_{ftd} = \varepsilon_{ftd} \cdot E_f$ or if 90° bent bars are provided for proper anchorage (see Figure 5-4). Otherwise (distance of the section under verification from the bar end smaller than its anchorage length provided by (5.3)), the ultimate strain for the bar can be computed as

$\varepsilon_{ftd} = \frac{\sigma_{fd}}{E_f} < f_{ftd}$, where σ_{fd} is given by Eqs. (5.5) as a function of the distance ℓ_b between the section under verification and the FRP bar end, and of the bond quality class of the FRP bars.

(6) In failure region 2, failure occurs due to crushing of the concrete, while the strain in the FRP reinforcement remains below its ultimate value. In this case, given the ultimate compressive strain in concrete, ε_{cu}, the section strains can be computed assuming linear strain distribution as follows (see Figure 6-1):

- Strain at the compressed edge of concrete: $\varepsilon_c = \varepsilon_{cu}$ (6.5)
- Strain in FRP bars: $\varepsilon_f = \varepsilon_{cu} \cdot \frac{d - x}{x} \leq \varepsilon_{ftd}$ (6.6)

The evaluation of ε_{ftd} follows the same considerations described in point (5).

(7) In case of pure bending, for both failure types of failures (region 1 and 2), the distance x of the neutral axis from the compressed edge is determined from the equilibrium of longitudinal forces:

$$\psi \cdot b \cdot x \cdot f_{cd} - A_f \cdot E_f \cdot \varepsilon_f = 0 \tag{6.7}$$

When an axial force is applied to the section, the first term of Eq. (6.7) is not equal to 0, but has to be equal to the the design value of the applied axial force, N_{Ed}, and the failure regions may be also different from the two ones plotted in Figure 6-1 for pure bending. In case of combined bending and axial load, an N_{Rd}-M_{Rd} interaction diagram could be constructed by means of Eq. (6.7) and (6.9) introduced in the following. In Eq. (6.7), f_{cd} is the design compressive strength of the concrete evaluated according to the current Standards, ψ is a dimensionless coefficient equal to 0.8095 for failure region 2, and for failure region 1 is expressed by the following Eq. (6.8) where, for sake of simplicity, it is assumed $\overline{\varepsilon_c} = 1000\varepsilon_c$:

$$\psi = \begin{cases} \overline{\varepsilon_c}\left(0.5 - \frac{\overline{\varepsilon_c}}{12}\right) & \text{per } \overline{\varepsilon_c} \leq 2.0 \\ 1 - \frac{2}{3\overline{\varepsilon_c}} & \text{per } 2.0 \leq \overline{\varepsilon_c} \leq 3.5 \end{cases} \tag{6.8}$$

In failure region 1, Eq. (6.7) must be solved iteratively since ψ it is a function of the concrete compressive strain $\varepsilon_c < \varepsilon_{cu}$. It should be noted that, for failure region 2, the fixed values $\psi = 0.8095$ and $\lambda = 0.4160$ correspond to the condition of reaching the ultimate compressive strain in concrete ($\varepsilon_c = \varepsilon_{cu}$) and are consistent with the simplified constant stress distribution (*stress block*).

The design bending moment, M_{Rd}, can finally be obtained from the equilibrium of moments respect to the centroid of the concrete section:

$$M_{Rd} = \psi \cdot b \cdot x \cdot f_{cd} \cdot (0.5h - \lambda \cdot x) + A_f \cdot E_f \cdot \varepsilon_f \cdot (0.5h - c) \tag{6.9}$$

In (6.9), λ is a dimensionless coefficient equal to 0.4160 for failure region 2 and, for failure region 1, being $\overline{\varepsilon_c} = 1000\varepsilon_c$:

$$\lambda = \begin{cases} \dfrac{8-\overline{\varepsilon_c}}{4\left(6-\overline{\varepsilon_c}\right)} & \text{per } \overline{\varepsilon_c} \le 2.0 \\ \dfrac{\varepsilon_c\left(3\overline{\varepsilon_c}-4\right)+2}{2\overline{\varepsilon_c}\left(3\overline{\varepsilon_c}-2\right)} & \text{per } 2.0 \le \overline{\varepsilon_c} \le 3.5 \end{cases} \tag{6.10}$$

6.2 PRINCIPLES OF FLEXURAL DESIGN UNDER FIRE CONDITIONS

(1) In fire design verifications of RC structures with FRP bars, for a given exposure time and under specific environmental conditions, the thermal analysis provides the temperature field within the cross-section of the structural element. Consequently, a temperature-dependent stress–strain relationship $\sigma(\varepsilon, T_i)$, must be considered for each material of the cross-section. The mechanical properties required for fire verification (elastic modulus, ultimate strength, and ultimate strain) of FRP bars at elevated temperatures shall be provided by the Manufacturer and evaluated in accordance with standardized national or international testing procedures. In the absence of a standardized procedure, these properties may be determined using the same setup as for tensile tests at room temperature, employing a climatic chamber capable of uniformly heating the specimen in the central region where the strain field is measured (using well-established photogrammetric techniques for strain evaluation) and where specimen failure occurs.

(2) For RC structures with FRP bars, it should be noted that:

- a higher fire resistance can be achieved by increasing the thickness of the cover. The temperature reached in the bars largely depends on the concrete cover, whereas the overall fire resistance depends on the fibers' high-temperature strength and, therefore, on the fiber type;
- the type of aggregate used in concrete affects fire performance, both because of differences in thermal conductivity and varying susceptibility to spalling. For thermal conductivity, reference may be made to the conductivity curves provided in the current standards or in validated references (EN 1992-1-2) for RC elements with steel reinforcement. The effect of spalling is generally neglected in safety verifications;
- due to resin softening, the bar loses its bond with concrete when the FRP bar temperature exceeds its glass transition temperature (T_g)**.** Therefore, the first possible flexural failure mechanism is the loss of tensile load-carrying capacity of the bar due to bond failure. This highly unfavorable mechanism can be avoided if the bar ends is able to maintain an adequate bond strength. Under such conditions, the flexural failure mode to be verified corresponds to the reduction in the tensile strength of the FRP bars as the temperature increases;
- to ensure adequate anchorage of the bars, a “cold zone” shall be provided at the end of the structural element, having a length at least equal to the anchorage length of the bar calculated at room temperature according to Eqs. (5.2). The evaluation of temperatures in the anchorage zones may consider the use of specific passive fire protection systems (e.g., boards or coatings), applied only over the length required to guarantee the cold zone. Alternatively, thermal analyses and advanced bond-mechanics models may be employed to minimize or eliminate the need for additional protective systems;
- the use of spliced bars in the fire-exposed zone may lead to premature failure of the RC element, as bond degradation in the exposed region may occur before the FRP bars' tensile strength reduces. To prevent premature failure, continuous reinforcement should be used in regions of the concrete element that may be exposed to fire.

(3) Considering the parameters that play a key role in the behavior of FRP-reinforced elements, Appendix F presents a simplified method for design and verification under fire conditions.

6.3 SHEAR RESISTANCE

(1) Shear verifications of RC elements with FRP bars are to be performed only with respect to the ultimate limit states (ULS); the cases of elements with and without transversal reinforcements specific for shear made by FRP stirrups are treated separately.

6.3.1 Elements without transverse shear reinforcement

(1) The construction of slabs, plates, or other members with analogous structural behavior without stirrups is permitted, provided that they are able to exhibit an adequate capacity for transverse load redistribution.

(2) At the ultimate limit state (ULS), the design shear resistance of an element longitudinally reinforced with FRP bars and without transverse reinforcement may be evaluated using empirical expressions, which account for the various shear-resisting mechanisms mobilized in concrete beams. Two formulations are proposed: one based on the equation provided by the current national Code for concrete elements reinforced with steel bars (Approach 1), the second based on the equation provided by the recent Eurocode 2 (EN 1992-1-1:2023).

Approach 1: the shear resistance of concrete elements provided of longitudinal FRP bars and without shear reinforcement is given by:

$$\mathrm{V_{Rd,ct}} = \frac{k_s}{\gamma_V} \cdot k \cdot \left(100\rho_l \cdot \frac{\mathrm{E_f}}{210} \cdot f_{ck} \right)^{1/3} \cdot b_w \cdot d \geq \mathrm{V_{Rd,ct,min}} \tag{6.11a}$$

where $\mathrm{V_{Rd,ct,min}}$ is the minimum value of the shear resistance provided by strength mechanisms associated to concrete and equal to:

$$\mathrm{V_{Rd,ct,min}} = 0.035 \cdot k^{3/2} \cdot \sqrt{f_{ck}} \cdot b_w \cdot d \tag{6.11b}$$

Eq. (6.11a), as the following Eq. (6.11c), is based on an alternative formulation to Eq. (4.1) since the partial factor γ_V, assumed equal to 1.5, is applied to whole resistance $\mathrm{V_{Rd,ct}}$ and not to the material strength; for this reason in Eq. (6.11a) and (6.11c) the characteristic value, and not the design value, of compressive strength f_{ck} is used. Moreover, in the above expressions, the symbols have the following meanings:

- k_s is an experimentally calibrated coefficient, equal to 0.20 for longitudinal reinforcement consisting of either glass or carbon FRP bars;
- b_w and d are the width and the effective depth of the concrete section, respectively; for non-rectangular sections, b_w is the minimum width of the concrete section;
- $\rho_l = \mathrm{A_f}/(b \cdot d) \leq 0.02$ is the longitudinal tensile reinforcement ratio, where $\mathrm{A_f}$ is the total area of FRP bars properly anchored, meaning extending not less than $\ell_{ad} + d$ beyond the considered section, with ℓ_{ad} as the anchorage length defined in §5.3;
- f_{ck} is the characteristic value of the compressive strength of concrete;
- γ_c the partial factor for concrete, assessed based on the current Standards;
- $k = 1 + \sqrt{\frac{200}{d}} \leq 2$;

- E_f is the modulus of elasticity of the longitudinal FRP bars (in GPa).

Approach 2: the shear resistance of concrete elements provided of longitudinal FRP bars and without shear reinforcement is given by:

$$V_{Rd,ct} = \frac{k'_s}{\gamma_V} \cdot \left(100\rho_l \cdot \frac{E_f}{210} \cdot f_{ck} \cdot \frac{d_{dg}}{d} \right)^{1/3} \cdot b_w \cdot d \geq V_{Rd,ct,min} \qquad (6.11c)$$

where, in addition to the symbols already defined,

- $\gamma_V = 1.4$, is the partial factor for the shear resistance model in concrete elements without transversal reinforcement as used in (EN 1992-1-1:2023),

- k'_s is an experimentally calibrated coefficient, equal to 0.82 for longitudinal reinforcement consisting of either glass or carbon FRP bars,

- d_{dg} is a size parameter depending on the concrete type and its aggregate properties, which may be taken as:

  - d_{dg} = 16 mm + $D_{min} \leq$ 40 mm for $f_{ck} \leq$ 60 MPa;
  - d_{dg} = 16 mm + $D_{min} \left(\frac{60}{f_{ck}} \right)^2 \leq$ 40 mm for f_{ck} > 60 MPa;

where D_{min} is the smallest diameter of the largest sieve size, which can be substituted by the maximum aggregate diameter, D_{max}.

In Eq. (6.11c), $V_{Rd,ct,min}$ is given by Eq. (6.11b).

6.3.2 Elements with FRP transverse shear reinforcement

(1) With reference to concrete elements provided of transverse shear reinforcement fully made by FRP stirrups or made by both FRP and steel stirrups, the design indications herein provided are valid only for FRP and steel stirrups placed orthogonally to the element axis.

(2) At the Ultimate Limit State (ULS), the design shear resistance of a member reinforced with both longitudinal and transverse FRP bars can be evaluated using a truss model. The resisting elements of the ideal truss are: the FRP stirrups, the longitudinal FRP reinforcement, the concrete compression chord, and the concrete compression struts in the web, inclined at an angle θ. Such an assumption leads that the shear resistance of the element, V_{Rd}, can be expressed as:

$$V_{Rd} = \min(V_{Rd,f} + V_{Rd,ct}; V_{Rd,c}) \qquad (6.12)$$

where:

- $V_{Rd,c}$ is the resistance associated with the crushing of the concrete, (shear–compression failure of the truss),
- $V_{Rd,f}$ is the contribute to the shear–tension failure of the truss associated to the tensile failure of the FRP stirrups;
- $V_{Rd,ct}$ is the contribute to the shear–tension failure of the truss associated to the concrete shear-resisting mechanisms, which activates also in absence of transversal reinforcement.

(3) The contribution corresponding to the tensile failure of the FRP stirrups, to be introduced in Equation (6.12), is calculated as:

$$V_{Rd,f} = 0.9d \frac{A_{fw}}{s} f_{ubd} \cot\theta \tag{6.13}$$

In the absence of more specific information—and given the limited experimental data currently available, it is recommended to assume $\theta = 45°$ ($\cot\theta = 1$).

Moreover, in Equation (6.13), A_{fw} is the total cross-sectional area of the FRP stirrups where s is their spacing, f_{ubd} is the design tensile strength of the bent portion of the FRP stirrup, evaluated as:

$$f_{ubd} = \eta_a \cdot \eta_T \cdot \frac{f_{ubk}}{\gamma_f} \tag{6.14}$$

where η_T and η_a are the conversion factors accounting for temperature and environmental conditions (as defined in § 4.6), f_{ubk} is the characteristic tensile strength of the bent portion of the FRP stirrup, γ_f is the partial factor for FRP stirrups equal to 1.40, as specified in §4.5 for verifications at SLU under shear stresses, and having the same meaning of the partial factor γ_V previously introduced to calculate the contribute $V_{Rd,ct}$.

It has to be noted that, according to Table 3-1 of this Document, the strength f_{ubk} is a mandatory property for the FRP stirrups and shall be greater than 40 % of the characteristic tensile strength of the straight portion of the stirrup, $f_{ftk,st}$. Both values of strength, f_{ubk} and $f_{ftk,st}$, shall be available from the manufacturer's qualification tests in accordance with *EAD–FRP Bars* or *LG–FRP Bars*; in particular, the value $f_{ftk,st}$ determines the class of the bar used for realizing the stirrup on the basis of the limits listed in Table 3-3 (see point (4) of §3.3). If the manufacturing process for the bar used to realize the stirrup is the same of the straight bar with equal diameter, the class of the stirrup is the same of the straight bar, individuated by its tensile strength f_{ftk0}, and the strength of the stirrup f_{ubk} shall be higher than 40% of f_{ftk0}. In the design phase, lacking information on f_{ubk}, in Eq. (6.14) it will be possible to use the 40% of the characteristic value of tensile strength associated to the class of the bar chosen for realizing the stirrup.

For seismic design, the following limit also applies in the Eq. (6.14): $f_{ubd} \le 0.005 \cdot E_f$.

(4) The contribution of the concrete shear-resisting mechanisms, $V_{Rd,ct}$, to be used in Equation (6.12), is given by Equation (6.11a) or (6.11c).

(5) The design resistance associated with the crushing of the concrete web, $V_{Rd,c}$ is calculated as:

$$V_{Rd,c} = 0.9b \cdot d \cdot \alpha_c \cdot \nu \cdot f_{cd} \frac{\cot\theta}{(1+\cot\theta^2)} \tag{6.15}$$

The selection of θ follows the same assumptions as in item (3).

In Equation (6.15), $\nu = 0.5$ is a reduction coefficient, α_c is a coefficient accounting for the effect of axial compression in the section, function of the mean compressive stress acting in the element, $\sigma_{cp} = \frac{N_{Ed}}{A_c}$, being N_{Ed} the design applied axial force and A_c the cross-sectional area of the element, as follows:

$$\begin{aligned}
&\alpha_c = 1 && \text{for} \quad \sigma_{cp} = 0 \\
&\alpha_c = 1 + \frac{\sigma_{cp}}{f_{cd}} && \text{for} \quad 0 \le \sigma_{cp} \le 0.25\, f_{cd} \\
&\alpha_c = 1.25 && \text{for} \quad 0.25\, f_{cd} \le \sigma_{cp} \le 0.50\, f_{cd} \\
&\alpha_c = 2.5\left(1 - \frac{\sigma_{cp}}{f_{cd}}\right) && \text{for} \quad 0.50\, f_{cd} \le \sigma_{cp} \le f_{cd}
\end{aligned} \tag{6.16}$$

where f_{cd} is the design value of the compressive strength of concrete

(6) The longitudinal reinforcement shall be designed by shifting the bending moment diagram horizontally by:

$$a_1 = \frac{0.9d \cdot \cot\theta}{2} \tag{6.17}$$

where θ is set as indicated in item (3).

6.3.3 Shear design under fire conditions

(1) For verifications under fire conditions, the contribution of both longitudinal and transverse FRP reinforcement shall be neglected when the temperature distribution within the structural element indicates that the glass transition temperature T_g has been exceeded. Therefore, in this case the shear resistance shall be determined using Equation (6.11b) for elements both with and without shear reinforcement, neglecting the contribution due to the dowel effect of the longitudinal bars.

6.4 TORSIONAL RESISTANCE

(1) For the calculation of the torsional resistance of concrete elements reinforced with FRP longitudinal bars and FRP stirrups, and in the absence of specific provisions, the formulations provided by the applicable standards or by other validated references for concrete elements reinforced with steel bars and stirrups may be adopted, under the following assumptions:

- the areas of steel longitudinal bars and stirrups are replaced by the nominal areas of the FRP longitudinal bars and FRP stirrups;
- the yield strength of the steel longitudinal reinforcement is replaced by the design tensile strength of the FRP bars, f_{ftd};
- the yield strength of the steel stirrups is replaced by the design tensile strength of the bent portion of the FRP stirrups, f_{ubd}, which shall also satisfy $f_{ubd} \le 0.005 \cdot E_f$ in the design of elements for seismic actions.
- $\cot\theta = 1$;
- $\nu = 0.35$.

6.5 CONFINEMENT

(1) Experimental research has shown that the compressive strength of FRP bars is significantly lower than their tensile strength, primarily due to the occurrence of more pronounced instability phenomena compared to those observed in steel bars. This behavior is related to the lower elastic modulus of FRP materials. Therefore, although further research is still needed to confirm the available experimental data, the contribution of FRP bars under compression shall be neglected. However, it is necessary to prevent instability of FRP bars in compression, since it may influence the behavior of the whole

section, by providing a suitable confinement of the bars. The confinement of compressed FRP bars may be achieved by means of FRP stirrups, placed perpendicular to the element's axis and spaced according to the following requirement:

$$s \le \min\left(d_{\min}, 16d_{\mathrm{b}}, 48d_{\mathrm{bs}}\right) \tag{6.18}$$

where $d_{\min}$ is the minimum transverse dimension of the section, d_{b} is the nominal diameter of the longitudinal FRP bars, and d_{bs} is the nominal diameter of the FRP stirrups.

(2) In addition to preventing instability of the FRP bars in compression, adequate confinement with FRP stirrups of compressed concrete elements may also improve their overall performance, allowing for:

- an increase in the ultimate strength of elements subjected to axial or slightly eccentric axial load;
- an increase in the ultimate compressive strain of concrete in elements subjected to combined compression and bending in case of high eccentricity.

In particular, to estimate the effect of confinement, lacking specific formulations for FRP stirrups, validated expressions or those provided by the current Standards for elements confined with steel stirrups may be used. In such cases, the contribution of the FRP stirrups may be considered analogous to that of steel ones, replacing the steel yield strength with the design tensile strength f_{ubd} of the FRP stirrups, according to the following expression:

$$f_{\mathrm{ubd}} = \min\left(\eta_{\mathrm{T}} \cdot \eta_{\mathrm{a}} \frac{f_{\mathrm{ubk}}}{\gamma_{\mathrm{f}}}; 0.004 \cdot \mathrm{E_f}\right) \tag{6.19}$$

being γ_{f} the partial factor of the FRP stirrups equal to 1.40, as specified in §4.5, η_{T} and η_{a} the conversion factors taking into account the effect of temperature and environmental conditions depending of the exposure conditions of the structure, as defined in §4.7, f_{ubk} the characteristic value of the bent part of the FRP stirrup, and $\mathrm{E_f}$ the elastic modulus of the FRP stirrup. In Eq. (6.19), the first term is related to the linear-elastic behavior of FRP, which provides a confining pressure increasing with the axial load: as the axial strain of the concrete increases, the confinement pressure continues to rise with the concrete's lateral expansion until the tension failure of the FRP stirrups occurs. The second term takes into account that the stress level in the FRP stirrups should also be limited to maintain the integrity of the concrete.

6.6 RESISTANCE IN CASE OF HYBRID REINFORCEMENT

6.6.1 Ultimate moment resistance without and with axial force

(1) It is assumed that flexural failure, in case of pure bending moment or combined with axial force, occurs when one of the following conditions is reached:

- the ultimate compressive strain of the concrete, $\varepsilon_{\mathrm{cu}}$;
- the ultimate tensile strain of the FRP bars, $\varepsilon_{\mathrm{ftd}}$, as defined in Equation (6.2).

(2) The constitutive laws of the materials are assumed to be the same as those given in §6.1.1 for sections reinforced exclusively with FRP bars. For steel reinforcement, the constitutive law prescribed by the current Standards shall be applied.

(3) The design resistant moment of the section shall be evaluated in accordance with the assumptions stated in §6.1.1.

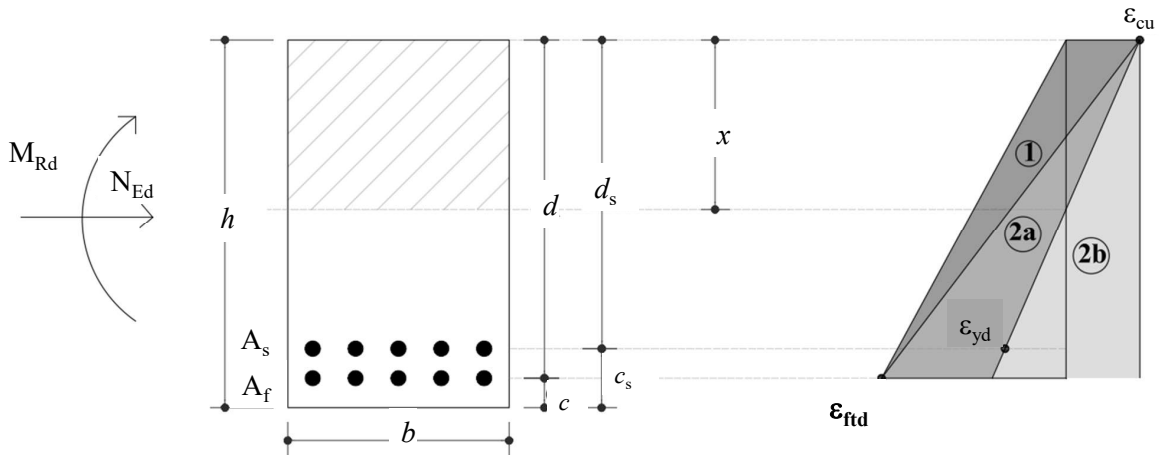

Figure 6-2 - Failure modes of a concrete section reinforced with hybrid steel–FRP reinforcement under pure bending moment or combined with axial force.

(4) For the rectangular section shown in Figure 6-2, A_f is the total area of the tensile FRP reinforcement; E_f is the modulus of elasticity of the FRP, A_s is the total area of the tensile steel reinforcement; x is the neutral axis depth, measured from the most compressed fiber, c and c_s are the distances of the centroids of the FRP and steel reinforcement from the tensioned edge of the section, respectively. Three possible failure regions can be distinguished depending on which strain limit is reached:

- Failure region 1: the ultimate strain in the FRP bars, ε_{ftd}, is reached and the steel bars in tension are yielded ($\varepsilon_s > \varepsilon_{yd}$);
- Failure region 2a: the ultimate compressive strain in the concrete, ε_{cu}, is reached and the steel bars in tension are yielded ($\varepsilon_s > \varepsilon_{yd}$);
- Failure region 2b: the ultimate compressive strain in the concrete, ε_{cu}, and the steel bars in tension are in the elastic range ($\varepsilon_s < \varepsilon_{yd}$).

(5) In failure region 1, failure occurs when the ultimate strain in the tensile FRP reinforcement is reached; the steel bars in tension are yielded, while the concrete does not reach its ultimate compressive strain: $\varepsilon_f = \varepsilon_{ftd}$, $\varepsilon_s \geq \varepsilon_{yd}$, $\varepsilon_c \leq \varepsilon_{cu}$.

The strains ε_c and ε_s can be calculated from the linear strain distribution as:

- maximum strain in concrete in compression: $$\varepsilon_c = \frac{x}{d-x}\varepsilon_{ftd} \quad (6.20)$$
- strain in steel bars in tension: $$\varepsilon_s = \frac{d_s - x}{d-x}\varepsilon_{ftd} \quad (6.21)$$

where d is the distance from the compressed edge to the centroid of the FRP reinforcement and d_s is the distance from the compressed edge to the centroid of the steel reinforcement.

In this failure mode, the stress in the steel bars equals the design yield strength, f_{yd}.

(6) In failure region 2a, failure always occurs by crushing of the concrete, while the tensile FRP bars do not reach their ultimate strain, and the steel bars in tension are yielded: $\varepsilon_c = \varepsilon_{cu}$, $\varepsilon_f < \varepsilon_{ftd}$, $\varepsilon_s \geq \varepsilon_{yd}$

The strains ε_f and ε_s can therefore be calculated as a function of the concrete ultimate strain, assuming linear strain distribution, as follows:

- strain in the FRP bars in tension: $\varepsilon_f = \frac{d-x}{x}\varepsilon_{cu}$ (6.22)
- strain in the steel bars in tension: $\varepsilon_s = \frac{d_s-x}{x}\varepsilon_{cu}$ (6.23)

In this failure domain, the stress in the steel bars in tension equals the design yield strength, f_{yd}.

(7) In failure region 2b, failure also occurs by crushing of the concrete, while the FRP bars in tension do not reach their ultimate strain and the steel bars in tension are in the elastic range:

$\varepsilon_c = \varepsilon_{cu}$, $\varepsilon_f < \varepsilon_{ftd}$, $\varepsilon_s < \varepsilon_{yd}$.

The strains ε_f and ε_s can therefore be calculated as a function of the concrete ultimate strain, assuming linear strain distribution along the section, through the following relationships:

- strain the FRP bars in tension: $\varepsilon_f = \frac{d-x}{x}\varepsilon_{cu}$ (6.24)
- strain in the steel bars in tension: $\varepsilon_s = \frac{d_s-x}{x}\varepsilon_{cu}$ (6.25)

In this domain, the stress in the steel bars in tension shall be evaluated by multiplying the strain from Eq. (6.25) by the elastic modulus of steel, E_s.

(6) In case of pure bending moment, for all failure regions, the position of the neutral axis, x, measured from the compressed edge of the section, is determined from the equilibrium of axial forces:

$$\psi \cdot b \cdot x \cdot f_{cd} - A_f \cdot E_f \cdot \varepsilon_f - A_s \cdot \sigma_s = 0 \quad (6.26)$$

In case of combined presence of axial force, the first term of Eq. (6.26) is not equal to 0, but to the design value of the axial force, N_{Ed}. The design moment resistance, M_{Rd}, is obtained from the equilibrium of moments with respect to the centroid of the concrete section:

$$M_{Rd} = \psi \cdot b \cdot x \cdot f_{cd} \cdot (0.5h - \lambda \cdot x) + A_f \cdot E_f \cdot \varepsilon_f \cdot (0.5h - c) + A_s \cdot \sigma_s \cdot (0.5h - c_s) \quad (6.27)$$

The coefficients ψ and λ shall be taken as defined in §6.1.2 for members reinforced with FRP reinforcement.

In Eqs (6.26) and (6.27), σ_s is the stress in the steel bars in tension and may be taken as $\sigma_s = f_{yd}$ in failure regions 1 and 2a, while in failure region 2b, since the steel remains elastic $\sigma_s = E_s \cdot \varepsilon_s$, where ε_s is computed from Eq. (6.25).

6.6.2 Shear resistance

(1) For structural elements provided with hybrid shear reinforcement, consisting of a double arrangement of stirrups (inner steel stirrups and outer GFRP stirrups), lacking experimental data and numerical analyses capable of accurately defining the load-carrying capacity of this configuration, on safety side, it is recommended to assume the contribution of the only steel or FRP stirrups. Thus, the shear resistance at the ultimate limit state may be determined in accordance with Eq. (6.12), considering in the calculation of $V_{Rd,f}$ the contribution of only one type of stirrups present in the section, while $V_{Rd,ct}$ is given by Eq. (6.11a) or Eq. (6.11c). The contribution of the concrete web, $V_{Rd,c}$, may be calculated using Equation (6.15).

6.7 BEHAVIOR OF STATICALLY INDETERMINATE STRUCTURES

(1) In the case of statically determinate (isostatic) structures, the distribution of internal forces is governed solely by the equilibrium equations.

(2) In the case of statically indeterminate (hyperstatic) structures, the internal stresses depend on the stiffness characteristics of the cross-sections, which are determined by their moment–curvature relationships. FRP bars exhibit an elastic–brittle behavior so, if we exclude the stiffness contribution of the concrete in tension, the moment–curvature diagram of a RC section with such reinforcement is monotonically increasing and remains approximately linear up to failure. As a consequence, structural members reinforced with FRP bars exhibit low ductility (limited to the concrete's nonlinear behavior), which prevents significant redistribution of stress resultants, and, thus:

- a linear elastic structural analysis may be carried out;
- limit analysis theorems cannot be applied to hyperstatic structures;
- The corollaries of the fundamental limit analysis theorems are not valid, meaning that:
  a. any distortions in the structure (for example, due to thermal variations) may influence its load-carrying capacity;
  b. the elastic properties of the structure affect its ultimate resistance;
  c. the load-carrying capacity of a hyperstatic structure may decrease when the resistance of some of its parts is increased.

6.8 CONSTRUCTION DETAILS

6.8.1 Concrete cover

(1) The relatively high values of transverse thermal expansion of FRP bars compared with concrete, together with the Poisson effect in the case of compressed reinforcement, may induce significant circumferential tensile stresses in the concrete around the bar, initiating radial cracking (Figure 6-3). These cracks can damage the bond at the concrete–FRP bar interface, with adverse effects on the structural behavior under both service and ultimate conditions, as well as on the structure's durability.

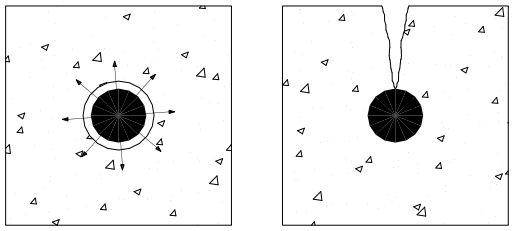

Figure 6-3 - Cracking induced by FRP transverse expansion and consequent normal stresses in the concrete surrounding the bar.

(2) To prevent the formation of radial cracks around the bars, it is recommended to adopt a sufficiently large geometric concrete cover c_{geom} (i.e., the distance from the outer face of the bar to the element surface), whose minimum value is given by the following relationship:

$$c_{\text{geom}} \geq c_{\text{min,b}} + \Delta c_{\text{dev}} \tag{6.28}$$

where Δc_{dev} is the additional cover allowance accounting for construction tolerance, defined in

accordance with Eurocode 2 (Table 6.7, EN 1992-1-1: 2023) and $c_{\mathrm{min,b}}$ is a minimum value related to the bond shear stresses transferred by the bar to the surrounding concrete that shall be: $1.5d_{\mathrm{b}} \le c_{\mathrm{min,b}} \le 50\mathrm{mm}$, being d_{b} the nominal diameter of the FRP bar.

When FRP stirrups are presents, c_{geom} is the distance of the outer face of the stirrup to the element surface and shall be calculated according to Eq. (6.28), but adopting the following indication: $\min(1.5d_{\mathrm{b}};10\mathrm{mm}) \le c_{\mathrm{min,b}} \le 38\mathrm{mm}$.

It has to be noted that in concrete elements reinforced with FRP bars, in Eq. (6.28) there is no term related to the durability, that on the contrary for steel bars is present and depends on the exposure environmental conditions and on the design service life of the structure.

6.8.2 Requirements for longitudinal reinforcements

(1) The minimum nominal diameter that may be used for FRP bars as longitudinal reinforcement is d_b = 8 mm.

(2) The area of the longitudinal tensile FRP reinforcement, $\mathrm{A_f}$, shall not be less than a minimum value, $\mathrm{A_{f,min}}$, capable of ensuring that:

$$\mathrm{M_{Rd}} \ge 1.5 \cdot \mathrm{M_{cr}} \tag{6.29}$$

where $\mathrm{M_{cr}}$ represents the cracking moment, to be determined in accordance with the applicable standards. Eq. (6.29) can be equivalently rewritten as:

$$\mathrm{A_{f,min}} = 0.34 \cdot \frac{b \cdot d \cdot f_{\mathrm{ctm}}}{f_{\mathrm{ftd}}} \tag{6.30}$$

(3) The recommended minimum compression reinforcement, $\mathrm{A_{fc}}$, shall be not lower than the following value:

$$\mathrm{A_{fc,min}} = 0.001 \cdot \mathrm{A_c} \tag{6.31}$$

(4) For members without shear reinforcement, the area of tensile longitudinal FRP reinforcement, A_{f}, shall be provided such that the corresponding percentage ρ_{l} is not lower than the following minimum value:

$$\rho_{\mathrm{l,min}} = \frac{\mathrm{A_{f,min}}}{b \cdot d} = 0.01 \tag{6.32}$$

(5) The lap splicing of tensile FRP bars shall be carried out only in regions where the stress in the bars is less than 80% of the design tensile strength evaluated at the Ultimate Limit State, f_{ftd}. The minimum lap splice length, ℓ_{s}, shall be taken as:

$$\ell_{\mathrm{s}} = 1.25 \cdot \ell_{\mathrm{ad}} \tag{6.33}$$

where ℓ_{ad} is given by Equation (5.3).

6.8.2.1 Specific requirements for columns

(1) The area of the longitudinal reinforcement $\mathrm{A_f}$ in columns subjected to combined compression and bending shall be not lower than the following minimum value:

$$A_{f,min} = \max\left(0.1 \cdot \frac{N_{Ed}}{f_{ftd}}; 0.01 \cdot A_c\right) \tag{6.34}$$

where N_{Ed} is the design axial load, f_{ftd} is the design tensile strength of the FRP reinforcement, and A_c is the area of the concrete section.

(2) The maximum value of the total longitudinal reinforcement for columns, A_f, shall be:

$$A_{f,max} = 0.04 \cdot A_c \tag{6.35}$$

In case of lap slicing of the bars, the value ofc $A_{f,max}$ shall be double the one provided by Eq. (6.35).

(3) The longitudinal reinforcement in columns shall also comply with the following additional requirements:

- at least one bar in each corner for polygonal sections and a minimum of six bars for circular sections;
- the reinforcement shall be symmetrically arranged;
- in polygonal sections, all bars shall be restrained by stirrups or ties and placed at a maximum spacing of 150 mm.

6.8.2.2 Specific requirements for slabs

(1) For concrete slabs reinforced with FRP bars, the total area of the longitudinal reinforcement in tension, A_f, shall be, in both directions, non lower than the following minimum value is:

$$A_{f,min} = 0.0025 \cdot A_c \tag{6.36}$$

(2) When the analysis of slabs is performed using beam-type models—that is, without adopting a two-dimensional plate model—only the reinforcement in the primary bending direction may be determined from the analysis. In addition to this reinforcement, a secondary (distribution) reinforcement shall be provided, placed orthogonally to the primary one. The specific area of secondary reinforcement (per unit length) shall not be less than 20% of the primary reinforcement area, also referred to per unit width.

6.8.3 Requirements for transverse reinforcement

(1) For beams and columns, the minimum diameter of stirrups, d_{bs}, shall be the greater of 6 mm and of one quarter of the nominal diameter d_b of the longitudinal bars.

6.8.3.1 Specific requirements for beams

(1) For beams with transversal reinforcement, the minimum value of the percentage of transverse reinforcement, ρ_s, shall be:

$$\rho_{s,min} = \frac{0.08\sqrt{f_{ck}}}{\varepsilon_{ftd} \cdot E_f} \tag{6.37}$$

In addition, at least three stirrups per meter shall be provided, and the stirrup spacing, s, shall satisfy the following limitation:

$$s \le 0.75d \tag{6.38}$$

where d is the effective depth of the section.

(2) In support regions and in the presence of concentrated loads, over a length equal to the effective depth d of the section, the stirrup spacing shall satisfy the following condition:

$$s \le \min\left(\frac{d}{4}; 12\ \min(d_b); 150\ \text{mm}\right) \tag{6.39}$$

where $\min(d_b)$ is the minimum diameter of the longitudinal bars present in the element.

6.8.3.2 Specific requirements for columns

(1) In columns, the stirrup spacing, s, shall satisfy the following limitation:

$$s \le \min\left(15 \cdot \min(d_b); 250\ \text{mm}\right) \tag{6.40}$$

where $\min(d_b)$ is the minimum diameter of the longitudinal bars present in the element.

(2) The stirrup spacing shall be appropriately reduced at the end regions of columns, over a length not less than the greater of:

- the larger side of the concrete cross-section;
- one-sixth of the clear height of the column (one-third for isostatic columns);
- 450 mm.

Within these regions, the stirrup spacing shall satisfy the following condition:

$$s \le \min\left(\frac{l_{min}}{4}; 100\ \text{mm}\right) \tag{6.41}$$

where l_{min} is the smaller side of the cross-section.

6.8.4 Additional construction details

(1) For bent bars and stirrups, in order to prevent damage to the FRP fibers, the minimum bending diameter to be used for bending operations in the manufacturing facility, shall be at least seven times the nominal diameter of the bar, d_b (Table 3-1). The Manufacturer shall specify the mandrel diameter used for bending (see Appendix A).

(2) The design stress in bent FRP bars and in FRP stirrups shall be less than $25f_{cd}$, where f_{cd} is the design value of the compressive strength of the concrete, in order to prevent concrete damage in the vicinity of the bend.

(3) The minimum anchorage lengths for FRP bars are given in § 5.4.

Essential References

1. EN 1992-1-1:2023 (2023) *Eurocode 2: Design of concrete structures - Part 1-1: General rules and rules for buildings, bridges and civil engineering structures*, European Committee for Standardization (CEN), Brussels, Belgium.

7 SERVICEABILITY LIMIT STATES (SLS)

7.1 BASIC ASSUMPTIONS

(1) Structural elements shall also be verified with respect to the Serviceability Limit States (SLS), the most relevant of which concern:

- limitation of stresses in the materials (concrete in compression and FRP reinforcement in tension);
- control of deformations (limitation of deflections);
- control of cracking (limitation of crack widths).

Because of the low elastic modulus of FRP reinforcement—particularly in the case of glass FRP (GFRP)—these serviceability verifications may become governing criteria for the design of members reinforced with FRP bars.

Other serviceability limit states may be relevant in specific situations, even though they are not explicitly listed in these Guidelines.

(2) The combinations of actions to be considered for serviceability verifications shall be those defined by the applicable Standards.

In particular, the following load combinations are identified for SLS verifications:

- Rare (or characteristic) combination – generally used for irreversible SLS; it corresponds to a load having a 5% probability of being exceeded during the design service life of the structure.
- Frequent combination – generally used for reversible SLS; it corresponds to a load that is exceeded for 10% of the design service life.
- Quasi-permanent combination – generally used for long-term effects; it corresponds to a load that is exceeded for 50% of the design service life.

(3) Under the various service load combinations, the following conditions shall be verified:

- Material stress limitations: stress levels in the materials shall be limited to avoid nonlinear behavior of both the FRP bars and the concrete, for both the characteristic and quasi-permanent combinations of actions. In particular, under quasi-permanent loads, stresses due to sustained actions shall be limited to mitigate creep in the concrete and static fatigue in the FRP bars, which could reduce the long-term strength of the reinforcement.
- Deformation control: the structural deformations, and particularly the deflections of members under flexure, shall not reach excessive values that could impair the normal use of the structure, cause damage to non-structural elements, or produce psychological discomfort for occupants. The limiting values of deflection-to-span ratios depend on the structural type and intended use of the structure and may refer either to the total deflection or to that due to the variable component of the load. Because of the relatively low modulus of elasticity of FRP bars—especially those made of glass fibers—the deformation check may govern the minimum amount of FRP reinforcement required to satisfy all serviceability conditions.
- Crack control: cracking shall be adequately limited, since excessive width or closely spaced cracks could significantly reduce the durability, functionality, or appearance of the structure, and could also impair the bond integrity at the FRP–concrete interface. Nevertheless, as FRP reinforcement is less susceptible to corrosion than steel reinforcement, the allowable crack widths may be less stringent than for conventional RC.

(4) Serviceability verifications may be performed under linear elastic conditions, considering either the uncracked or cracked section, depending on whether the tensile stress in the concrete under the adopted load combination is below or above its tensile strength.

The assumptions underlying the analysis are:

- sections remain plain, resulting in a linear strain distribution in compressed concrete and in the tensile FRP bars;
- linear-elastic compressive behavior of the concrete;
- limited tensile capacity of concrete, possibly accounting for tension-stiffening effects between cracked sections;
- linear-elastic behavior of FRP bars in tension;
- negligible contribution of FRP bars in compression.

These assumptions make it possible to define a modular ratio, $\alpha_f = \frac{E_f}{E_c}$, representing the ratio between the elastic moduli of the FRP and the concrete. In service conditions, this coefficient allows the use of the transformed-section method for linear-elastic materials, introducing the equivalent FRP reinforcement area, appropriately homogenized through α_f, in the calculation of the moment of inertia and the neutral axis. In all cases, the contribution of FRP reinforcement in compression is neglected, but it is permissible not to deduct the corresponding concrete area.

(5) For long-term load effects (i.e., under the quasi-permanent loading combinations), the value of the modular ratio, α_f, shall take into account the time-dependent deformations of concrete. When calculating stresses and deflections, it is necessary, where relevant, to consider not only the effects of loads but also those of temperature variations, creep, shrinkage, and any other imposed deformations.

(6) For serviceability verification, it must be considered that the structural member may include portions where the tensile stress in concrete is below its tensile strength (uncracked zones) and portions where the tensile strength is exceeded, leading to the formation of transverse cracks at a specific spacing. In the presence of cracked regions, appropriate tension-stiffening models may be adopted (see § 7.3 and §7.4).

7.2 STRESS LIMITATIONS

(1) For the rare (characteristic) load combination, the stress in the FRP bars shall satisfy the following limitation:

$$\sigma_f \le \eta_T \cdot \eta_a \cdot 0.8 \cdot \frac{f_{ftk0}}{\gamma_f} \tag{7.1}$$

where f_{ftk0} is the characteristic tensile strength of the FRP bars, η_T and η_a are the conversion factors defined in § 4.6 and in Table 4-1), γ_f is the partial factor for the FRP material, which, for serviceability limit-state verifications, shall be taken as 1.0.

The compressive stresses in the concrete shall be limited in accordance with the applicable standards.

(2) Under the quasi-permanent load combination, the stress in the FRP bars shall satisfy the following condition:

$$\sigma_f \le \eta_T \cdot \eta_a \cdot \frac{f_{ftk,c}}{\gamma_f} \tag{7.2}$$

where the symbols have the same meaning introduced in point (1) and $f_{ftk,c}$ is the characteristic static fatigue strength (*creep rupture*) of the FRP bars at 100 years. If $f_{ftk,c}$ is not available, Eq. (7.2) becomes, since $f_{ftk,c} = \eta_c \cdot f_{ftk0}$:

$$\sigma_f \le \eta_T \cdot \eta_a \cdot \eta_c \cdot \frac{f_{ftk0}}{\gamma_f} \tag{7.2b}$$

being η_c the conversion factor for static fatigue (*creep rupture*) at 100 years defined in § 4.6 and in Table 4-2.

The compressive stresses in the concrete shall be limited in accordance with the applicable Standards.

(3) In the case of members subjected to simple bending, being M the bending moment due to the applied loads corresponding to the SLS verification combination, the stresses in the materials may be calculated for the cracked section as follows:

- Compressive stress in the concrete:

$$\sigma_c = \frac{M}{I_2} x_2 \tag{7.3}$$

- Tensile stress in the FRP reinforcement:

$$\sigma_f = \frac{\alpha_f \cdot M}{I_2} \left(d - x_2\right) \tag{7.4}$$

where I_2 is the moment of inertia of the cracked RC section, neglecting the contribution of compressed FRP bars and transforming the FRP bars in tension using the modular ratio α_f; x_2 is the distance from the compressed edge to the neutral axis of the cracked section and d is the effective depth of the section. In the calculation of the modular ratio $\alpha_f = \frac{E_f}{E_c}$, the elastic modulus of concrete, E_c shall be evaluated based on the load combination used for the serviceability verification. It may be taken as an effective modulus to account for the development of time-dependent deformations, according to $E_{c,eff} = \frac{E_c}{1+\varphi(t,t_0)}$, where $\varphi(t,t_0)$ is the creep coefficient of concrete, to be determined in accordance with the applicable standards or other reliable sources.
This approach neglects potential linear creep effects in FRP bars, which are generally much smaller than those in concrete. In the absence of specific information on conditions producing significant creep effects, a simplified value $\varphi(t,t_0) = 1$ may be assumed for the calculation of I_2 and x_2 and the corresponding stresses.

7.3 DEFLECTIONS

(1) The deformations exhibited by structures reinforced with FRP bars shall comply with the limitations established by the applicable standards for RC structures with steel bars of comparable type and use.

(2) The analytical model adopted shall realistically simulate the actual behavior of the structure, with a level of accuracy consistent with the design objectives. The increased deformability due to possible cracking of the concrete in tension—caused by the exceedance of its tensile strength—shall be duly considered. In particular, the mechanical model shall account for:

- the different behavior of sections in uncracked and cracked stages;
- the stiffening effect of the tensile concrete between cracks (tension-stiffening effect) in the regions where cracking occurs; if this contribution is neglected, the calculated deflection will be greater, and the resulting assessment will therefore be safe;
- the influence of imposed deformations, such as thermal effects;
- the variation of the modulus of elasticity of concrete depending on its degree of curing at the time of loading;
- the effects of creep and shrinkage in the concrete;
- the type of loading, whether static or cyclic.

(3) The deflection of FRP-RC flexural members may be calculated by integrating the curvature diagram. Curvatures may be obtained from a nonlinear analysis that accounts for cracking and for the tension-stiffening effect of the tensile concrete. In the case of nonlinear deflection analysis, the principle of superposition of effects does not apply.

(4) Alternatively to point (3), for beams in flexure, simplified analytical procedures similar to those used for conventional RC beams with steel bars may be adopted. Interpretation of experimental results confirms the validity—also for FRP-reinforced beams—of the simplified tension-stiffening model, in which the deflection is expressed as a combination of the deflection in the uncracked stage (stage 1) and that in the fully cracked stage (stage 2):

$$f = f_1 \cdot (1-\gamma) + f_2 \cdot \gamma$$
$$\gamma = 1 - \beta_1 \cdot \beta_2 \left(\frac{M_{cr}}{M_{max}} \right)^m \tag{7.5}$$

where:

- f is the total deflection of the structural element;
- f_1 is the deflection calculated for the uncracked beam, corresponding to the moment of inertia I_1 of the uncracked section, with the FRP tensile reinforcement transformed by the modular ratio α_f;
- f_2 is the deflection calculated for the fully cracked beam, corresponding to the moment of inertia I_2 of the cracked section, already defined in § 7.2;
- γ is the tension-stiffening coefficient, where:
  - M_{max} is the bending moment at the most stressed section of the element, evaluated under the characteristic load combination (representing the maximum moment acting during the structure's design service life);
  - M_{cr} is the cracking moment corresponding to the same section subjected to M_{max};
  - *m* is a coefficient, to be taken as 2 in the absence of more specific information;
  - β_1 is a dimensionless coefficient accounting for the bond quality of the bars, to be taken as 0.85 for Bond class 1 and 0.70 for Bond class 2, with bond classes defined in § 5.3; for exposure condition 3, the coefficient β_1 shall be multiplied by the environmental conversion coefficient η_a (Table 4-1);
  - β_2 is a dimensionless coefficient accounting for the duration of loading, equal to 1.0 for short-term loads and 0.5 for long-term or cyclic loads. In the case of long-term loads, creep effects in concrete shall be considered through the previously defined effective modulus,

$$E_{c,eff} = \frac{E_c}{1+\varphi(t,t_0)}.$$

(5) The coefficients m and β_1 depend on the bond characteristics between the FRP bars and the concrete. To achieve a more accurate evaluation of the deflection behavior of beams, which may govern the minimum required amount of FRP reinforcement to satisfy the serviceability criteria, one may refer to the procedure described in Appendix D, which guides the specific calibration of these coefficients.

7.4 CRACKING

(1) Although FRP bars possess significantly greater durability than conventional steel reinforcement, it is nevertheless advisable to impose limitations on crack width under service conditions, to protect the bars themselves, to enhance the durability of the concrete, and for aesthetic reasons.

(2) For the verification of crack width in concrete members reinforced with FRP bars, the characteristic crack width, w_k, shall not exceed the limiting values, w_{max}, reported in Table 7-1.

Table 7-1 - Limiting values of crack width for FRP-reinforced elements under different exposure conditions and load combinations

Exposure Condition	**Exposure Class**	**SLS Load Combination**	w_{max} **[mm]**
1-2 (dry internal or external environment)	X0, XC1 (dry), XS1	Frequent	0.7
		Quasi-permanent	0.6
3 (permanently or cyclically wet environment, or buried in natural soil or groundwater)	XC1 (humid), XC2, XC3, XC4, XD1, XD2, XD3, XS2, XS3, XF3, XF4, XF1, XF2 XA1, XA2, XA3	Frequent	0.5
		Quasi-permanent	0.4

(3) For the calculation of crack width in FRP-RC members, the classical Model Code approach may be adopted. This method removes the assumption of equal strains in tension between the FRP reinforcement and the adjacent concrete at the same depth from the neutral axis, and instead computes:

- the maximum crack spacing, $s_{r,max}$;
- the difference between the mean strains developed in the FRP bars and in the tensile concrete between two adjacent cracks $(\varepsilon_{fm} - \varepsilon_{cm})$.

This approach simplifies computation of the tension-stiffening effect of tensile concrete around FRP bars, arising from bond stresses at the bar–concrete interface. Accordingly, by analogy with formulations for RC members reinforced with steel bars, the characteristic crack width of an FRP-RC element can be calculated as follows:

$$w_k = k_{1/r} \cdot s_{r,max} \cdot (\varepsilon_{fm} - \varepsilon_{cm}) \tag{7.6}$$

where:

- $k_{1/r} = \dfrac{h - x_2}{d - x_2}$ is a geometric factor accounting for the effect of beam curvature on crack width, where h is the section height, d is the effective height, and x_2 is the distance from the compressed edge to the neutral axis of the cracked section;
- $s_{r,max}$ is the maximum spacing between two consecutive cracks;
- ε_{fm} and ε_{cm} are the mean strains in the FRP reinforcement and in the tensile concrete between two adjacent cracks, respectively.

In Equation (7.6), the maximum crack spacing $s_{r,max,}$ can be calculated as:

$$s_{r,max} = \beta_w \cdot \left(k_c \cdot c_{geom} + k_{\phi/r} \cdot k_{fl} \cdot k_b \frac{f_{ctm} \cdot d_b}{\tau_{mf} \cdot \rho_{l,ef}} \right) \tag{7.7}$$

where:

- β_w is a coefficient relating the maximum to the mean crack spacing, which may be taken as 1.7 under stabilized cracking conditions;
- k_c is an empirical coefficient, taken as 1.5 (EN 1992-1-1:2023);
- c_{geom} is the concrete cover, defined as the greater of the clear distances from the FRP bars to the bottom or side surfaces of the section, measured to the bar surface (i.e., excluding bar diameter);
- $k_{\phi/r}$ is a coefficient depending on the bond stress distribution along the bars; under the simplifying assumption of constant bond stress between adjacent cracks; it may be taken as 0.25;
- k_{fl} is a coefficient accounting for stress distribution prior to cracking. For rectangular sections in bending: $k_{fl} = \dfrac{h - h_{c,ef}}{h}$**,** where $h_{c,ef}$ is the height of the effective tensile concrete area, defined below. For members in pure tension, k_{fl} =1.00;
- k_b is a coefficient accounting for the position of the FRP bars during casting, taken as 0.9 when bars are placed at the bottom (better bond → smaller crack spacing) and 1.2 when bars are placed at the top (poorer bond → larger crack spacing);
- f_{ctm} is the mean tensile strength of concrete;
- d_b is the nominal diameter of FRP bars. If multiple bar diameters are used, an equivalent diameter may be defined as:

$$d_{b,eq} = \frac{n_1 d_{b1}^2 + n_2 d_{b2}^2}{n_1 d_{b1} + n_2 d_{b2}} \tag{7.8}$$

where n_1 is the number of bars with diameter $d_{b1,}$ and n_2 is the number of bars with diameter d_{b2}.

- τ_{mf} is the mean bond stress between the FRP bars and the concrete, under serviceability loading conditions, equal to: $\tau_{mf} = k_{bond} f_{ctm}$, where, for stabilized cracking, k_{bond} = 1.50 for Bond class 1, and k_{bond} = 1.25 for Bond class 2. For exposure condition 3, the value of τ_{mf} shall be multiplied by the environmental conversion coefficient η_a (Table 4-1). Alternative values of k_{bond} may be derived from experimental data following the "design by testing" procedures described in Annex D of EN 1990.
- $\rho_{l,ef}$ is the effective reinforcement ratio defined as:

$$\rho_{l,ef} = \frac{A_f}{A_{c,ef}} \tag{7.9}$$

where $A_{c,ef}$ is the effective tensile concrete area (Figure 7-1). For rectangular or T-shaped sections with the web in tension:

$$A_{c,ef} = b \cdot h_{c,ef} \tag{7.10}$$

where b is the width of the beam or of the web in tension, and $h_{c,ef}$ is the effective height, calculated as follows:

- for a single layer of tensile bars (Figure 7.1a):

$$h_{c,ef} = \min\left\{c + 5d_b; 10d_b; 3.5c; h - x_2; h/2\right\} \tag{7.11}$$

- for n layers of tensile bars, spaced vertically by δ_c (Figure 7.1b):

$$h_{c,ef} = \min\left\{\min(c + 5d_b; 10d_b; 3.5c) + (n-1)\delta_c; h - x_2; h/2\right\} \tag{7.12}$$

where c is the distance from the centroid of the FRP bars to the tensioned face of the section (mechanical cover).

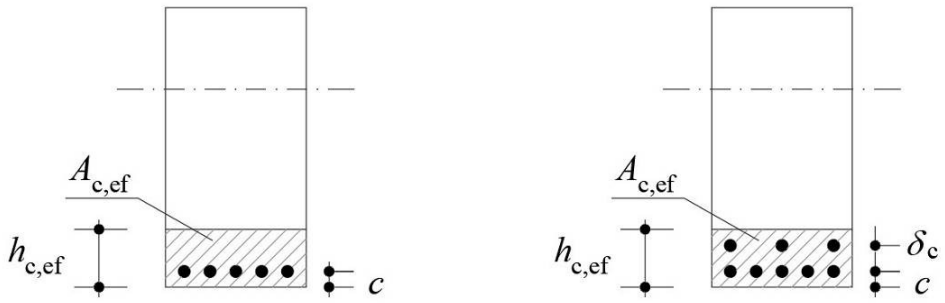

Figure 7.1: Definition of the effective tensile concrete area: (a) single layer of reinforcement; (b) multiple layers of reinforcement.

(4) In Equation (7.6), the difference between the mean strains in the FRP reinforcement and in the tensile concrete between two consecutive cracks may be calculated as:

$$\varepsilon_{fm} - \varepsilon_{cm} = \left(\frac{\sigma_f}{E_f} - k_t \frac{f_{ctm}}{E_f \cdot \rho_{l,ef}} + k_t \frac{f_{ctm}}{E_c}\right) \geq \frac{\sigma_f}{E_f}(1 - k_t) \tag{7.13}$$

where:

- σ_f is the stress in the FRP bars under the service load combination, calculated for the cracked section in accordance with § 7.2;
- E_c is the instantaneous modulus of elasticity of the concrete;
- k_t is a coefficient depending on the duration and nature of the applied load, equal to:
  - k_t = 0.6 for short-term or instantaneous loads;
  - k_t = 0.4 for long-term or repeated loads;
- $\rho_{l,ef}$ is the effective reinforcement ratio defined by Eq. (7.9).

(5) As an alternative to Eqs. (7.6), (7.7), and (7.13), refined models may be employed, provided they

are supported by adequate experimental evidence.

7.5 VERIFICATIONS SERVICEABILITY AT SLS FOR HYBRID REINFORCEMENT

(1) For stress verification of concrete members with hybrid reinforcement, the assumptions listed in points (4) and (5) of § 7.1 shall be applied. For concrete and steel reinforcement, the stress limitations established by the applicable Standards for conventional RC elements shall be adopted, while for FRP reinforcement, the limitations defined in Eqs. (7.1) and (7.2) shall be applied. In calculating the moment of inertia of the section and the corresponding neutral axis, the steel reinforcement—both in tension and in compression—may be taken into account using the modular ratio $\alpha_s = \frac{E_s}{E_c}$, where E_s is the modulus of elasticity of steel. The tensile FRP reinforcement shall be considered using the modular ratio α_f, as previously defined in § 7.2.

(2) For deflection verification of concrete members with hybrid reinforcement, and in the absence of specific validated provisions, it is acceptable—on the conservative side—to use Equation (7.5), adopting for the coefficient β_1 the value corresponding to the bond class of the FRP bars. In this way, the tension-stiffening behavior of the steel reinforcement is assumed to be analogous to that of the FRP bars for deflection calculation.

(3) For crack width verification of concrete members with hybrid reinforcement, in order to take into account the different bond stresses transferred by the two reinforcement typologies, lacking validated alternative indications, the calculation of the maximum crack width can be done using Equation (7.6), (7.7) and (7.13), where the effective tensile reinforcement ratio, $\rho_{l,ef}$, comprising both steel and FRP reinforcement, may be calculated as:

$$\rho_{l,ef} = \frac{A_f + \xi_1 A_s}{A_{c,ef}} \qquad \xi_1 = \frac{1.8}{k_{bond}} \cdot \frac{d_b}{d_{ba}} \tag{7.14}$$

where:

- d_b and d_{ba} are the nominal diameters of the FRP and steel bars, respectively;
- k_{bond} is the bond quality coefficient, defined previously as 1.50 for FRP bars of Bond class 1 and 1.25 for Bond class 2.

The value of crack width provided by Eq. (7.6) is always referred to the level of the reinforcement more proximal to the tensile edge of the section (i.e., the level of both reinforcements if they are placed at the same level, the level of the FRP bars if the steel bars are placed more internal in the section). Moreover, if the FRP and steel bars are placed at the same level ($d = d_s$, being d and d_s the distance of the FRP and the steel bars from the compressed edge of the section, see Figure 6-2), in Eq. (7.13), the term $\frac{\sigma_f}{E_f}$ can be calculated as the strain at the reinforcement level (being $d = d_s$) under the usual assumptions of cracked section and plane section conservation. Conversely, if the steel bars are placed at a distance from the tensile edge higher than that of the FPR bars (thus, $d > d_s$), the strain $\frac{\sigma_f}{E_f}$ in Eq. (7.13) and the distance d in Eq. (7.6) refer to the only FRP bars.

In case of FRP and steel bars having different diameters, Eq. (7.8) can be used for calculating the equivalent diameter in Eq. (7.7), where the concrete cover refers to the reinforcement closest to the tension edge of the concrete section.

If the FRP and steel bars are placed at the same level ($d = d_s$), the crack width calculated at the reinforcement level according to Eq. (7.6) shall be limited by the same values provided by the current Code for concrete elements reinforced with steel bars.
If the steel bars are placed at a distance from the tensile edge of the concrete section higher than the FRP bars, i.e., $d_s < d$, the crack width calculated at d, i.e. at the level of the FRP bars, according to Eq. (7.6) shall be compliant with the limits provided for elements reinforced with FRP bars listed in Table 7.1; moreover, the crack width calculated at the level d_s of the steel bars shall be compliant with the limits provided by the current Code for concrete elements reinforced with steel bars. Note that, for the latter case, the crack width at the level of steel bars can be calculated multiplying the crack width at the level of the FRP bars according to Eq. (7.6) by the coefficient $\frac{d_s - x_2}{d - x_2}$, being x_2 the distance of the neutral axis from the compressed edge of the cracked concrete section (State 2), d and d_s the distances previously defined.

Essential References

1. EN 1990:2023, *Eurocode 0: Basis of structural and geotechnical design*, European Committee for Standardization (CEN), Brussels, Belgium.
2. EN 1992-1-1:2023, *Eurocode 2: Design of concrete structures – Part 1-1: General rules and rules for buildings, bridges and civil engineering structures*, European Committee for Standardization (CEN), Brussels, Belgium.

8 DESIGN PROVISIONS IN SEISMIC AREAS

8.1 INTRODUCTION

(1) The lack of ductility and the limited energy dissipation capacity are inherent characteristics of FRP bars and shall be carefully considered in situations where seismic actions may be significant. Consequently, it is not possible to directly apply the seismic design criteria established for RC structures with steel reinforcement to structures reinforced with FRP bars. However, in many cases, it is still possible to design such structures without requiring ductility from the reinforcement, at least for some structural elements. Moreover, there are several potential applications of FRP-RC in which static design requirements are more demanding than seismic ones; in these cases, the design approach may follow the provisions described in Chapter 6 of these Guidelines. Additionally, in prefabricated construction, certain elements that do not belong to the primary seismic-resisting system may also be reinforced with FRP bars.

(2) In general, structural elements made of FRP-RC constituting the primary seismic-resisting system shall not be used in high-seismicity zones, defined as those where, at the Life-Safety Limit State, the anchoring acceleration of the design spectrum exceeds $S\,a_g > 0.375$g ([1]). This limitation stems from the current lack of sufficient experimental research on the behavior of FRP-RC structures subjected to seismic actions that may induce large displacements. In this context, potential applications of concrete structures with non-metallic reinforcement can be grouped into the following three categories:

a) Structures in which seismic actions cause only limited variations in internal forces compared with those evaluated under non-seismic load combinations, as well as structures not belonging to the seismic-resisting system.
b) Structures forming part of the seismic-resisting system and designed as non-dissipative systems, with a behavior factor $1 \le q \le 1.5$.
c) Structures forming part of the seismic-resisting system and designed to exhibit dissipative behavior in accordance with ductility-based design principles. In this case, it is necessary to adopt hybrid reinforcement, i.e., to use both steel and FRP bars.

These categories, which, as noted, may apply either to the entire structure or to individual structural elements, are described in detail in the following sections, together with the corresponding criteria for evaluation of actions, internal forces, verification procedures, and the specific design provisions to be applied in each case.

8.2 STRUCTURES FOR WHICH SEISMIC ACTION CAUSES LIMITED VARIATIONS IN INTERNAL FORCES COMPARED WITH NON-SEISMIC COMBINATIONS

(1) This category of structures is applicable in areas of low to medium seismicity, where, at the Life-Safety Limit State (LSLS), the anchoring acceleration of the spectrum satisfies the condition $S\,a_g < 0.375$g ([2]). This category includes:

a) Structures in which seismic action produces only small or negligible increases in internal

([1]) The value of the anchoring acceleration of the spectrum $S\,a_g = 0.375$g corresponds to the boundary between seismic zone 2 (medium seismicity) and zone 1 (high seismicity) as defined by OPCM 3274 and OPCM 3519, in terms of the peak ground acceleration with a 10% probability of exceedance in 50 years ($a_g = 0.25$g) referred to ground type A (rigid soil), and assuming a soil coefficient S=1.5, which includes both stratigraphic and topographic amplification effects.

([2]) Areas characterized by an anchoring acceleration of the spectrum $S\,a_g < 0.375$g correspond to zones of medium to very low seismicity, in accordance with the definitions provided in OPCM 3274 and OPCM 3519. See also Footnote 1.

forces compared with those evaluated under non-seismic load combinations;
b) Structural elements that do not participate in the lateral load-resisting system.

To qualify under this category, it shall be verified - either for the entire structure or for individual structural elements - that the Ultimate Limit State (ULS) verifications under non-seismic load combinations are more stringent than those under seismic load combinations (Life-Safety Limit State - LSLS), taking into account the higher partial safety factors for loads applied in the non-seismic case.

Examples of structures belonging to this category include:

- Roof structures supported by vertical load-bearing elements, such as prefabricated roof panels;
- Bridge decks (slabs);
- Pavements and secondary elements, such as curbs and embedded conduits.

(2) The non-relevance of seismic actions for the specific application shall be evaluated by general considerations, through simplified assessments of the element's behavior within the structural system, or by means of a more detailed analysis of the overall structural behavior and of the corresponding actions acting on the element of interest. A simplified and conservative evaluation of the seismic action may be performed using the elastic response spectrum (with q=1) and, with regard to the vibration period, by referring either to the plateau of the response spectrum or, for ground-supported structures, to the anchoring acceleration of the spectrum. For this category of structures, design verifications may be carried out in accordance with the criteria described in Chapter 6, without any additional requirements.

(3) If the primary structure is designed to resist seismic actions using steel reinforcement, the structural elements reinforced with FRP bars that do not form part of the lateral load-resisting system shall nevertheless be capable of accommodating the deformations imposed by the displacements of the main structure.

8.3 STRUCTURES DESIGNED AS NON-DISSIPATIVE

(1) This category of structures applies in areas of very low or low seismicity, where, at the Life-Safety Limit State (LSLS), the anchoring acceleration of the design response spectrum satisfies the condition S a_g < 0.225g ([3]).

(2) This category includes structures or structural elements in which, for the demand and capacity assessment, all members and connections remain within the elastic or substantially elastic range. The behavior factor may be selected within the range $1 \leq q \leq 1.5$, adopting values greater than 1 when a limited deviation from perfectly elastic behavior (e.g., due to concrete in compression or tension due to cracking) can be assumed to provide some hysteretic energy dissipation in the force–deformation response. Examples of structures belonging to this category include:

- Structures intended to remain substantially elastic even during an earthquake, in order to avoid damage, such as:
  - structures vulnerable to rocking;
  - precast infill elements;
- Structures equipped with supplemental energy dissipation or isolation systems;

([3]) Areas characterized by an anchoring acceleration of the spectrum S a_g < 0.225g correspond to zones of low to very low seismicity, in accordance with the definitions provided in OPCM 3274 and OPCM 3519, and consistent with the explanation given in Footnote 1.

- Shallow and deep foundation structures (see also § 8.5);
- Coastal protection structures and retaining walls.

For bridges, a non-dissipative design approach requires $q = 1$.

(3) Among the examples listed above, particular importance is given to structures designed to remain elastic even during an earthquake. This design choice is recommended when the residual deformations that may occur in dissipative structures after a seismic event could cause significant economic losses, up to and including the need to demolish and reconstruct the works. In such cases, the design criteria are similar to those for conventional non-dissipative RC structures, and, in general, no additional detailing is required beyond that used for structures not specifically designed for seismic actions. For beam–column joints, it shall be verified that the bars are anchored adequately within the joint region. In particular, the seismic actions shall be calculated with reference to the design spectrum reduced by the behavior factor q (if the evaluation of q, as described in point (2), yields a value greater than 1).

(4) For structural types that are particularly vulnerable to seismic action, it is recommended to assume $q = 1$. For instance:

- Concrete structures: torsionally flexible structures, inverted pendulum structures, and single-story inverted pendulum frame structures (the latter if irregular in height);
- Precast structures: monolithic cell-type structures, and structures with fixed-base columns and hinged floor diaphragms (the latter if irregular in height).

(5) For the verification of structural elements, the design moment resistance shall be calculated assuming substantially elastic section behavior (see Chapter 6).

8.4 STRUCTURES DESIGNED WITH DISSIPATIVE BEHAVIOR

(1) This category of structures can be adopted in areas of very low to medium seismicity, for which, at the Life-Safety Limit State (LSLS), the value of the spectral anchoring acceleration is $S\ a_g < 0.375g$([4]).

(2) This category includes structures for which, in the calculation of seismic actions and in the verification of structural elements, nonlinear and dissipative structural behavior is explicitly considered.

(3) Design in the dissipative range is recommended for building frame structures or bridges located in areas of medium seismicity, unless supplemental seismic reduction systems are installed, such as base isolation systems. For bridges designed with dissipative structural behavior, the bridge system shall be conceived and proportioned so that, under the seismic action corresponding to the LSLS, a stable dissipative mechanism develops in which energy dissipation is concentrated in the piers.

(4) Compliance with the rules for design in the dissipative range requires, at least in those portions of the structure where plastic hinges are expected to form, the use of metallic reinforcement.

(5) In the design of dissipative structures, the ductility class requirements CD “A” or CD “B” established by the applicable codes for conventional RC structures with steel reinforcement shall be satisfied — both in terms of detailing and verifications, including curvature ductility checks at the Collapse Limit State (CLS). The behavior factor q shall be determined in accordance with the applicable

([4]) Zones characterized by a value of the spectral anchoring acceleration S_{ag} < 0.375g correspond to areas of very low to medium seismicity, in accordance with the definitions provided in Ordinance OPCM 3274 and Ordinance OPCM 3519 (see also Footnote 1).

Standards, with reference to the selected ductility class (CD “A” or CD “B”).

(6) Among the design provisions for ductility classes CD “A” and CD “B” (depending on the chosen class), the most relevant are the capacity design criteria. For the correct application of these criteria — particularly the requirement that columns have greater resistance than beams — it is necessary to consider, in the evaluation of the beam moment resistance, the possible presence of FRP bars, which may increase the flexural capacity if they are anchored within the joints. Accordingly, the overstrength factors used in design shall be determined with reference to the actual FRP reinforcement provided, and the standard overstrength factors applicable to RC sections cannot be used.

(7) Various design strategies can be adopted for a dissipative structure with hybrid reinforcement. A common principle is to place the steel reinforcement in the inner layers—where it is better protected from aggressive agents—and the FRP reinforcement in the outer layers. Some examples of deisgn strategies are:

a) Approach No. 1 for design hybrid reinforcements

- Longitudinal reinforcement consists of inner steel bars and outer FRP bars.
- Transverse reinforcement consists of:
    - Inner steel stirrups in the critical regions, confining the concrete together with the longitudinal steel bars;
    - Outer FRP stirrups forming, together with the longitudinal FRP bars, the reinforcement cage along the entire non-critical portion of the element, responsible for providing shear resistance.

b) Approach No. 2 for design hybrid reinforcements

- Longitudinal reinforcement consists of both steel and FRP bars, where:
    - The steel reinforcement, placed mainly in the critical regions, ensures compliance with all requirements specified by the current codes for ductility classes CD “A” or CD “B”;
    - The FRP reinforcement supplements the steel reinforcement for static loading conditions (ULS checks) and in regions with reduced seismic demands. In these regions, the ultimate moment shall be calculated assuming substantially elastic behavior.
- Transverse reinforcement consists of:
    - Steel stirrups in the critical regions, to confine the concrete;
    - FRP stirrups, together with the longitudinal FRP bars and the outer reinforcement cage along the non-critical portions of the element, are responsible for providing shear resistance.

(8) If a design approach different from those described in point (7) is adopted — and if GFRP stirrups are used in the critical regions — it is essential to ensure that they remain within the elastic range. Furthermore, the axial stiffness equivalence (EA) of the GFRP stirrups shall be ensured with respect to that obtained using steel stirrups, in order to provide adequate concrete confinement, considering that the elastic modulus of GFRP is lower than that of steel.

8.5 FOUNDATIONS

(1) For RC structures with steel bars, the applicable Standards prescribe that foundation structures shall be designed based on the demand transmitted by the superstructure, assigning them a non-dissipative structural behavior, regardless of the behavior attributed to the supported structure. For this reason, foundations may be designed and constructed with FRP reinforcement, offering clear durability advantages.

(2) The actions transmitted to the foundations derive from the analysis of the overall structural behavior, which is generally conducted by examining only the superstructure. The loads acting on the foundations, transmitted by the superimposed elements, may be determined using one of the following approaches:

- Performing the structural analysis assuming non-dissipative behavior;
- From the flexural strength capacity of the elements, together with the shear determined by equilibrium considerations;
- From the actions transmitted by the superstructure under the assumption of dissipative behavior**,** amplified by a factor equal to 1.30 for ductility class CD “A” and 1.10 for CD “B”.

(3) When FRP reinforcement is used in foundation structures, since no ductility reserve can be relied upon, the first two approaches are recommended, as they ensure that the transmitted forces do not exceed the calculated values. Consequently, the design of foundation elements in terms of resistance shall always be based on the values of bending moment derived from one of the two first approaches.

(4) In the case of pile foundations located in seismic areas, the use of FRP reinforcement in the piles is not recommended, due to the lack of ductility of FRP bars and the impossibility of verifying potential post-earthquake damage.

9 EXECUTION REQUIREMENTS

9.1 MATERIAL SHIPMENT TO THE CONSTRUCTION SITE

(1) Each bar shall be clearly identified with the following information:

- batch number;
- name of the Manufacturer and of the certified commercial product;
- nominal bar diameter, in accordance with Table 3-2;
- class designation, in accordance with Table 3-3.

(2) If the Manufacturer is unable to mark this information directly on the bars, it is essential that all bars shipped together include at least one identification tag per bundle, indicating the information listed above.

Each bundle of bars, for each bar type, shall have its own identification tag.

(3) In the case of bent bars, in addition to the above information, the minimum certified bending radius provided by the Manufacturer shall also be indicated.

9.2 STORAGE AT THE CONSTRUCTION SITE

(1) FRP bars shall be stored with care to prevent surface damage that could compromise their durability, load-bearing capacity, or bond strength with concrete.

(2) Although FRP bars are corrosion-resistant, they may degrade if exposed to UV radiation for extended periods or subjected to high temperatures. Therefore, bars should be stored on pallets to avoid direct contact with the ground—particularly for long-term storage. When stored outdoors, and unless otherwise specified by the Manufacturer, the bars shall be protected from UV exposure using opaque coverings and shielded from chemical contaminants. For bars with enhanced bond properties obtained by surface sand coating, direct contact with running water should be avoided to prevent loss of the quartz coating, unless otherwise indicated by the Manufacturer.

(3) The Manufacturer shall clearly specify the recommended storage duration and conditions for the bars. These Guidelines shall be strictly followed on site.

9.3 HANDLING AT THE CONSTRUCTION SITE

(1) FRP bars shall be handled with care to avoid surface damage, such as deep scratches or notches, which could compromise the strength and durability of the material.

(2) Unless otherwise specified by the Manufacturer, personnel shall wear protective gloves during handling to prevent splinters, cuts, or skin irritation that may result from contact with the fibers contained in the bars.

(3) Cutting operations shall be performed using high-speed grinders with diamond blades or fine-tooth saws. The use of clippers or bolt cutters is strictly prohibited, as these may cause cracks in the resin matrix or fiber damage.

(4) Lifting operations shall employ multiple support points to distribute the load and avoid localized stresses. This requirement is particularly critical when lifting reinforcement cages, due to the lower shear strength of FRP reinforcement compared to steel.

(5) When the material is supplied in coils, special care shall be taken during uncoiling operations to prevent damage to the bars and injury to personnel.

9.4 INSTALLATION

(1) The installation of FRP bars shall be carried out strictly in accordance with the instructions of the Field Engineer and any additional recommendations provided by the Manufacturer. The following provisions, consistent with international Standards, ensure the structural integrity and durability of FRP reinforcement used in concrete construction

(2) Any bar exhibiting surface damage or alteration during transport or handling shall be rejected or subjected to verification, in consultation with the Manufacturer and the Field Engineer. Instructions concerning bar placement and tolerances shall be defined prior to installation and approved by the Engineer of Record.

(3) FRP bars shall not be bent on site. The Manufacturer must realize any bends or hooks during fabrication. Bars bent shall not be accepted on site if the bending radius, r_t, is smaller than the minimum certified bending radius established by the Manufacturer during qualification testing.

(4) During concrete casting, the bars shall be securely tied to prevent movement or flotation. Tying procedures are the same as for steel reinforcement; however, non-corrosive materials such as plastic or nylon ties may also be used—particularly when carbon FRP bars are involved—to prevent galvanic corrosion. For carbon FRP (CFRP) bars, direct contact between steel and carbon FRP shall be avoided. For glass FRP (GFRP) bars, no contraindications exist regarding direct contact with steel reinforcement.

(5) During concrete vibration, care shall be taken to avoid damaging the reinforcement.

9.5 QUALITY CONTROL AND INSPECTION

(1) All activities related to the installation of FRP reinforcement shall be subject to systematic inspection to verify compliance with the design documents, the Manufacturer's specifications, and the requirements of this Guideline.

(2) The Field Engineer shall ensure that the following checks are carried out before and during installation:

- verification of identification and traceability of each batch of FRP bars (Manufacturer, product, diameter, and material class);
- confirmation that storage and handling have prevented surface deterioration, contamination, or mechanical damage;
- verification that bar placement, concrete cover, alignment, and spacing comply with the approved drawings and tolerances;
- confirmation that bent bars or prefabricated cages meet the certified minimum bending radius and are documented by the Manufacturer.

(3) Any bar showing cracks, delamination, discoloration, fiber exposure, or surface abrasion shall be rejected and replaced unless the Manufacturer and the Field Engineer jointly approve its use after evaluation.

(4) During concrete placement, the Field Engineer shall verify that the **r**einforcement remains correctly positioned and that vibration operations do not induce impact or stress on FRP bars or stirrups.

(5) After casting, a final report shall be prepared documenting:

- identification of the installed FRP reinforcement;
- reference to batch certificates and test reports;
- results of on-site inspections and any corrective measures taken;
- confirmation of compliance with the design and Manufacturer's specifications.

(6) All records, including delivery notes, certificates of conformity, and inspection reports, shall be attached to the declaration of correct execution prepared by the Field Engineer for the duration of the structure’s design service life or for the period specified by applicable regulations.

10 OTHER APPLICATIONS

10.1 INTRODUCTION

FRP bars can be used in a wide range of applications, not only for the construction of new RC structures.

Although these Guidelines primarily provide design criteria for this type of construction, it is useful to note several additional fields of application for FRP bars — both in the realization of other structural systems and in the strengthening of existing structures.

10.2 FRP BARS AS STRENGTHENING SYSTEMS FOR EXISTING STRUCTURES

10.2.1 External strengthening with NSM technique

(1)) FRP bars can be used as external reinforcement for existing RC and masonry structures, by inserting them into pre-cut surface grooves (NSM – *Near Surface Mounted technique*) filled with resin or high-strength mortar (Figure 10-1a–b). These applications are now well established and show great promise (De Lorenzis & Teng, 2007; Bilotta et al., 2016; Dias et al., 2018; Ferretti et al., 2024), owing to the high durability and low weight of FRP bars, which facilitate both handling and installation.

(2) The use of FRP bars with the NSM technique can represent a highly efficient strengthening solution for reinforced and prestressed concrete infrastructure, thanks to their lightness, strength, and durability (Figure 10-1c). Their use increases the load-carrying capacity of structural members without significantly increasing their self-weight, making them particularly suitable for bridges, viaducts, and tunnels. Furthermore, FRP bars' corrosion resistance makes them ideal for use in aggressive environments, where traditional steel reinforcement is prone to deterioration. Consequently, in the specific case of infrastructures, FRP reinforcement improves durability, reduces maintenance costs, and extends the design service life of the structure.

(a) (b) (c)

Figure 10-1 - Application of FRP bars using the NSM technique - a) bar placement in the surface groove; b) strengthening of a RC slab at the soffit (fib Bulletin 90, 2019); c) strengthening of a roadway structure at the top surface (courtesy of Sireg Geotech S.r.l.).

(3) Specific design recommendations for evaluating the increase in load-carrying capacity of elements strengthened with FRP bars installed using the NSM technique are provided in CNR DT 200/R2-2026. The geometric and mechanical properties of FRP bars used for NSM applications shall be evaluated according to the provisions contained in the present Guidelines.

10.2.2 Repointing of mortar joints with FRP bars

(1) FRP bars can be used in structural repointing interventions of deteriorated mortar joints in masonry elements (structural repointing, Figure 10-2). This type of strengthening increases both the strength and the stiffness of the masonry, depending on the wall thickness and the depth of repointing, and is even more effective when the intervention is carried out on both faces of the wall. Connecting the FRP bars inserted into the mortar joints with additional tensile elements that act as transverse connectors between wall wythes creates a continuous three-dimensional reinforcement system, further enhancing the overall effectiveness of the intervention.

(2) The evaluation of the increase in load-carrying capacity of masonry elements strengthened by repointing with FRP bars inserted into mortar joints can be performed according to the design provisions of CNR DT 200/R2-2026 for the NSM technique, adopting the mechanical properties of the mortar used for the repointing as the substrate properties. The geometric and mechanical characteristics of the FRP bars used for deep repointing of mortar joints shall be assessed in accordance with the provisions of the present Guidelines.

Figure 10-2 - Application of FRP bars as reinforcement for the structural repointing of mortar joints in masonry walls.

10.2.3 Improving of connections between masonry elements

(1) FRP bars can be used as connection systems between masonry elements at corners or intersections of orthogonal walls, by inserting them into drilled holes subsequently filled with grout (grouted anchors, Figure 10-3a), in order to reduce the vulnerability of such elements to out-of-plane overturning mechanisms. The increase in capacity of the masonry element due to the presence of FRP connections—expressed in terms of the activation acceleration of the overturning mechanism—can be estimated through rigid-body mechanism analysis (Figure 10-3b), following the procedures specified in the applicable Standards, taking into account the stabilizing contribution of the FRP bars (Maione et al., 2023). The maximum contribution provided by a given FRP bar, when combined with a specific injection mortar, shall be determined through experimental pull-out tests performed on the masonry substrate involved in the intervention, or through reliable literature data (Ceroni and Di Ludovico, 2020). As an upper bound, the design tensile strength at the Ultimate Limit State (ULS) shall be taken as defined by Equation (4.2). The geometric and mechanical characteristics of FRP bars used in grouted-anchor applications shall be evaluated in accordance with the provisions of the present Guidelines.

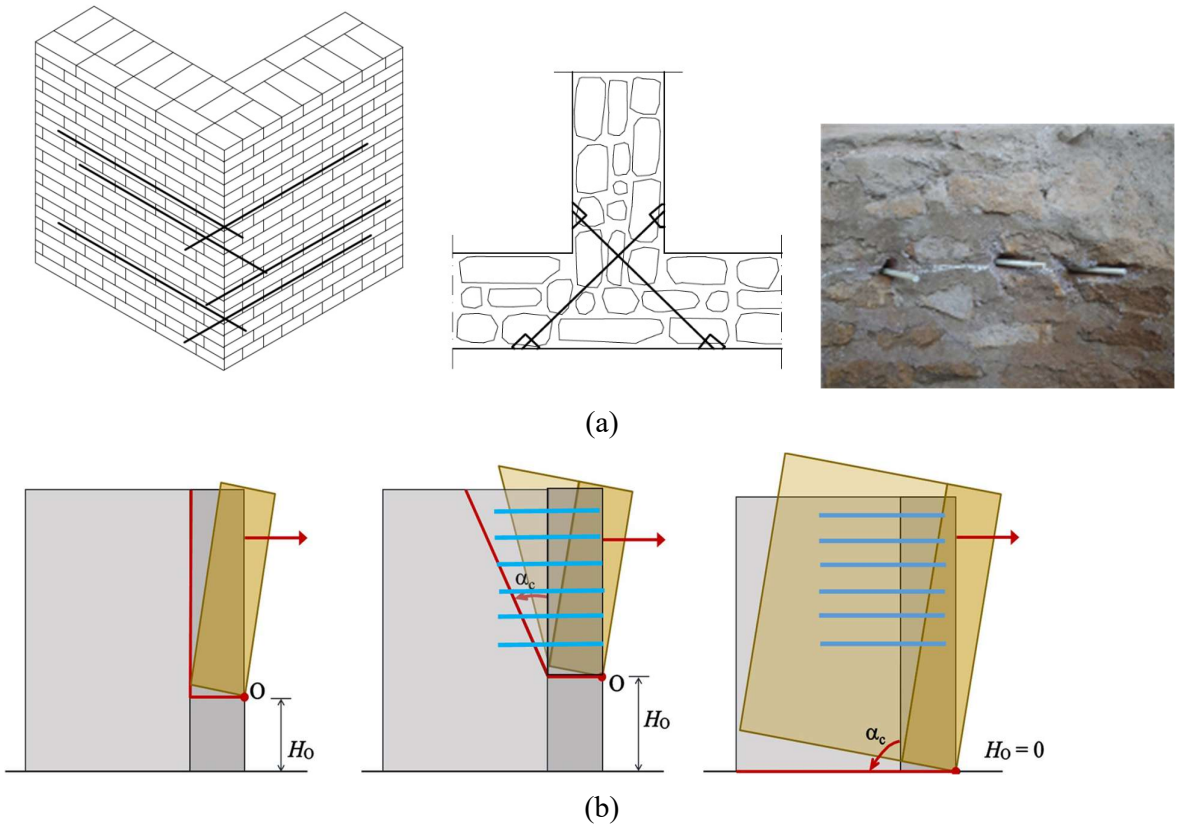

Figure 10-3 - a) Use of FRP bars as grouted anchors in masonry elements; b) connection effect of FRP bars on the shape and size of the macro-block involved in the out-of-plane mechanism, identified by the hinge height H_0 and the crack inclination angle α_c (Maione et al., 2023).

(2) FRP bars with circular or rectangular cross-sections can also be used as ties (chains) to provide a connection between walls in existing masonry buildings, in order to improve the box-like behavior of the entire structure (Figure 10-4a). The geometric and mechanical properties of FRP bars used as ties shall be evaluated in accordance with the provisions of the present Guidelines. The design of the bars may follow the same criteria used for steel ties, considering that the tensile strength of the FRP bars at the Ultimate Limit State (ULS) is given by Equation (4.2). Special attention shall be paid to the anchorage system of the FRP bars to ensure adequate resistance to out-of-plane displacements of the connected walls (passive ties) or to achieve the desired pretension level in cases where a tensile load is applied to the FRP bar (active ties). The anchorage system (see example in Figure 10-4b for rectangular-section GFRP bars) shall be appropriately designed and proportioned to avoid both excessive stress concentration in the masonry and damage to the FRP bars in the anchorage region, taking into account that the mechanical properties transverse to the fiber direction are much lower than those along the fibers themselves.

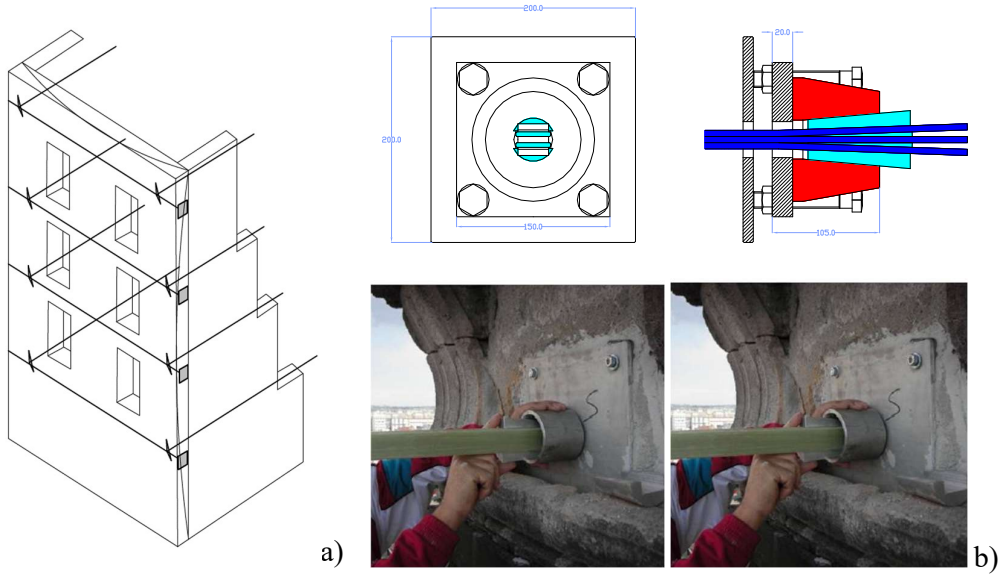

Figure 10-4 - a) Application of FRP bars as ties in masonry buildings; b) example of end-anchorage system for rectangular-section GFRP bars (Ceroni and Prota, 2009).

Essential References

1. Ceroni F., Prota A. (2009) *Case study: Seismic upgrade of a masonry bell tower by GFRP ties*, ASCE Journal of Composite for Construction, 13 (3): 188-197.
2. Ceroni F., Di Ludovico M. (2020) *Traditional and innovative systems for injected anchors in masonry elements: experimental behaviour and theoretical formulations*, Construction and Building Materials, 254, 10.1016/j.conbuildmat.2020.119178.
3. De Lorenzis, L., Teng, J.G. (2007) *Near-surface mounted FRP reinforcement: an emerging technique for structural strengthening*." Compos., Part B, 38, 119–143.
4. Dias S.J.E., Barros J.A.O., Janwaen W. (2018) *Behavior of RC beams flexurally strengthened with NSM CFRP laminates*, Composite Structures, 201, 363-376.
5. Bilotta A., Ceroni F., Barros J., Costa I., Palmieri A., Szabo Z., Nigro E., Matthys S., Balazs G., Pecce M., (2016) *Bond of NSM FRP strengthened concrete: Round Robin Test initiative*, ASCE Journal of Composites for Construction, 20 (1), 10.1061/(ASCE)CC.1943-5614.0000579.
6. Istruzioni CNR DT200/R2-2026 (2026) *Guidelines for the Design, Execution, and Inspection of Structural Strengthening Interventions Using Fiber-Reinforced Composites*, National Research council, Rome, Italy.
7. Ferretti F., Incerti A., Savoia M. (2025) *In-plane shear strengthening of masonry panels using pultruded FRP rebars*, Construction and Building Materials, 493, 10.1016/j.conbuildmat.2025.143144
8. *fib* bulletin 90 (2019) *Externally applied FRP reinforcement for concrete structures*, Technical Report, Task Group 5.1, the International Federation for Structural Concrete, ISBN: 978-2-88394-132-8.
9. Maione A., Casapulla C., Di Ludovico M., Prota A., Ceroni F. (2023) *Limit analysis and design-oriented approach for out-of-plane loaded masonry walls strengthened by grouted anchors*, Engineering Structures, 285, 10.1016/j.engstruct.2023.115991.

10.3 APPLICATIONS OF FRP BARS FOR SOIL RETENTION

(1) FRP bars can be used as post-tensioned anchors for maintaining excavation faces during digging

operations or for the permanent stabilization of unstable slopes and artificial embankments — either as post-tensioned tendons for RC retaining walls (Figure 10-5a) or inserted directly into pre-drilled and grouted holes (*soil nails*, Figure 10-5b). FRP bars are particularly suitable for this type of application because they are non-corrosive and can be used even in chemically aggressive soils. The design of FRP bars for such applications may follow the same procedures used for steel anchors, considering that the maximum strength of the FRP bars at the Ultimate Limit State (ULS) is given by Eq. (4.2).

(a)

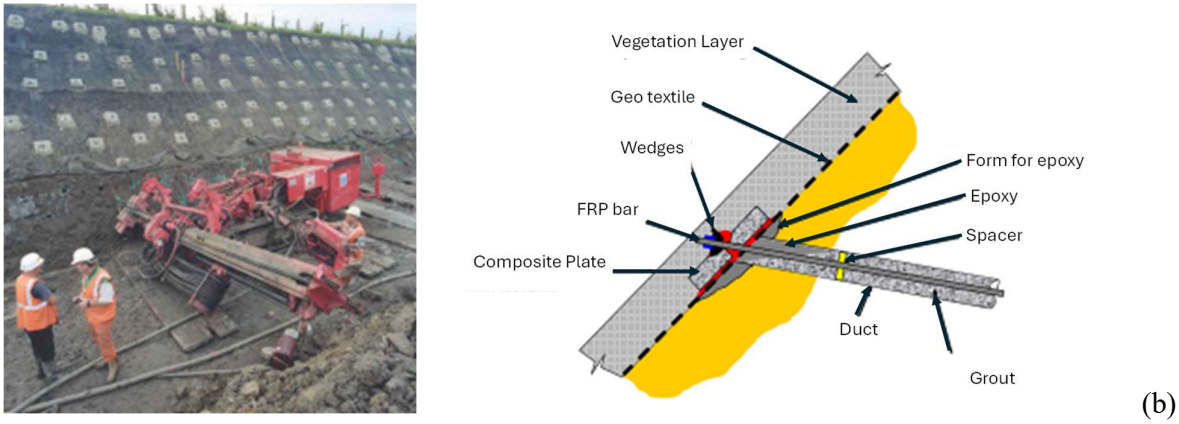

(b)

Figure 10-5 - a) Application of FRP bars as post-tensioned anchors (courtesy of ATP); b) application of FRP bars as soil nails (courtesy of Sireg Geotech S.r.l.).

(2) FRP bars can also be effectively used as reinforcement for concrete pile walls forming coastal flood-protection barriers (sea dikes or sea walls, Figure 10-6; Steputat et al., 2022). The corrosion resistance of FRP bars extends the design service life of coastal structures and allows for a significant reduction in maintenance and repair costs compared to traditional steel reinforcement—particularly since these structures are generally subjected to moderate stress levels.

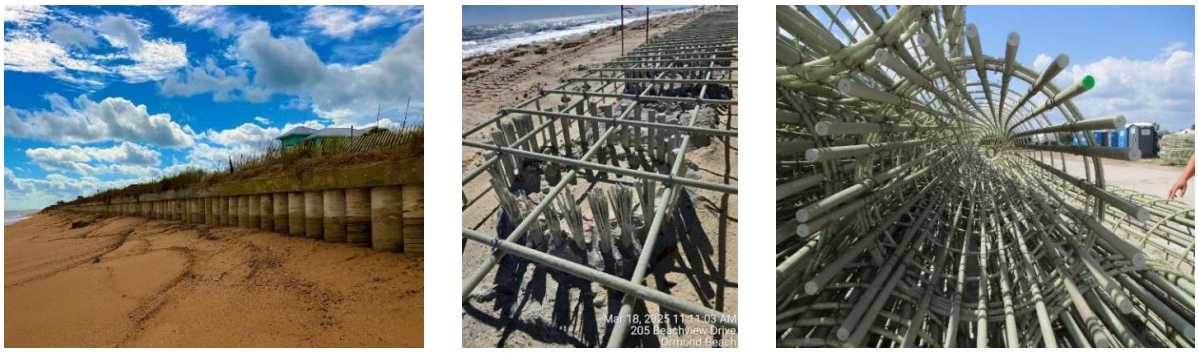

Figure 10-6 - Examples of application of FRP bars as reinforcement of seawalls.

Essential References

1. Steputat C.C., O'Connor J., Arrants M., Beech J., Nanni A. (2022) *GFRP-RC seawalls as a means of coastal fortification and extended service life*, Concrete International, November 2022, pp. 36–42.

10.4 APPLICATIONS OF FRP BARS FOR TEMPORARY STRUCTURES

(1) FRP bars can be used as soft-eyes (Mohameda et al., 2020) for the construction of underground excavations, such as metro tunnels. The easiness of cutting the FRP bars—particularly those made of glass fiber (GFRP)—makes them especially suitable for temporary diaphragm walls that must later be partially cut through by a full-face Tunnel Boring Machine (TBM). A soft-eye consists of a reinforcement cage made of GFRP bars and stirrups (Figure 10-7a-b), which the TBM can easily cut during excavation (Figure 10-7c). The lightweight of FRP bars also facilitates transportation and on-site assembly of the reinforcement cage. This technique enables a significant reduction in the time required for diaphragm wall construction.

(a)

(b)

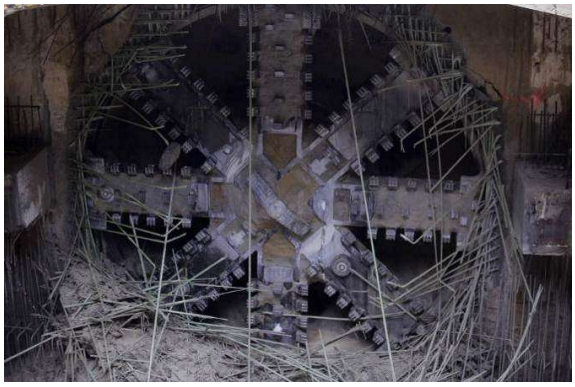

(c)

Figure 10-7 - Examples of FRP bar applications for the construction of temporary diaphragm walls (soft-eyes) in tunnel excavation - a) *fib* Bulletin 40; b) Rome Metro (courtesy of ATP); c) https://www.dextragroup.com/ground-engineering/tunneling/astec-soft-eyes/.

Essential References

1. Mohameda H.M., Alia A.H., Hadhooda A., Mousab S., Abdelazima W., Benmokrane B. (2020) *Testing, design, and field implementation of GFRP RC soft-eyes for tunnel construction*, *Tunnelling and Underground Space Technology*, 106, 103626.

2. *fib Bulletin 40* (2007) *FRP Reinforcement in RC Structures*, Technical Report, ISBN 978-2-88394-080-2.

10.5 FRP BARS AS REINFORCEMENT IN NON-STRUCTURAL ELEMENTS

(1) FRP bars, including FRP meshes, can be used as reinforcement for non-structural concrete elements, such as floor pavements or non-load-bearing precast elements (Roghani et al., 2022). The advantages of using FRP bars are particularly evident in aggressive environments where steel reinforcement is susceptible to corrosion (e.g., coastal or marine areas). The use of FRP reinforcement in such elements primarily aims to control cracking caused by temperature variations and shrinkage. For this purpose, the same detailing rules used for steel reinforcement (e.g., minimum bar spacing as a function of slab thickness and bar diameter, minimum concrete cover) may be adopted; however, more extensive experimental studies could justify a reduction in concrete cover, mainly when the cover is prescribed solely for corrosion protection of the reinforcement.

(2) FRP bars are also used as reinforcement for concrete boat-launch ramps (Figure 10-8), as they are resistant to chloride-induced corrosion and other aggressive agents, thereby preventing or significantly reducing degradation due to marine exposure.

Figure 10-8 - Application of FRP bars as reinforcement in concrete boat-launch ramps (courtesy of Sireg Geotech).

Essential References

1. Roghani H., De Caso F., Nanni A. (2022) *Constructability of slabs-on-ground with FRP meshes as secondary reinforcement*, 15th International Conference on Fibre-Reinforced Polymers for Reinforced Concrete Structures (FRPRCS-15) and 8th Asia-Pacific Conference on FRP in Structures (APFIS-2022), 10–14 December 2022, Shenzhen, China.

10.6 APPLICATIONS OF FRP BARS AS INTERNAL REINFORCEMENT FOR ELEMENTS EXPOSED TO ELECTROMAGNETIC INTERFERENCES

(1) In transportation infrastructures, various electrical systems may be sensitive to electromagnetic interference (EMI) — such as train detection systems, railway and tramway switching equipment, automated metro control systems, and highway toll detection systems, among others. Traditional steel reinforcement can interfere with the electromagnetic waves of these systems, potentially compromising their proper operation. Conversely, GFRP bars allow the construction of reinforcement cages made of non-conductive materials (Figure 10-9), which are transparent to electromagnetic waves, thus eliminating the risk of interference and ensuring the safe and reliable operation of these infrastructures.

Figure 10-9 - Example of an FRP bar application as reinforcement for elements exposed to electro-magnetic interference (courtesy of Sireg Geotech S.r.l.).

11 APPENDIX A: QUALIFICATION AND ON-SITE ACCEPTANCE OF MATERIALS AND PRODUCTS

11.1 QUALIFICATION OF FRP BARS

According to the current regulations (D.M. 17 January 2018, hereinafter NTC 2018), the qualification of construction materials and products intended for structural use is mandatory and regulated by Chapter 11, which defines the following three cases:

A. Products falling within the scope of a harmonized European Standard (hEN). In this case, the product shall be CE marked (in accordance with EU Regulation 2024/3110). For such products, CE marking represents the only recognized qualification pathway.
B. Products not covered by a hEN but whose qualification requirements are explicitly defined by the technical Standards.
C. Products not falling within either case A or case B.

For products belonging to Case C, qualification may be obtained alternatively through one of the following procedures:

- CE marking based on a *European Technical Assessment* (ETA), issued in accordance with a specific European Assessment Document (EAD);
- a *Technical Evaluation Certificate* (*Certificato di Valutazione Tecnica* – CVT) issued by the President of the Italian Superior Council of Public Works, following the assessment carried out by the Central Technical Service, and, where applicable, based on a dedicated qualification guideline issued by the same Council.

As indicated in Case A, CE marking for construction products is governed by EU Regulation 2024/3110 (Construction Products Regulation - CPR), which establishes harmonized procedures for the marketing of construction products within the European Union (EU). CE marking certifies that the information accompanying the product, summarized in the Declaration of Performance and Conformity (DoPC), has been obtained in accordance with the Regulation UE 2024/3110. Such information shall be therefore considered accurate and reliable. The manufacturer prepares the DoPC when placing the product on the market, assuming full responsibility for the product's conformity with the declared performance. For additional information on the meaning of CE marking and Technical Evaluation Certificates (CVT), reference may be made to CNR DT 200/R2-2025. At present, no harmonized European Standards (hEN) are available for FRP bars.

For the qualification of FRP bars, the following reference documents are available:

- *European Assessment Document EAD 260023-00-0301, Carbon, glass, basalt and aramid fibre reinforced polymer bars as reinforcement of structural elements*, published in the Official Journal of the European Union by Decision (EU) 2024/1944 (herein referred to as *EAD–FRP Bars*. Based on this document, CE marking may be obtained through the issuance of a European Technical Assessment (ETA).
- *Guideline for the Identification, Qualification and Acceptance of Fibre-Reinforced Composite Bars and Stirrups for Structural Use*, issued by the Italian Superior Council of Public Works in December 2021 (herein referred to as *LG–FRP Bars*), which supports the issuance of Technical Evaluation Certificates (CVT).

European Assessment Documents (EADs) are available on the EOTA website (eota.eu/eads); Technical Documents issued by the National Research Council of Italy (CNR) are also accessible via the CNR website (https://www.cnr.it/it/norme-tecniche-costruzioni).

11.2 PROPERTIES OF FRP BARS

Compliance with the strength classes defined in Table 3-3, as well as the authorization for use of a given product, shall be verified through the achievement, during the qualification process, of mechanical properties equal to or greater than those specified in Table 3-1. These properties shall be determined in accordance with the procedures set out in the *EAD–FRP Bars* or *LG–FRP Bars*. In addition to the characteristics reported in Table 3-1, further physical and mechanical properties of FRP bars may be qualified, particularly those listed in Table 11-1. For the test methods and evaluation procedures of these properties, reference may be made to the *EAD–FRP Bars* or the *LG–FRP Bars* documents.

Essential References

1. EAD 260023-00-0301 (2024) *Carbon, glass, basalt and aramid fibre reinforced polymer bars as reinforcement of structural elements*, Adopted on January 2019, EOTA, OJ Publication: Decision (EU) 2024/1944.

2. LG-barre FRP (2021) *Linea guida per l'identificazione, la qualificazione e l'accettazione di barre e staffe in composito fibrorinforzato per uso strutturale*, Consiglio Superiore dei Lavori Pubblici, Dicembre 2021.

Table 11-1 - Additional physical and mechanical properties of FRP bars through experimental testing

N°	Property	Symbol [Unit]	Reference Document
1	Compressive strength (mean and characteristic)	f_{fc}, f_{fck} [MPa]	*EAD-FRP Bars* §2.2.3 *LG-FRP Bars* – Tab. 2
2	Longitudinal modulus in compression (mean)	E_{fc} [GPa]	*EAD-FRP Bars* §2.2.3 *LG-FRP Bars* – Tab. 2
3	Tensile strain at failure (mean and characteristic)	ε_{ft0}, ε_{ftk0} [mm/mm]	*EAD-FRP Bars* §2.2.2 *LG-FRP Bars* – Tab. 2
4	Bond strength (pull-out) from concrete substrate (mean values): - C20/25 concrete, centered position (*alkaline conditions*) - C20/25 concrete, eccentric position (*standard conditions*) - C20/25 concrete, centered position (*at maximum service temperature*) - C50/60 concrete, centered position (*standard conditions*)	$\tau_{b,a}$ [MPa] $\tau_{b,cb}$ [MPa] $\tau_{b,Tmax}$ [MPa] $\tau_{b,C50/60}$ [MPa]	*EAD-FRP Bars* §2.2.4 *LG-FRP Bars* – Tab. 2
5	Tensile fatigue (2×10^6 cycles, stress ratio R = 0.1, frequency 1–10 Hz)	$f_{fatigue}$ [MPa]	*EAD-FRP Bars* §2.2.7 *LG-FRP Bars* – Tab. 3
6	Static fatigue (characteristic values): - Creep rupture strength at one million hours (≈ 100 years) – *standard conditions* - Creep rupture strength at one million hours (≈ 100 years) – *alkaline exposure at 60 °C*	$f_{ftk,c}$ [MPa] $f_{ftk,ca}$ [MPa]	*EAD-FRP Bars* §2.2.8 *LG-FRP Bars* – Tab. 3
7	Longitudinal coefficient of thermal expansion	$\alpha_{sp,L}$ [°C^{-1}]	*EAD-FRP Bars* §2.2.9 *LG-FRP Bars* – Tab. 1
8	Transverse coefficient of thermal expansion	$\alpha_{sp,T}$ [°C^{-1}]	*EAD -FRP Bars* §2.2.10 *LG-FRP Bars* – Tab. 1
9	Melting temperature (for thermoplastic or semi-crystalline FRP bars)	T_{pm} [°C]	*EAD-FRP Bars* §2.2.11
10	Relaxation: - Relaxation rate after 10, 120 and 1000 hours - Relaxation rate after one million hours (≈ 100 years)	Y_{10}, Y_{120}, Y_{1000} [%] $Y_{million}$ [%]	*EAD-FRP Bars* §2.2.12 *LG-FRP Bars* – Tab. 3
11	Alkali resistance: - Mass-loss rate (at 1000 h and 3000 h) - Residual mean tensile strength after 1000 h under sustained load - Residual mean interlaminar shear strength after 1000 h - Residual mean interlaminar shear strength after 3000 h	$R_{\Delta m}$ [%] $R_{et,t}^{1000}$ [%] $R_{et,i}^{1000}$ [%] $R_{et,i}^{3000}$ [%]	*EAD-FRP Bars* §2.2.16 *LG-FRP Bars* – Tab. 2
13	Reaction to fire (class rating)	Fire Class	*EAD-FRP Bars* §2.2.17 *LG-FRP Bars* – Tab. 2

12 APPENDIX B – CALIBRATION OF PARTIAL MATERIAL FACTORS

12.1 INTRODUCTION

This Appendix provides information on the procedure for the calibration of the partial factors for FRP bars referred to in Chapter 4. The concept of safety adopted herein is consistent with EN 1990 Basis of Structural Design (EN 1990, 2023). In defining the design value of a generic resistance property R_d of a material, it is possible to distinguish the partial factor γ_{Rd}, which accounts for uncertainties related to the resistance model and the geometry, and the partial factor γ_m which accounts for uncertainties in the material properties:

$$R_d = R\left\{X_{d,i}; a_{d,i}\right\} = R\left\{\eta \frac{X_{k,i}}{\gamma_m \cdot \gamma_{Rd}}; a_{d,i}\right\} \tag{12.1}$$

where (as also suggested by EN 1990 §8.3.5.1(2)) the factors γ_m and γ_{Rd} can be combined into a single partial factor for material properties γ_f (EN 1990, § C.4.3):

$$\gamma_f = \gamma_m \cdot \gamma_{Rd} \tag{12.2}$$

In Eq. (12.1) $R\{\cdot\}$ is a function depending on a specific resistance model of the mechanical X_i and geometrical a_i parameters, represented by $X_{d,i}$ and $a_{d,i}$ in terms of design values (EN 1992-1-1:2023). η is a conversion factor that takes into account the reduction of the mechanical properties due to exposure to non-standard environmental conditions, as humidity and temperature, aging, scale effects and other relevant parameters.

In the following sections, for the FRP bars, based on statistical analysis of experimental results and on literature models, these partial factors will be evaluated:

- the partial factor, γ_m, which takes into account only uncertainties in the material property, considering possible unfavorable deviations of the property from its characteristic value, and which will be assessed in §12.2;
- the partial factor γ_{Rd}, which is associated with uncertainties in the resistance model and geometric deviations, unless explicitly accounted for within the resistance model itself, and which will be assessed in §12.3.1 for the flexural resistance model and in §12.4 for the resistance models associated to shear and confinement;
- the partial factor of the FRP bar, γ_f, according to Eq. (12.2) for evaluating the design strength of the FRP bars, which will be evaluated in §12.3.2 and §12.3.3 for flexural verifications and in §12.5 for the shear and confinement.

12.2 DERIVATION OF THE MATERIAL PARTIAL FACTOR, γ_m

To determine the partial material factor, a statistical analysis was conducted on tensile-strength test results from the qualification of eight different GFRP bars, with diameters ranging from 6 mm to 25 mm, produced by both domestic and international manufacturers. Testing was conducted in five different university laboratories in Europe, following the same test procedure (EAD 260023-00-0301, §2.2.2).

The experimental results were grouped in datasets of equal diameter and it was observed that the statistical distribution of strengths can be well approximated by a three-parameter log-normal distribution, satisfying the Kolmogorov–Smirnov log-normality criterion (Massey, 1959). By adopting this distribution for interpolation of the experimental data, the design and characteristic values defined in Eurocode 0 (EN 1990, 2023) for the three-parameter log-normal case can be expressed as follows:

Design strength: $$X_d = \vartheta + (\mu_X - \vartheta) \cdot e^{-\left[\frac{1}{2}\ln\left(1+\frac{\sigma_X^2}{(\mu_X-\vartheta)^2}\right)+sign(\gamma)\cdot\alpha_R\cdot\beta\sqrt{\ln\left(1+\frac{\sigma_X^2}{(\mu_X-\vartheta)^2}\right)}\right]} \quad (12.3)$$

Characteristic strength: $$X_k = \vartheta + (\mu_X - \vartheta) \cdot e^{-\left[\frac{1}{2}\ln\left(1+\frac{\sigma_X^2}{(\mu_X-\vartheta)^2}\right)-sign(\gamma)\Phi^{-1}(p)\sqrt{\ln\left(1+\frac{\sigma_X^2}{(\mu_X-\vartheta)^2}\right)}\right]} \quad (12.4)$$

where:

- μ_X, σ_X and ϑ are the parameters of the three-parameter log-normal distribution (mean, standard deviation, and threshold, respectively), γ is the skewness,
- α_R is the sensitivity factor according to the First Order Reliability Method (FORM),
- β is the target reliability index, which depends on the consequence class of the structure and the reference period (EN 1990, 2023),
- Φ is the cumulative probability function of the standard normal distribution, and $\Phi^{-1}(p)$ is the corresponding quantile function (for p = 5%, $\Phi^{-1}(0.05) = -1.645$).

The partial material factor γ_m is therefore given by:

$$X_d = \eta \frac{X_k}{\gamma_m} \quad \rightarrow \quad \gamma_m = \frac{X_k}{X_d} \quad (12.5)$$

where the design and characteristic values are determined from Eqs. (12.3) and (12.4) for each tested bar diameter. In Eq. (12.5) the conversion factor η is not considered, since the tensile tests were carried out under standard environmental conditions. The values of η_i listed in Tables 4-1 and 4-2 were fixed based on literature information.

In Eq. (12.3), the following parameters were adopted:

- α_R=0.8, since it is supposed that the variable X related to the strength of the material is dominant in comparison with the other variables (uncertainties of resistance model and of geometry) that influence the γ_f according to Eq. (12.2) (EN 1990, 2023), and
- β = 3.8 (corresponding to Consequence Class CC2, reference period 50 years, EN 1990, Table C.3).

Equation (12.5) gives γ_m values ranging from 1.02 to 1.07, depending on bar diameter (Franco et al., 2025). When values were grouped in the strength classes defined in Table 3-3, γ_m ranges between 1.04 and 1.07. For safety, a partial material factor γ_m=1.07 is therefore recommended. In this case, the coefficient of variation of the tensile strength is $V_X = \sigma_X/\mu_X$ 0.07.

12.3 DERIVATION OF THE PARTIAL FACTOR FOR FRP BARS γ_f FOR FLEXURAL VERIFICATIONS

12.3.1 Assessment of the partial factor related to uncertainties of the flexural

resistance model and of geometry, γ_{Rd}

The partial factor γ_{Rd} related to the uncertainties related to the flexural behavior of the bar embedded in concrete and subject to normal stresses (such as those related to bending) can be expressed as the product of two terms: one accounting for the uncertainty in the resistance model ($\gamma_{Rd,mod}$) and the other for geometric deviations ($\gamma_{Rd,geo}$):

$$\gamma_{Rd} = \gamma_{Rd,mod} \cdot \gamma_{Rd,geo} \tag{12.6}$$

Assuming a normal distribution for both uncertainties, the partial coefficients can be defined as follows (fib Bulletin 80, 2016):

$$\gamma_{Rd,mod} = \frac{\mu_{\theta R,mod}}{\theta_{Rd,mod}} = \frac{1}{1-\alpha_R \cdot \beta \cdot V_{\theta R,mod}} = \frac{1}{1-0.4 \cdot 0.8 \cdot \beta \cdot V_{\theta R,mod}} \tag{12.7}$$

$$\gamma_{Rd,geo} = \frac{\mu_{\theta R,geo}}{\theta_{Rd,geo}} = \frac{1}{1-\alpha_R \cdot \beta \cdot V_{\theta R,geo}} = \frac{1}{1-0.4 \cdot 0.8 \cdot \beta \cdot V_{\theta R,geo}} \tag{12.8}$$

where $\mu_{\theta R,mod}, V_{\theta R,mod}$ and $\mu_{\theta R,geo}, V_{\theta R,geo}$ are, respectively, the mean values and coefficients of variation of the random variables $\theta_{R,mod}$ and $\theta_{R,geo}$, which describe the uncertainties related to the resistance model and geometry. In Eq. (12.7) and (12.8), a reduced value of the factor $\alpha_R = 0.4 \cdot 0.8 = 0.32$, as suggested in *fib* bulletin 80 (§ 4.1.3, eq. 4.1-20), since the uncertainties of the resistance model and of geometry are assumed as not dominant variables, but the variable X, associated to the material strength is assumed dominant (see also §12.2).

For RC members with steel reinforcement, statistical evaluations from experimental pure bending tests, EN 1992-1-1 (EN 1992-1-1, 2023, Appendix A) suggests adopting a model coefficient of variation equal to $V_{\theta R,mod} = 0.045$. In the absence of analogous statistical evaluations for RC elements with FRP bars and in consideration of the brittle behavior of the FRP bars, a conservative value for the coefficient of variation of $V_{\theta R,mod} = 0.06$ is adopted here.

The geometric uncertainties associated with the reinforcement area are implicitly accounted for in the resistance variability, since the latter is defined in terms of the effective cross-sectional area. Therefore, for pure tension members, geometric uncertainty can be neglected. For bending, however, where resistance also depends on the section dimensions and the position of the bars (through the effective depth and, consequently, the concrete cover), geometric uncertainties may have a non-negligible influence. It can be assumed that this factor does not depend on the material, and that it is taken the same used for steel, which in EN 1992-1-1 (EN 1992-1-1, 2023, Appendix A) is defined as a function of the effective depth *d* (in mm):

$$V_{\theta R,geo} = 0.05[200 / d]^{2/3} \tag{12.9}$$

Such a coefficient of variation is usually calculated for concrete element reinforced with steel bars adopting in Eq. (12.9) d = 200 mm, that provides $V_{\theta R,geo} = 0.05$. Using for concrete elements reinforced with FRP bars the value for $V_{\theta R,geo}$ and introducing, thus, $V_{\theta R,mod} = 0.06$ and $V_{\theta R,geo} = 0.05$ in Eqs. (12.7) and (12.8), the following result is obtained:

$$\gamma_{Rd,mod} = 1.08\,,\ \gamma_{Rd,geo} = 1.06 \tag{12.10}$$

These values are lower or comparable with the partial factor estimated for the material in §12.2 (γ_m =1.08) and, thus, justify the assumption of considering the material strength as dominant variable,

also in consideration of the safe choice adopted for the uncertainty related to the resistance model.

Using for $\gamma_{Rd,mod}$ and $\gamma_{Rd,geo}$ the values given by Eq. (12.10), the global partial factor for model and geometry uncertainties, γ_{Rd}, for FRP bars under flexural stresses, is therefore equal to:

$$\gamma_{Rd} = \gamma_{Rd,mod} \cdot \gamma_{Rd,geo} = 1.08 \cdot 1.06 = 1.15 \tag{12.11}$$

For comparison, it should be noted that the partial factor for model uncertainty for FRP bars is taken in the fib Model Code 2020 §17.8.1.1 (*fib* MC 2020, 2024) as $\gamma_{Rd,mod} = 1.10$, while in the *fib* Model Code 2010 (fib Bulletin 65, 2012) the factor for geometric uncertainty used for steel was assumed as $\gamma_{Rd,geo} = 1.05$. The combined use of these two values in Eq. (12.11) provides $\gamma_{Rd} = 1.16$, in agreement with the calculated values.

12.3.2 Assessment of the partial factor of the FRP bars γ_f according to EN 1990

Considering the values reported in §12.3.1 for the partial factors related to uncertainties of the geometry and of the resistance model ($\gamma_{Rd,mod}$ = 1.08 and $\gamma_{Rd,geo}$ =1.06, that provided $\gamma_{Rd} = \gamma_{Rd,mod} \cdot \gamma_{Rd,geo} = 1.15$) and adopting the highest value of the partial factor of the material ($\gamma_m = 1.08$) calculated in §12.2, the overall partial factor for FRP bars can therefore be determined as:

$$\gamma_f = \gamma_{Rd} \cdot \gamma_m = 1.15 \cdot 1.08 \cong 1.24 \tag{12.12}$$

12.3.3 Assessment of the partial factor of the FRP bars γ_f according to EN 1992-1-1

As an alternative to the approach described in § 12.4 and to the corresponding procedures developed in §12.2 and §12.3, according to Annex A of EN 1992-1-1 (EN 1992-1-1, 2023), the overall partial factor for the material, γ_f, can be calculated using the following expression, assuming a log-normal distribution of the material strength:

$$\gamma_f = \frac{\exp\left(\alpha_R \cdot \beta \cdot V_{Rf}\right)}{\mu_{Rf}} \tag{12.13}$$

where:

- α_R is the sensitivity factor of the resistance, equal to 0.8;
- β is the reliability index, equal to 3.8 (for consequence class CC2 and a 50-year reference period);
- V_{Rf} is the coefficient of variation of the resistance, calculated as:

$$V_{Rf} = \sqrt{V_m^2 + V_{\theta R,mod}^2 + V_{\theta R,geo}^2} \tag{12.14}$$

The individual terms under the square root represent the coefficients of variation associated with the uncertainties of the material, V_m, of the model, $V_{\theta R,mod}$, and of the geometry, $V_{\theta R,geo}$, as reported in Table 12-1. In particular:

- V_m is taken from the statistical analysis of the available experimental database assuming a three-parameter log-normal distribution (0.07, as defined in §12.2);
- $V_{\theta R,geo}$ = 0.05 as adopted in §12.3.1 for d=200 mm in Eq. (12.9);
- $V_{\theta R,mod}$ = 0.06, as discussed in § 12.3.1, as a safe assumption.

The bias factor of the resistance, μ_{Rf}, can be computed as:

$$\mu_{Rf} = \mu_m \cdot \mu_{\theta R,mod} \cdot \mu_{\theta R,geo} \tag{12.15}$$

where each term represents the bias factor associated with the material, the model, and the geometry, respectively, as indicated in Table 12-1.

Using Equation (12.13) together with the values in Table 12-1, the following value of the overall partial factor is obtained:

$$\gamma_f = \frac{\exp\left(\alpha_R \cdot \beta \cdot V_{Rf}\right)}{\mu_{Rf}} = \frac{\exp\left(0.8 \cdot 3.8 \cdot 0.105\right)}{1.16} = 1.18 \tag{12.16}$$

Table 12-1: Statistical parameters adopted for the calculation of the partial factor γ_f

Variable	Coefficient of variation	Bias factor
Tensile strength	$V_m = 0.07$	$\mu_m = \exp(1.645\, V_m)$
Geometrical uncertainty (effective depth d in mm)	$V_{\theta R,geo} = 0.05[200/d]^{2/3}$	$\mu_{\theta R,geo} = 1 - 0.05[200/d]^{2/3}$
Model uncertainty	$V_{\theta R,mod} = 0.06$	$\mu_{\theta R,mod} = 1.09$
Resistance (for d = 200 mm)	$V_{Rf} = \sqrt{V_m^2 + V_{\theta R,mod}^2 + V_{\theta R,geo}^2} = 0.105$	$\mu_{Rf} = \mu_m \cdot \mu_{\theta R,mod} \cdot \mu_{\theta R,geo} = 1.16$

12.3.4 Partial factor for FRP bars γ_f adopted in this document for flexural verifications

In this document, it is assumed that the flexural verifications at SLU in concrete elements reinforced with FRP bars shall be carried out by adopting in the calculation of the design tensile strength of the FRP bars, the partial factor $\gamma_f = 1.25$, slightly safer in comparison with the value (1.24) provided by Eq. (12.12) according to the procedure suggested in (EN 1990:2023) and described in §12.3.1 and in §12.3.2. Such a value is comprehensive of all the previously described uncertainties (uncertainties of the resistance model and of the geometry in case of bending moment, uncertainty of the tensile strength of the FRP bars) and, thus, can be used without any further reduction factor in order to calculate, starting from the characteristic value of the tensile strength associated with a given class of the FRP bars, the design value to be used in the evaluation of the resistant bending moment of concrete sections reinforced with these bars. Depending on the exposure conditions of the structure, the design value of the tensile strength of FRP bars shall take into account also the conversion factors indicated in Eq. (4.4).

12.4 DERIVATION OF THE PARTIAL FACTOR FOR FRP BARS γ_f IN CASE OF SHEAR STRESS AND FOR CONFINAMENT

In order to assess the partial factor γ_f to be used for the calculation of the shear resistance of concrete elements reinforced with FRP stirrups, considering the approach described in §12.1, it is necessary to estimate the partial factors γ_m, $\gamma_{Rd,mod}$ and $\gamma_{Rd,geo}$.

For straight FRP bars, in §12.2 the partial factor associated to the uncertainty of the tensile strength is estimated ($\gamma_m = 1.08$) based on detailed statistical analyses carried out on a wide database of experimental results of tensile tests. Since for the tensile strength of the FRP stirrups, individuated by the strength of the bent part, f_{ub}, an analogous number of experimental results is not available at the moment, on the safe side, an higher value of the partial factor is assumed, $\gamma_m = 1.15$, obtained

assuming a lognormal distribution of the strength with coefficient of variation $V_m = 0.10$ under the hypothesis that the strength f_{ub} is more scattered than the tensile strength of the straight FRP bars.

The partial factor $\gamma_{Rd} = \gamma_{Rd,mod} \cdot \gamma_{Rd,geo}$ should be estimated on the basis of the comparisons between experimental data and predictions provided by shear resistance models, but, lacking these comparisons, it is possible to follow the same methodology used for flexural verifications. In particular, for the uncertainty related to geometry, the same value of the coefficient of variation used for flexural verification, $V_{\theta R,geo}$=0.05, is adopted, while for the uncertainty related to the shear resistance model a higher coefficient of variation, $V_{\theta R,mod} = 0.10$, is adopted, as suggested in literature. Therefore, based on these assumptions, the two procedures described in §12.3.2 and §12.3.3 provide:

- EN 1990: $$\gamma_f = \gamma_{Rd} \cdot \gamma_m = 1.39 \quad (12.17)$$
- EN 1992-1-1: $$\gamma_f = \frac{\exp\left(\alpha_R \cdot \beta \cdot V_{Rf}\right)}{\mu_{Rf}} = 1.29 \quad (12.18)$$

On the safe side, in this Document, the verifications at SLU for shear stresses in concrete elements reinforced with FRP stirrups shall be carried out adopting in the calculation of the design tensile strength of the FRP stirrups the partial factor $\gamma_f = 1.40$, slightly safer in comparison with the value provided by Eq. (12.17). Because of the linear dependence of the shear resistance related to the FRP stirrup contribution on the tensile strength of the stirrups (see Eq. 6.13), this partial factor can be intended also as partial factor related to the whole shear resistance, similarly to the partial factor γ_V used to calculate the contribute of the shear resistant mechanisms of concrete, $V_{Rd,ct}$, in elements without specific shear reinforcement (see Eq. (6.11a) and (6.11c)).

The same value of the partial factor $\gamma_f = 1.4$ is suggested for calculating the design tensile strength of the FRP stirrups when the effect of confinement induced by FRP stirrups has to be evaluated in concrete elements under axial loads or combined flexural and axial loads.

For both types of verification, the value $\gamma_f = 1.4$ is comprehensive of all the previously described uncertainties (uncertainties of the resistance model and of the geometry in case of shear, uncertainty of the tensile strength of the FRP stirrups) and, thus, it can be used without any further reduction factor in order to calculate the design value of the tensile strength of FRP stirrups, starting from the characteristic value of the tensile strength associated with a given strength class. Depending on the exposure conditions of the structure, the design value of the tensile strength of FRP stirrups shall take into account also the conversion factors indicated in Eq. (4.4).

Essential References

1. EAD 260023-00-0301 (2024) *Carbon, glass, basalt and aramid fibre reinforced polymer bars as reinforcement of structural elements*. Adopted on January 2019, EOTA, OJ Publication: Decision (EU) 2024/1944.
2. EN 1990:2023 (2023) *Eurocode - Basis of structural and geotechnical design*. European Committee for Standardization (CEN), Brussels, Belgium.
3. EN 1992-1-1:2023 (2023) *Eurocode 2: Design of concrete structures - Part 1-1: General rules and rules for buildings, bridges and civil engineering structures*, European Committee for Standardization (CEN), Brussels, Belgium.
4. Massey F.J. (1951) *The Kolmogorov–Smirnov test for goodness of fit*, J Am Stat Assoc 46(2539): 68–78.
5. *fib* Bulletin 80 (2016) *Partial factor methods for existing concrete structures*, CEB-FIP *fib*.

6. *fib* Bulletin 65 (2012) *Model Code 2010* - Final draft, Vol. 1, CEB-FIP *fib*.
7. *fib* MC 2020 (2024) *fib Model Code for concrete structures 2020*, v. 1.2, CEB-FIP *fib*.
8. Franco A., Ceroni F., Bonati A., Occhiuzzi A. (2025) Partial factors for FRP rebars in reinforced concrete structures, *12th International Conference on Fiber-Reinforced Polymer (FRP) Composites in Civil Engineering*, CICE 2025 July 14-16, 2025, Lisbon, Portugal.

APPENDIX C: Duties and responsibilities of stakeholders in the selection and quality control of FRP bars

Manufacturer

- The production of FRP bars, as well as that of their individual components (fibres and matrices), shall be subject to continuous quality control programs.
- For products qualified through CE marking, Manufacturer shall provide the *Declaration of Performance and Conformity (DoPC)* in accordance with EU Regulation 2024/3110, or other available certifications, to ensure that each production batch complies with the declared specifications.
- For products qualified through a *Technical Evaluation Certificate (CVT)*, Manufacturer shall provide the CVT and accompanying technical documentation, such as data sheets, with the product delivery.
- Whenever possible, products shall bear a permanent marking ensuring complete traceability. Otherwise, marking shall be supplied with labels or tags indicating all the information required for the traceability of the materials.

Designer

- Shall clearly specify in the design documents the quality and characteristics (geometric, mechanical, and physical) of the FRP bars, as indicated in Table 3-1, and shall define the class in accordance with Table 3-3.
- Shall recommend to the Field Engineer, depending on the importance and scale of the application, the execution of tests to be performed to verify some or all of the geometric, mechanical, or physical properties provided by the manufacturer in the technical data sheets.

Contractor

- Shall select and use FRP bars with the properties specified by the Designer, purchased from Manufacturers that have completed the qualification process described in §11.1.
- Shall verify that the products are accompanied by comprehensive technical data sheets that specify the values of their mechanical and physical properties.
- Shall confirm, together with the Field Engineer, that the products comply with the Designer's specifications. If materials with the specified properties are unavailable, possible alternatives shall be agreed upon with both the Designer and/or the Field Engineer.

Field Engineer

- Plays a decisive role in product acceptance.
- Shall verify, both during the procurement phase and upon delivery, that the supplied material complies with the designer's specifications.
- Shall confirm the origin of the supplied material. FRP bars may bear the Manufacturer's mark or be supplied in bundles provided with labels or tags containing all necessary traceability information.
- Shall verify the geometric, mechanical, and physical properties of the products by reviewing the Declaration of Performance and Conformity (DoPC) under EU Regulation 2024/3110 in

the case of CE-marked products (also checking that the Certificate of Constancy of Performance and Conformity (CCPC) issued by a notified body is valid), or the equivalent certifications in other cases.
- Shall perform, for products qualified through CVT, acceptance checks in accordance with the procedures specified in *LG- FRP bars*.
- May, for CE-marked products, decide to perform additional on-site acceptance tests as indicated in Table 3-5, since the acceptance procedures of the *LG-FRP bars* are not mandatory.

Testing Laboratories

- Shall have proven experience in the experimental characterization of fibre-reinforced materials.
- Shall be equipped with appropriate testing and measurement facilities.
- Shall perform experimental tests in accordance with specific Standards for fibre-reinforced materials and, in particular, for FRP bars.
- Shall issue detailed test reports including all relevant information about the testing equipment and measured results.
- Shall operate in compliance with UNI CEI EN ISO/IEC 17025, "*Requisiti generali per la competenza dei laboratori di prova e di taratura*" (*General requirements for the competence of testing and calibration laboratories)*.

Compliance and Safety Inspector

- Shall verify the quality of the materials used by checking the Declaration of Performance and Conformity (DoPC) under EU Regulation 2024/3110 for CE-marked products, or through accompanying certificates for supplied materials.
- Shall verify the Field Engineer's acceptance of materials.
- Shall review the results of any acceptance tests required by the Field Engineer.

13 APPENDIX D – Experimental calibration of the deflection formula for FRP-reinforced concrete flexural members

The following procedure may be used to experimentally determine, with greater accuracy, the influence of the bond characteristics of specific FRP bars on the calculation of deflections in FRP-RC flexural members.

For the evaluation of deflections, the following expression can be adopted:

$$f = f_1 \cdot (1-\gamma) + f_2 \cdot \gamma$$
$$\gamma = 1 - \beta_1 \cdot \beta_2 \left(\frac{M_{cr}}{M_{max}} \right)^m \tag{14.1}$$

The parameters introduced above are defined in §7.3.

Based on a test population consisting of at least five concrete elements reinforced with FRP bars and tested in four-point bending, the midspan deflections shall be measured at specified load levels, ensuring that no less than 5 measurements are recorded for each test within the load range of 20% to 60% of the ultimate load.

Using the experimental data and the analytical formulation in Equation (14.1), the coefficients β_1 and m may be calibrated using an appropriate statistical analysis, such as the maximum likelihood method.

In accordance with §7.3, the coefficient β_2 shall be taken equal to 1.0, since the applied loads during the experimental tests may be considered short-term loads, unless the loading is cyclic, in which case $\beta_2 = 0.5$ shall be used.

14 APPENDIX E – The bond–slip relationship between FRP bars and concrete

14.1 INTRODUCTION

As described in Chapter 5, the proper composite action between an FRP bar and concrete is ensured by the bond mechanism that develops between the two through tangential stresses along their interface. The transfer of tangential stresses at the FRP bar–concrete interface can be analytically represented by an interface law $\tau(s)$ (the bond–slip relationship), which associates the slip s (relative displacement between bar and concrete) with the corresponding shear stress τ acting along the interface surface. This law mainly depends on: the mechanical properties of the materials (normal and shear elastic moduli, Poisson's ratio), the geometrical characteristics of the bars (shape, diameter, or equivalent dimension), the surface treatment of the bars (sand coating, grooves, ribs, indentations, or protrusions produced through various manufacturing techniques). Figure 14-1 shows examples of different types of FRP bars currently available on the market.

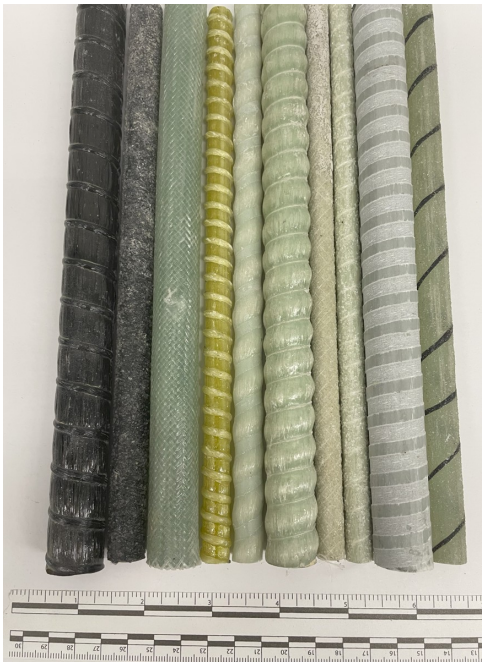

Figure 14-1 - Examples of various types of FRP bars available commercially.

The bond–slip relationship may be obtained experimentally through specific tests, as described in § 5.3. Depending on the surface treatment of the bars, the bar shape can vary and is characterized by different values of the bond strength τ_b. Bond failure of FRP bars may occur either: at the bar–concrete interface (where adhesion is governed primarily by chemical–physical bonding), or within the surrounding concrete, due to the formation of compressed struts (bond governed by both adhesion and mechanical interlocking), depending on the surface configuration. These mechanisms, in turn, influence the analytical formulations to be used to represent the experimental laws.

Although the FRP bar–concrete bond behavior may strongly depend on the specific geometrical and mechanical properties of the bar—and should ideally be characterized individually for each product—the following sections present analytical formulations that guide modeling the FRP bar–concrete bond

both in terms of the $\tau(s)$ relationship and the maximum bond stress τ_b.

14.2 THEORETICAL FORMULATIONS FOR THE FRP BAR–CONCRETE BOND RELATIONSHIP

The analytical model proposed by (Eligehausen et al., 1983, known as the BEP model), initially developed for deformed steel bars, was subsequently modified and recalibrated by Cosenza et al. (1996) (the so called modified BEP model) to represent better the bond mechanism of FRP bars (Figure 15-2a) and later simplified by (Pecce et al., 2001) by removing the residual stress branch (Figure 15-2b). Unlike steel bars with mechanical interlock, FRP bars often do not exhibit an apparent horizontal plateau after reaching the maximum bond stress. Consequently, in both formulations shown in Figure 14-2, the descending branch is modeled as a linear softening segment after the peak stress.

For the bond model with residual strength (Figure 15-2a), the three branches are defined as follows:

$$\tau(s) = \tau_b \cdot \left(\frac{s}{s_b}\right)^{\alpha} \qquad s \le s_b \tag{15.1}$$

$$\tau(s) = \tau_b - p\left(s - s_b\right) \qquad s_b < s \le s_r \tag{15.2}$$

$$\tau(s) = \tau_r \qquad s > s_r \tag{15.3}$$

$$\text{being } p = \frac{\tau_b - \tau_r}{s_r - s_b} \tag{15.4}$$

For the bond model without residual strength (Figure 15-2b), the first branch is given by Eq. (15.1), while the second branch is defined as:

$$\tau(s) = \tau_b - p\left(s - s_b\right) \qquad s_b < s \le s_u \tag{15.5}$$

$$\text{being } p = \frac{\tau_b}{s_u - s_b} \text{ e } \tau(s) = 0 \text{ per } s > s_u .$$

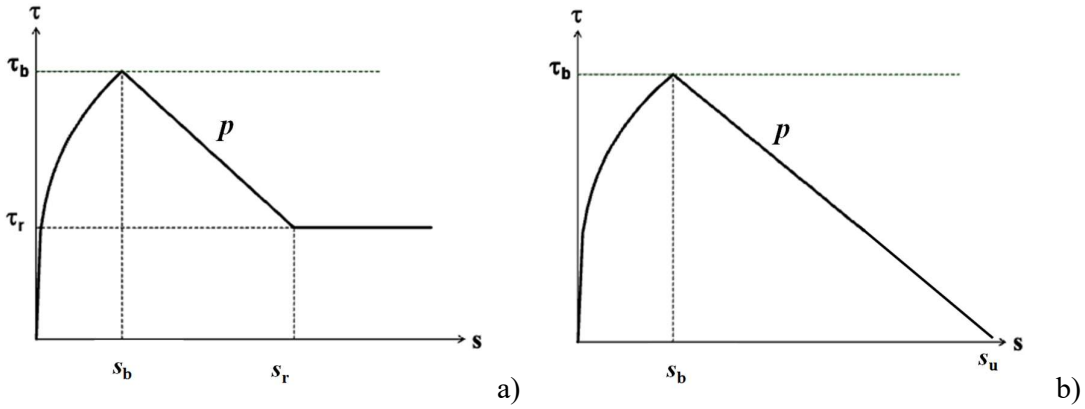

Figure 14-2 - Bond–slip laws for FRP bars: (a) modified BEP model with residual strength; (b) modified BEP model without residual strength

The number of parameters to be identified for the modified BEP model is five for the three-branch

formulation: $\tau_b, \tau_r, s_b, s_r, \alpha$ or τ_b, s_b, α, p and s_r (or τ_r). For the two-branches model, the parameters are only four: τ_b, s_b, α and p. The following section guides the determination of the maximum bond stress τ_b, in relation to the concrete strength and the bond class defined in § 5.3.

Referring to the model shown in Figure 14-2b (Eqs. 15.1 and 15.5), and based on literature data, two parameter ranges are suggested. For bond governed mainly by chemical–physical adhesion (Figure 14-3a): $s_b = 0.10 \div 0.35$ mm; $\alpha = 0.45 \div 0.50$, $p = 0.01 \div 0.05$ N/mm^3. For bond involving mechanical interlocking (Figure 14-3b): $s_b = 1.5 \div 1.75$ mm; $\alpha = 0.30 \div 0.45$, $p = 0.10 \div 0.20$ N/mm^3.

It is noted that, since $\alpha \leq 1$, the initial branch tends to exhibit a vertical slope as $s \rightarrow 0$.

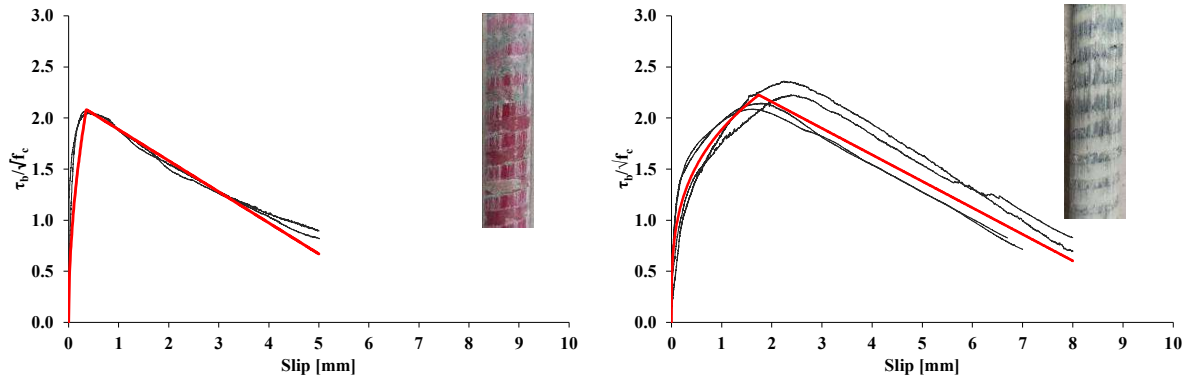

(a) (b)

Figure 14-3 - Experimental and analytical bond–slip relationships from Eqs. (15.1) and (15.5): (a) bond law based on chemical–physical adhesion; (b) bond law based on mechanical interlocking.

A slightly different formulation for the ascending branch was proposed by (Cosenza et al., 1997) and later discussed by (Focacci et al., 2020; 2024). In this model, the ascending portion of the bond–slip curve (Figure 14- 4a) is defined as:

$$\tau(s) = \tau_b \cdot \left(1 - \exp(-\frac{s}{s_b})\right)^{\beta} \qquad \tau \leq \tau_b \tag{15.6}$$

This formulation, characterized by a vertical initial slope at $s = 0$, accurately describes the early-stage bond mechanism governed by chemical adhesion at the FRP–concrete interface. The three parameters required to define the law fully are: τ_b, s_b, β. While the assessment of τ_b is discussed in the next section, the following typical ranges are suggested for the other parameters: $s_b = 1.70 \div 5.70$ mm; $\beta = 0.37 \div 1.17$.

Figure 14- 4b, compares the experimental ascending branches of the bond–slip curves obtained in experimental bond tests on CFRP bars and the analytical trend given by Eq. (15.6) where $\tau_b = 16.6$ MPa, $s_b = 4.14$ mm, $\beta = 0.7$ (Leone, 2005).

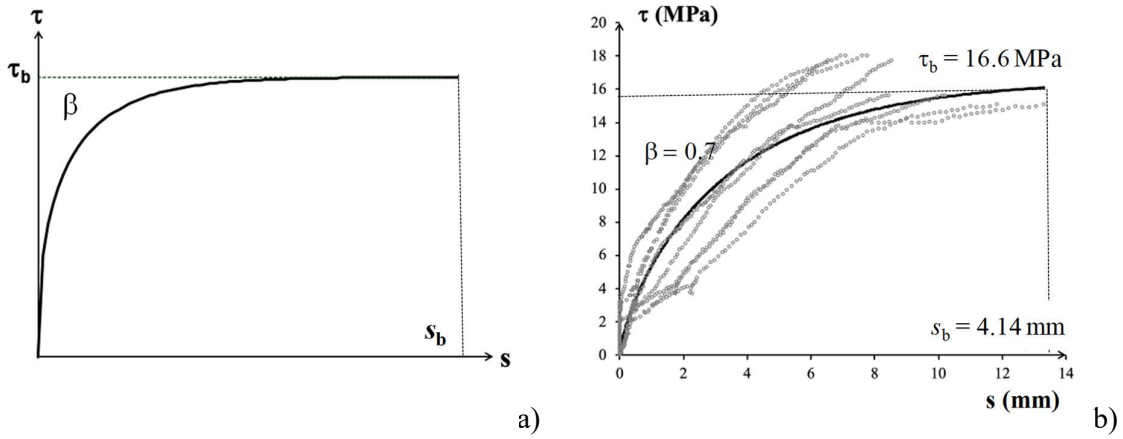

Figure 14- 4 - (a) Exponential ascending branch according to Eq. (15.6); (b) comparison between experimental and analytical bond–slip laws for the ascending branch given by Eq. (15.6) (Leone, 2005).

Essential References

1. Eligehausen R., Popov E.P., Bertero V.V. (1983) *Local bond stress–slip relationships of deformed bars under generalized excitations.* University of California, Berkeley, EERC Report UCB/EERC 83/23.
2. Cosenza E., Manfredi G., Realfonzo R. (1997) *Behavior and modeling of bond of FRP rebars to concrete.* J. Mater. Civ. Eng., 1(2): 40–51.
3. Cosenza E., Manfredi G., Realfonzo R. (1996) *Bond characteristics and anchorage length of FRP rebars.* Proc. 2nd Int. Conf. on Advanced Composites Materials in Bridge Structures (ACMBS-II), Montreal.
4. Pecce M., Manfredi G., Realfonzo R., Cosenza E. (2001) *Experimental and analytical evaluation of bond properties of GFRP bars.* J. Mater. Civ. Eng., 13(4): 282–290.
5. Leone M. (2005). *Interface analysis of FRP-reinforced concrete elements.* Ph.D. Thesis, University of Salento.
6. Focacci F., Nanni A., Bakis C.E. (2000) *Local bond–slip relationship for FRP reinforcement in concrete.* J. Compos. Constr., 4(1): 24–31.
7. Focacci F., Rahman M.M., D'Antino T., Carloni C. (2024) *FRP strips externally bonded to quasi-brittle substrates: discussions and advances of open research topics.* J. Compos. Constr., 28(6): 04024055.

14.3 EVALUATION OF THE MAXIMUM BOND STRESS

The peak stress of the bond–slip relationship, τ_b, can be obtained from experimental bond tests performed on embedment lengths equal to five times the effective bar diameter, as described in §5.3.
In the literature and design Guidelines, various formulations are provided to estimate τ_b primarily as a function of the bar diameter and the concrete compressive strength (Tighiouart et al., 1998; Okelo et al., 2005; Lee et al., 2008; *fib* Model Code 2020).
For this document, an extensive experimental database (622 tests) of bond (pull-out) tests on FRP bars of different types (in terms of surface treatment, fiber type, and diameter), embedded in concrete with compressive strength f_{cm} ranging from 22 MPa to 80 MPa and with bonded lengths equal to five times the bar diameter, was analyzed. The experimental results were examined in terms of peak shear stress, assuming it to be constant along the bonded length $\ell_b = 5d_{b,eff}$, hence, $\tau_b = \dfrac{F_{max}}{\pi d_{b,eff} \cdot \ell_b}$.

The experimental data were divided into two subgroups based on classification within the two bond quality classes defined in §5.3. Since these classes refer to a bond test carried out with concrete of a strength f_{ck} = 20 MPa (f_{cm} = 28 MPa), the assignment of each data point to one of the two classes was made by correcting the experimental value of the maximum bond shear stress, τ_b, by the ratio $\sqrt{\frac{28}{f_{cm}}}$ where f_{cm} is the mean compressive strength of the concrete used in the test.

For each subgroup, the following correlation laws were obtained:

Bond class 1: $\tau_b = 3.3 \cdot \sqrt{f_{cm}}$ (15.7a)

Bond class 2: $\tau_b = 2.2 \cdot \sqrt{f_{cm}}$ (15.7b)

Figure 14-5 shows the comparison between the experimental (not corrected by $\sqrt{\frac{28}{f_{cm}}}$) and theoretical values of the peak bond stress, τ_b, predicted by Eqs. (15.7) for the two bond classes. The comparison shows that Eqs. (15.7) predict in average quite well the experimental values of τ_b for the two bond classes and can be used to study the local bond behavior by means of numerical or analytical models, when specific experimental information about τ_b is not available.

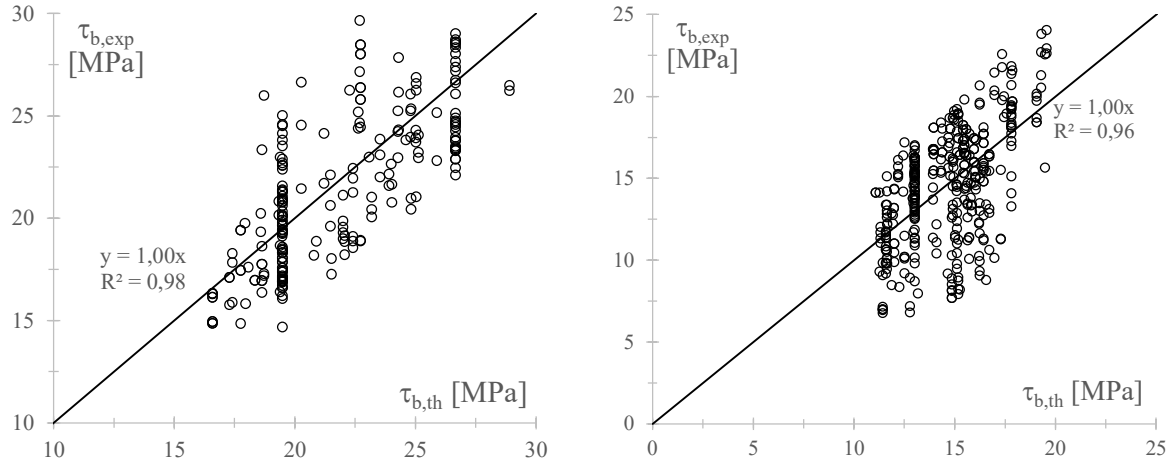

Figure 14-5 - Comparison between experimental and theoretical values given by Eqs. (15-7) for the peak bond stress, τ_b: (a) Bond class 1; (b) Bond class 2.

In some formulas reported in the literature and in design codes, the bond shear stress also depends on the bonded length of the bar, ℓ_b (Xue et al., 2016; Basaran et al., 2020; Sun-Jae Yoo et al., 2022; Wang et al., 2024; ACI 440.11-22). These formulations were calibrated based on bond-test results from bars with different bonded lengths, ℓ_b, also higher than $5d_b$ and assuming the shear stress computed at the experimental peak load constant along ℓ_b. Thus, these values are not comparable with τ_b, but they should be interpreted as predictive expressions of the average bond shear stress, $\overline{\tau_b}$, acting along the bar, under the simplified assumption of a uniform stress distribution. This average stress may be used to estimate the anchorage length required to reach a given normal stress, σ_f, in

the bar through the following expression:

$$\ell_a = \frac{A_b \cdot \sigma_f}{\pi d_{b,eff} \cdot \overline{\tau_b}} \tag{15.8}$$

The methods for calculating the anchorage length in this Document are discussed in detail in §15.4.

Essential References

1. ACI Committee 440 (2022) *ACI CODE 440.11-22 — Building code requirements for structural concrete reinforced with Glass Fiber Reinforced Polymer (GFRP) bars.* American Concrete Institute, Farmington Hills, MI.
2. Basaran B., Kalkan I. (2020) *Development length and bond strength equations for FRP bars embedded in concrete.* Composite Structures, 25.
3. *fib* (2024). *Model Code for Concrete Structures 2020, v1.2.* ISBN 978-2-88394-175-5.
4. Lee J.Y., Kim T.Y., Kim T.J., Yi C.K., Park J.S., You Y.C., Park Y.H. (2008) *Interfacial bond strength of glass fiber reinforced polymer bars in high-strength concrete.* Composites Part B: Engineering, 39(2), pp. 258-270.
5. Okelo R., Yuan R.L. (2005) *Bond strength of fiber reinforced polymer rebars in normal strength concrete.* Journal of Composites for Construction, 9(3), pp. 203-213.
6. Tighiouart B., Benmokrane B., Gao D. (1998) *Investigation of bond in concrete members with fibre reinforced polymer (FRP) bars.* Construction and Building Materials, 12(8), pp. 453-462.
7. Wang J., Xiao F., Lai Z., Yang J., Tian S. (2024) *Bond of FRP bars with different surface characteristics to concrete.* Structures, 59.
8. Xue W., Yang Y., Zheng Q., Fang Z. (2016) *Modeling of bond of sand-coated deformed glass fibre-reinforced polymer rebars in concrete.* Polymers and Polymer Composites, 24(1), pp. 45-56.

14.4 ANCHORAGE LENGTH

The evaluation of the anchorage length for FRP bars was carried out following the procedure proposed in the explanatory document (CEN/TC 250/SC 2 N2087) of Eurocode 2 (EN 1992-1-1, 2023) for steel reinforcement. For concrete elements reinforced with steel bars, the design value of the anchorage length, ℓ_a, for straight bars, is given by the following expression:

$$\ell_a = k_\ell \cdot k_{cp} \cdot \phi \cdot \left(\frac{\sigma_{sd}}{435}\right)^{3/2} \cdot \left(\frac{25}{f_{ck}}\right)^{1/2} \cdot \left(\frac{d_{ba}}{20}\right)^{1/3} \cdot \left(\frac{1.5 d_{ba}}{c_d}\right)^{1/2} \geq 10 d_{ba} \tag{15.9}$$

where:

- d_{ba} is the diameter of the steel bar;
- σ_{sd} is the design stress in the steel bar under the ULS combination of actions;
- f_{ck} is the characteristic cylindrical compressive strength of concrete;
- k_ℓ is a statistically calibrated coefficient: equal to 50 for design conditions under permanent and variable loads, or 35 for accidental load conditions;
- k_{cp} accounts for the effect of the position of the bar during the concrete casting on the bond behavior: in (EN 1992-1-1, 2023) it is taken as 1.0 or 1.2 for good or poor bond conditions, respectively;
- $c_d = \min(c_x, c_y, 0.5c_s, 3.75d_b)$ where c_x, c_y e c_s are defined in Figure 14-6;

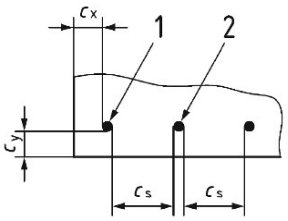

Figure 14-6 - Geometric quantities for the definition of c_d.

Eq. (15.9) was derived (CEN/TC 250/SC 2 N2087) by inverting the following regression formula for the stress in the bar as a function of the bonded length ℓ_a and of the dimensionless terms $\left(\frac{f_{ck}}{25}\right),\left(\frac{25}{d_{ba}}\right),\left(\frac{c_d}{d_{ba}}\right)$, as follows:

$$\sigma_{sd} = 54 \cdot \left(\frac{\ell_a}{d_{ba}}\right)^{11/20} \cdot \left(\frac{f_{ck}}{25}\right)^{1/4} \cdot \left(\frac{25}{d_{ba}}\right)^{1/5} \cdot \left(\frac{c_d}{d_{ba}}\right)^{1/4} \tag{15.10}$$

For this document, based on an extensive database of experimental pull-out tests (851 specimens) performed on FRP bars of different types (surface treatment, fiber type, diameter) embedded in concrete with compressive strength f_{ck} ranging from 15 MPa to 90 MPa, Eq. (15.10) was recalibrated for the two bond-quality classes defined in § 5.3. Specifically, 283 data points corresponded to Bond class 1 FRP bars, and 568 to Bond class 2; the tests covered bonded lengths ranging from $2.5d_{b,eff}$ to $40d_{b,eff}$, where $d_{b,eff}$ is the effective bar diameter.

Since these were pull-out tests, it was not possible to estimate the contribution of the term $\left(\frac{1.5d_{b,eff}}{c_d}\right)$ in (15.9). Therefore, to determine the new exponents of the terms $\left(\frac{f_{ck}}{25}\right),\left(\frac{20}{d_{b,eff}}\right),\left(\frac{\ell_a}{d_{b,eff}}\right)$, a multivariate regression analysis was carried out based on the comparison between the experimental values of the tensile stress acting in the FRP bar, $\sigma_{f,exp}$, corresponding to a bond failure for a fixed bond length ℓ_a, and the theoretical values $\sigma_{f,th,m}$ (see Figures 15-7) predicted by the following expressions:

- For bond quality Class 1: $\tau_b > 15$ MPa:

$$\sigma_{fd} = k \cdot \left(\frac{\ell_a}{d_{b,eff}}\right)^{1/2} \cdot \left(\frac{f_{ck}}{25}\right)^{2/5} \cdot \left(\frac{20}{d_{b,eff}}\right)^{1/5} \tag{15.11}$$

- For bond quality Class 2: 7 MPa $< \tau_b <$ 15 MPa:

$$\sigma_{fd} = k \cdot \left(\frac{\ell_a}{d_{b,eff}}\right)^{2/3} \cdot \left(\frac{f_{ck}}{25}\right)^{2/5} \cdot \left(\frac{20}{d_{b,eff}}\right)^{1/5} \tag{15.12}$$

In Eqs. (15.11) and (15.12), the symbols retain their previous meanings, except for the coefficient *k,* which was calibrated using the comparisons with experimental data, and the stress σ_{fd}, which represents the mean, the characteristic or the design value of the tensile stress acting in the FRP bar in case of bond failure for a fixed ℓ_a, in function of the value of *k*. The best fitting on the experimental values of $\sigma_{f,exp}$ allowed, indeed, estimating the mean value of *k*, while the '*design by testing*' procedure in

agreement with (EN 1990:2023) allowed estimating the fractile values 5% (characteristic value) and 0.1% (design value), as listed in Table 15-1 for the two datasets (FRP bars in Bond class 1 or 2). In Table 15-1, also the coefficient of variation (CoV) associated to the variable $\sigma_{f,exp} / \sigma_{f,th,m}$, the number of collected experimental data, and the range of variation of the mean compressive strength of concrete, f_{cm}, are listed.

Finally, by inverting Eq. (15.11) and (15.12), the following expressions for the anchorage length are obtained in order to warrant that the FRP bar can sustain the design tensile stress σ_{fd}:

- For bond quality Class 1: $\tau_b > 15$ MPa:

$$\ell_a = k_\ell \cdot d_b \cdot \left(\frac{\sigma_{fd}}{500}\right)^2 \cdot \left(\frac{25}{f_{ck}}\right)^{4/5} \cdot \left(\frac{d_{b,eff}}{20}\right)^{2/5} \qquad k_\ell = \left(\frac{500}{k}\right)^2 \tag{15.13}$$

- For bond quality Class 2: 7 MPa < τ_b < 15 MPa:

$$\ell_a = k_\ell \cdot d_b \cdot \left(\frac{\sigma_{fd}}{500}\right)^{3/2} \cdot \left(\frac{25}{f_{ck}}\right)^{3/5} \cdot \left(\frac{d_{b,eff}}{20}\right)^{3/10} \qquad k_\ell = \left(\frac{500}{k}\right)^{3/2} \tag{15.14}$$

Also Eq. (15.13) and (15.14) may have the meaning of mean, characteristic or design value depending on the adopted values of k_ℓ listed in Table 15-1.

Table 14-1 - Mean, characteristic, and design values of the coefficients k and k_ℓ

Bond class	k_ℓ			k			Database		
	mean	5%	design	mean	5%	design	CoV	data	f_{cm} [MPa]
1	12.0	19.0	30.0	144	115	92	0.13	283	22-80
2	19.3	34.0	65.0	69.5	48	31	0.24	568	26-77

Figure 14-7a and Figure 14-7b show the comparisons between the experimental, $\sigma_{f,exp}$, and the mean predicted values, $\sigma_{f,th,m}$, of the tensile stresses in FRP bars in case of bond failure, according to Eq. (15.11) for Class 1 and Eq. (15.12) for Class 2. In Figures 15-7, also the lines corresponding to the characteristic and deign values of the theoretical tensile stress are plotted.

For design purposes, the nominal diameter d_b of the bar shall be used in place of the effective diameter $d_{b,eff}$ employed during calibration.

The Eqs. (15.13) and (15.14) are plotted in Figure 14-8a and Figure 14-8b for FRP bars falling in Bond class 1 and 2, respectively, in terms of the dimensionless anchorage length, ℓ_a/d_b and with reference to mean (m), characteristic (k), and design (d) values. The formulas were applied assuming f_{ck} = 25 MPa and σ_{fd} = 490 MPa (for example: $\sigma_{fd} = \frac{f_{ftk}}{\gamma_f}\eta_T \cdot \eta_a \cdot \eta_{c,l} = \frac{1000}{1.25}0.9 \cdot 0.85 \cdot 0.8 = 490$ MPa).

Figure 14.9 presents the same curves assuming f_{ck} = 30 MPa and σ_{fd} = 490 MPa.

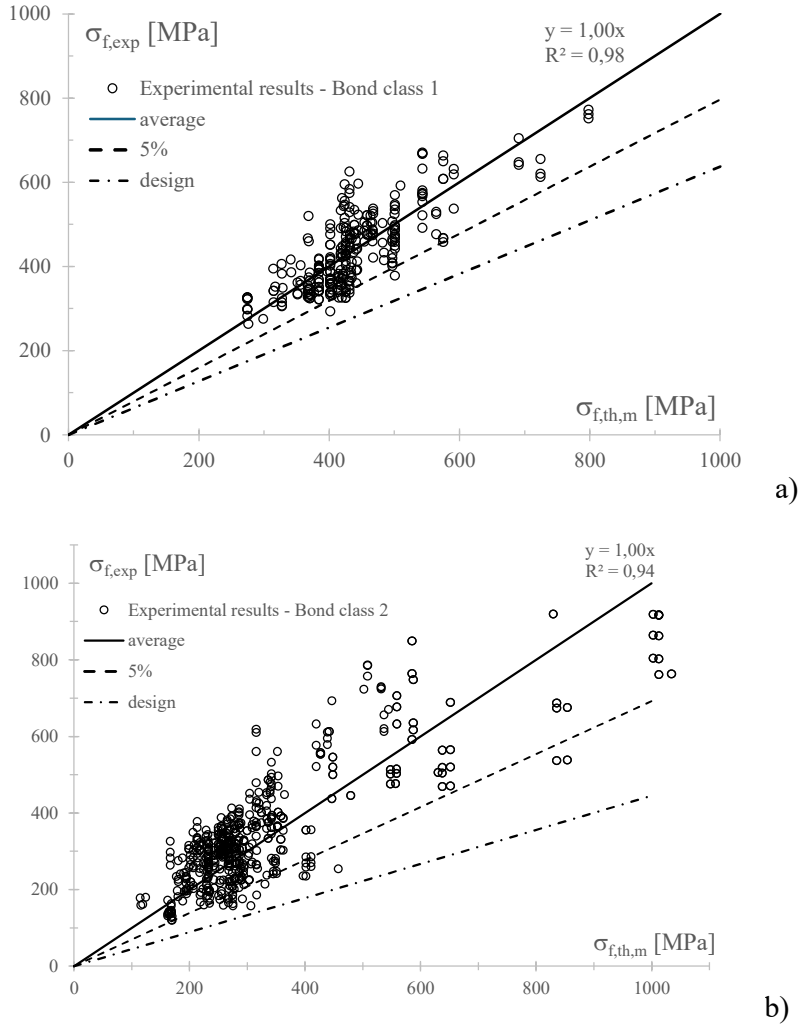

Figure 14-7 - Comparison between experimental and predicted tensile stresses in FRP bars from bond tests: (a) Class 1, Eq. (15.11); (b) Class 2, Eq. (15.12)

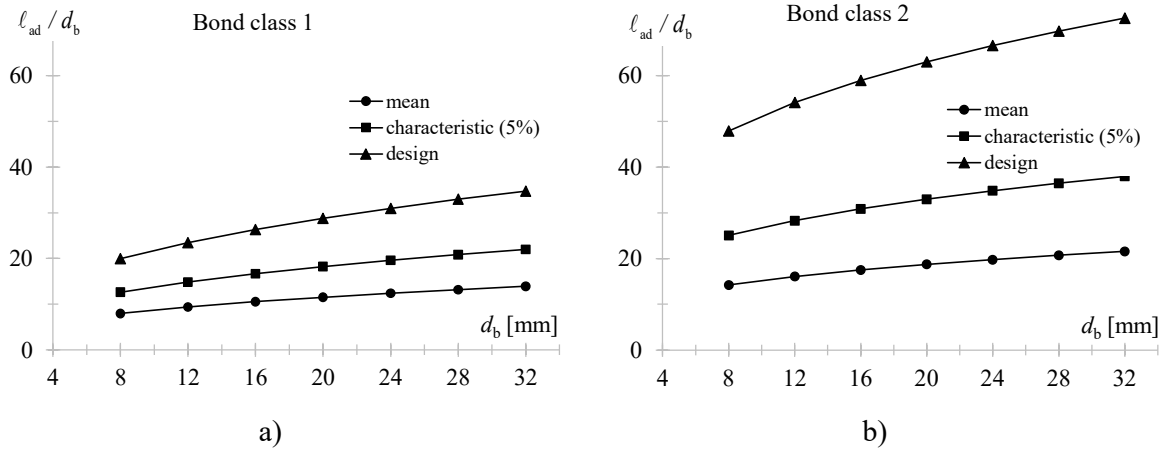

Figure 14-8 - Variation of ℓ_a/d_b with bar diameter for f_{ck} =25 MPa and σ_{fd} = 490 MPa: a) Bond class 1, Eq. (15.13); b) Bond class 2, Eq. (15.14).

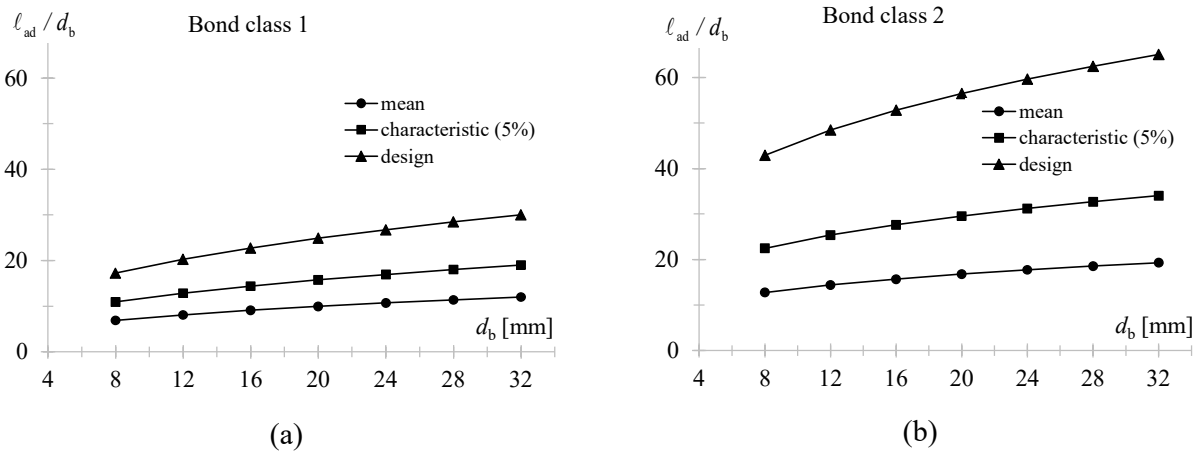

Figure 14.9 - Variation of ℓ_a/d_b with bar diameter for f_{ck} =30 MPa e σ_{fd} = 490 MPa: a) Bond class 1, Eq. (15.13); b) Bond class 2, Eq. (15.14).

Eqs. (5.13) and (15.14) are illustrated in Figure 14-10 for FRP bars falling in Bond class 1 and 2, as well as for conventional steel bars, assuming f_{ck} =30 MPa and the same applied stress for both FRP and steel bars equal to 383 MPa = 440/1.15 MPa. The plot shows that the ℓ_a/d_b ratio for FRP bars falling in Bond class 2 is only slightly higher than that required for steel bars, while FRP bars falling in Bond class 1 exhibit considerably shorter values of required anchorage lengths.

In applications, a minimum anchorage length not lower than 300 mm and 20 d_b for any diameter or Bond class is required. In Figure 15-10, dotted lines represent these limitations in function fo the bar diameter.

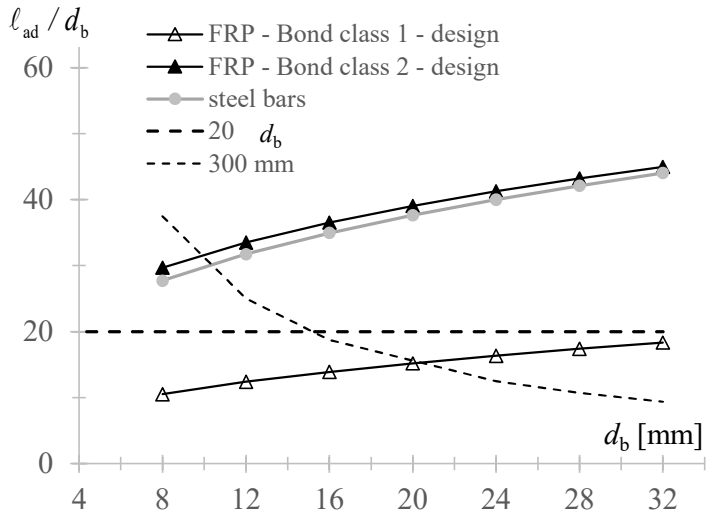

Figure 14-10 - Variation of ℓ_a/d_b with bar diameter for FRP bars falling in Bond class 1 (Eq. 15.13), Bond class 2 (Eq. 15.14), and steel bars (Eq. 15.9) for f_{ck} =30 MPa and σ_{fd} = 383 MPa.

Eqs. (15.13) and (15.14) do not account for the influence of concrete cover thickness, as they were calibrated on pull-out tests where bond failure always occurred thanks to high values of the concrete cover. Thus, for design purposes, the effect of cover thickness may be included by adding the

multiplicative factor $\left(\frac{1.5d_{\mathrm{b}}}{\mathrm{c_d}}\right)^{1/2}$ to Eqs. (15.13) and (15.14), by analogy with the provisions for steel bars in (EN 1992-1-1, 2023), provided it is greater than 1.

Finally, the term related to bar position during casting may also be introduced in Eqs. (15.13) and (15.14) via the coefficient k_{cp}, which accounts for the effect of bar position on the bond mechanism, as indicated in (EN 1992-1-1; 2023) for steel reinforcement (1.0 or 1.2 for good or poor bond conditions).

Essential References

1. CEN/TC 250/SC 2 N2087 (2023) *Background document EN 1992-1-1, Eurocode 2 – Design of concrete structures – Part 1-1: General rules and rules for buildings, bridges, and civil engineering structures.*
2. EN 1990 (2023) *Eurocode 0 – Basis of structural and geotechnical design.* European Committee for Standardization (CEN), Brussels.
3. EN 1992-1-1 (2023) *Eurocode 2 – Design of concrete structures – Part 1-1: General rules and rules for buildings, bridges, and civil engineering structures.* European Committee for Standardization (CEN), Brussels.

15 APPENDIX F: Simplified verification method under fire conditions

15.1 GENERAL CONCEPTS

The incremental–iterative procedure typically used to construct a moment–curvature relationship for nonlinear analysis of RC sections can be readily implemented in computational software, but it is less straightforward for manual calculations. Moreover, during fire exposure, the axial load N_{Ed}, may vary due to restraint effects. When adopting the member analysis approach in EN 1992-1-2, for flexural elements, it is reasonable to assume $N_{Ed}=0$.

A simplified method can therefore be used to evaluate the fire-resisting bending moment capacity of unprotected FRP-RC members exposed to fire on the tension-fiber side, $M_{Rd,fi,t}$, consistent with the 500 °C isotherm method of EN 1992-1-2 originally developed for steel-RC members. The temperature field is obtained through thermal analysis, and $M_{Rd,fi,t}$, is determined by considering a "reduced section" composed of:

(a) concrete at temperatures below 500 °C (with mechanical properties equal to those at 20 °C)
(b) FRP reinforcement with temperature-dependent mechanical properties, as specified in §6.2 (1).

It should be noted that the stress–strain relationship for concrete recommended by EN 1992-1-2—and applicable also at 20 °C for fire design—differs from the usual room-temperature law, as it includes a pronounced softening branch. For FRP bars, an elastic–brittle behavior can be assumed.

15.2 THERMAL ANALYSIS

The temperature field within a structural element can be evaluated using conventional thermal analyses under the design fire curve. Following approaches proposed in the literature and in international standards, simplified methods can also be adopted to estimate, with reasonable accuracy, the temperature of FRP bars in concrete elements exposed to fire from below. These methods refer to the ISO 834 standard temperature–time fire curve (EN 1363-1:2020) and to the thermal properties of concrete recommended by the Eurocodes.

For example, the temperature of the FRP bar, $T(t,c)$, may be evaluated as follows:

$$\begin{aligned} &t \le 30\,\text{min} : \mathrm{T}(t,c) = \mathrm{A}_1(c)\cdot t + 20 \qquad [°\mathrm{C}] \\ &t > 30\,\text{min} : \mathrm{T}(t,c) = \mathrm{A}_2(c)\cdot t + \mathrm{A}_3(c)\cdot t^{\mathrm{A}_4(c)} \qquad [°\mathrm{C}] \end{aligned} \tag{16.1}$$

where t is the exposure time to fire [min], c is the concrete cover [mm], and $A_i(c)$ are temperature-dependent coefficients listed in Table 15-1.

Table 15-1: Coefficients $A_i(c)$

c [mm]	A_1	A_2	A_3	A_4
20	11.538	-4586.1	4221.2	0.0470
30	8.032	-2326.8	1935.7	0.0854
40	5.685	-892.3	592.2	0.1774
50	3.997	-509.4	271.7	0.2561
60	2.792	-312.0	130.8	0.3400

15.3 MECHANICAL ANALYSIS

After determining the temperature distribution within the section and reducing the mechanical properties of the materials according to their temperature-dependent behavior, the fire design bending resistance, $M_{Rd,fi,t}$, can be calculated using the same assumptions as under normal temperature conditions (see §6.1).

The failure modes of the section remain the same as under ambient conditions:

- Failure mode 1: attainment of the maximum tensile strain in the FRP bars, $\varepsilon_{tot,f}$, while the concrete strain remains below the limit ε_{cu}^{*};
- Failure mode 2: attainment of the ultimate compressive strain in the concrete, ε_{cu}^{*}, while the FRP bar strain remains below its limit value, $\varepsilon_{tot,f}$.

The total strain in the FRP reinforcement can be expressed as:

$$\varepsilon_{tot,f} = \varepsilon_{fu,T} + \varepsilon_{T,f} \tag{16.2}$$

where $\varepsilon_{fu,T}$ is the ultimate strain of the FRP bar at temperature T and $\varepsilon_{T,f}$ is the thermal strain corresponding to the bar temperature. The ultimate strain $\varepsilon_{fu,T}$ must be provided in accordance with §6.2 (1).

Because the stress–strain relationship of concrete under fire conditions includes a descending branch (Figure 15-1), the maximum compressive strain of concrete, ε_{cu}^{*}, should be limited to a nominal value.

Figure 15-1 - Stress–strain relationship of concrete at 20 °C under fire conditions (EN 1992-1-2)

In case of Failure Mode 1 (FRP rupture), assuming plane sections remain plane, the maximum concrete compressive strain is given by:

$$\varepsilon_c = (\varepsilon_{fu,T} + \varepsilon_{T,f}) \cdot \frac{x}{d - x} \le \varepsilon_{cu}^{*} \tag{16.3}$$

where x is the neutral axis depth and d is the distance between the extreme compression fiber and the centroid of the FRP tension reinforcement.

In case of Failure Mode 2 (Concrete crushing), the maximum concrete strain equals its limiting value, and the FRP strain is related to it by:

$$\varepsilon_c = \varepsilon_{cu}^{*} \tag{16.4}$$

$$\varepsilon_{tot,f} = \varepsilon_{cu}^{*} \cdot \frac{d-x}{x} \le (\varepsilon_{fu,T} + \varepsilon_{T,f}) \tag{16.5}$$

In both failure modes, the neutral axis depth, x, is determined from axial force equilibrium:

$$N_c - N_f = 0 \tag{16.6}$$

where N_c and N_f are the compressive and tensile resultants, respectively.

The fire design bending resistance, $M_{Rd,fi,t}$, can then be determined from moment equilibrium, using the dimensionless coefficients ψ and λ corresponding to the stress–strain relationship of concrete at 20 °C under fire exposure (see Figure 15-2). In fire conditions, partial factors for materials are taken as unity, i.e., $f_{cd} = f_{ck}$.

For Failure Mode 1 (FRP rupture), the following equations can be written:

$$\psi \cdot b \cdot x \cdot f_{cd} - \rho_f(T) \cdot f_{ftd} \cdot A_f = 0 \tag{16.9}$$

$$M_{Rd,fi,t} = \rho_f(T) \cdot f_{ftd} \cdot A_f \cdot (d - \lambda x) = 0 \tag{16.10}$$

where $\rho_f(T)$ is the reduction factor of the tensile strength of the FRP bar, f_{ftd}, at time t and temperature T, provided by the manufacturer (see point (1) of § 6.2).

For Failure Mode 2 (Concrete crushing), the following equations can be written:

$$\psi \cdot b \cdot x \cdot f_{cd} - \rho_E(T) \cdot E_f \cdot A_f \cdot \left(\varepsilon_{cu}^{*} \frac{d-x}{x} - \varepsilon_{T,f} \right) = 0 \tag{16.11}$$

$$M_{Rd,fi,t} = \rho_E(T) \cdot E_f \cdot A_f \cdot \left(\varepsilon_{cu}^{*} \frac{d-x}{x} - \varepsilon_{T,f} \right) \cdot (d - \lambda \cdot x) = 0 \tag{16.12}$$

where $\rho_E(T)$ is reduction factor of the elastic modulus of the FRP bar at time t and temperature T provided by the manufacturer (see point (1) in§6.2).

In general, the coefficients ψ and λ depend on the limiting strain ε_{cu}^{*}. However, extensive parametric analyses (Nigro et al., 2014), based on the incremental–iterative procedure described earlier, showed that for estimating the bending resistance of any section, the values, $\varepsilon_{cu}^{*} = 0.010$, $\psi = 0.75$ and $\lambda = 0.50$ can be safely adopted.

To ensure the maximum bending resistance of FRP-reinforced members, adequate anchorage of the bars shall be provided. Under fire exposure, the anchorage length of the FRP bars at time t, $\ell_{ad,fi,t}$, and the ultimate anchorage stress, $\sigma_{fd,fi,t}$, can be determined using Eqs. (5.2) and (5.5), respectively, for ambient conditions, assuming bond loss occurs when bar temperature exceeds a conventional limit temperature. Based on (Katz et al., 2000), this limit temperature may conservatively be set at 50 °C, since for all tested bars, bond strength reductions below 10% were observed at bar temperatures below 50 °C.

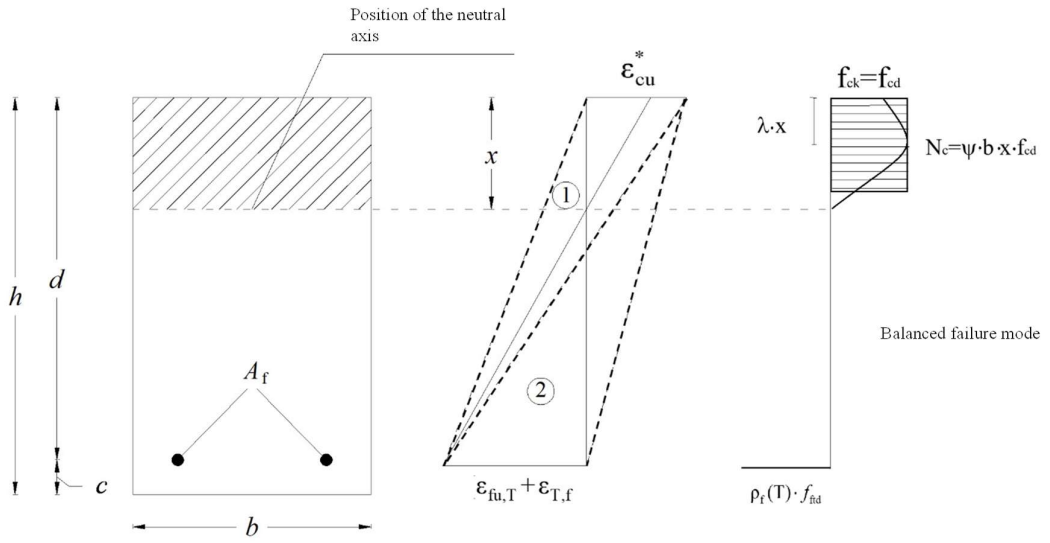

Figure 15-2 - Strains and stresses at the ultimate limit state (ULS).

For regions where the bar temperature exceeds 50 °C, the additional protected anchorage length, $\ell_{ad,fi,t,T>50°C}$, to be added to that from Eqs. (5.2), can be calculated as:

$$\ell_{ad,fi,t,T>50°C} = B_1(c) + B_2(c) \cdot t^{-B_3(c)} \quad [°C] \tag{16.15}$$

where t is the fire exposure time [min], c is the concrete cover [mm], $B_i(c)$ are the coefficients listed in Table 15-2. Eq. (16.15) was derived by interpolating thermal analysis results reported by (Nigro et al., 2012a).

The total anchorage length, $\ell_{ad,tot}$, required to ensure proper bond performance is the sum of the effective anchorage length, $\ell_{ad,fi,t}$, and the non-effective length, $\ell_{ad,fi,t,T>50°C}$ (see Figure 15-3 and Figure 15-4) .

Table 15-2: Coefficients $B_i(c)$

c [mm]	B_1	B_2	B_3
20	-23.43	15.38	0.4660
30	-104.68	58.45	0.2821
40	-159.79	87.28	0.2437
50	-2159.93	1995.44	0.0280
60	-13582.44	13347.56	0.0055

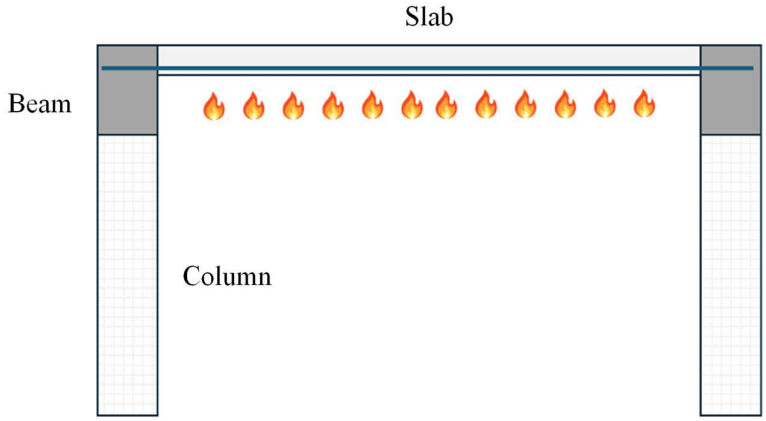

Figure 15-3 - Slab exposed to fire with anchorage of FRP bars in the supporting beam.

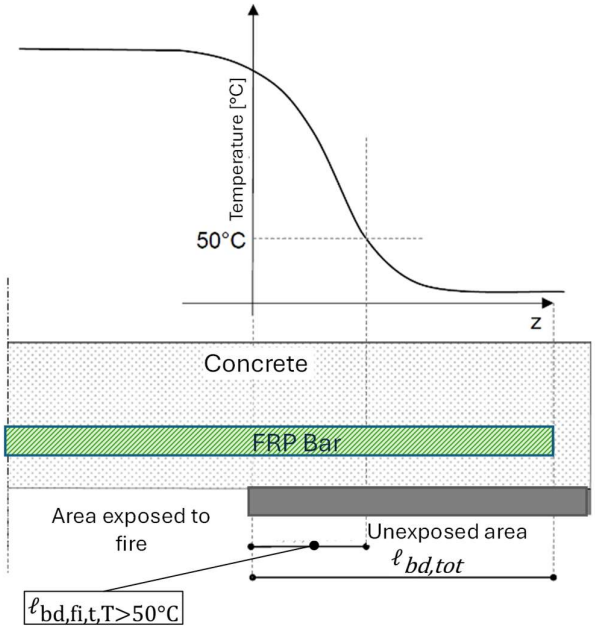

Figure 15-4 - Anchorage length of FPR bars in a not exposed area.

Essential References

1. Nigro E., Cefarelli G., Bilotta A., Manfredi G., Cosenza E. (2011) *Fire resistance of concrete slabs reinforced with FRP bars. Part I: experimental investigations on the mechanical behavior*, Composites: Part B, Engineering, 42, pp. 1739-1750, ISSN: 1359-8368

2. Nigro E., Cefarelli G., Bilotta A., Manfredi G., Cosenza E. (2011) Fire resistance of concrete slabs reinforced with FRP bars. Part II: experimental results and numerical simulations on the thermal field, Composites: Part B, Engineering, 42, pp. 1751-1763, ISSN: 1359-8368.

3. Nigro E., Cefarelli G., Bilotta A., Manfredi G., Cosenza E. (2012) *Performance under fire situations of concrete members reinforced with FRP rods: bond models and design nomograms*, J. of Composites for Construction, 16, pp. 395-406, ISSN: 1090-0268.

4. Nigro E., Cefarelli G., Bilotta A., Manfredi G., Cosenza E. (2014) *Guidelines for flexural resistance of FRP reinforced concrete slabs and beams in fire*, Composites: Part B, Engineering, pp. 103-112, ISSN: 1359-8368.

5. Bilotta A., Compagnone A., Esposito L., Nigro E. (2020) *Structural behaviour of FRP reinforced concrete slabs in fire*, Engineering Structures, 221, ISSN 0141-0296.

16 APPENDIX G: Design examples

16.1 FLEXURAL DESIGN OF RC BEAMS WITH FRP BARS

The following example illustrates the flexural verification at both ultimate (ULS) and serviceability (SLS) limit states for a simply supported RC beam reinforced with GFRP bars.

Each verification is performed by assuming the minimum number of bars required to satisfy the corresponding design condition, to determine which check governs the design.

Geometry of the Section

A rectangular section is considered, having the following dimensions:

- Width, b = 300 mm,
- Total height, h = 600 mm,
- Concrete cover (from bar centroid), c = 40 mm,
- Effective depth, d = 560 mm

The beam has a span of L = 5 m and is simply supported at both ends.

Material Properties

- Concrete class C30/37 with:
  - Characteristic cylinder strength: f_{ck} = 30 MPa
  - Mean compressive strength: $f_{cm} = f_{ck} + 8$ = 38 MPa.
  - Mean tensile strength: $f_{ctm} = 0.3 \cdot f_{ck}^{2/3} = 2.9$ MPa
  - Secant modulus of elasticity (mean value): $E_c = 22000 \cdot \left(\frac{f_{cm}}{10} \right)^{2/3} = 32837$ MPa
- Glass FRP (GFRP) bars of class E45/850, characterized by:
  - Characteristic tensile strength: f_{ftk0} = 850 MPa
  - Mean modulus of elasticity: E_f = 45 GPa
  - Nominal diameter: d_b = 14 mm.

Loads

The beam is subjected to the following uniformly distributed loads:

- Dead loads (structural + non-structural): $g_1 + g_2$ = 13.0 kN m
- Live load (characteristic value): q_k = 14.5 kN/m

The beam is placed under the exposure condition 2 (outdoor, dry environment), where the member is directly exposed to solar radiation.

16.1.1 Ultimate Limit State (ULS) Verification

For the ULS load combination, the stress in the FRP bars shall not exceed:

$$f_{ftd} = \eta_T \cdot \eta_a \cdot \eta_{c,l} \frac{f_{ftk0}}{\gamma_f}$$

with f_{ftk0} = 850 MPa, η_a = 0.85 e η_T = 0.9, γ_f=1.25.

The reduction coefficient $\eta_{c,l}$, accounts for the viscoelastic effects in the bars caused by the quasi-

permanent loads, and it is computed as (see Eq. (4.4a)):

$$\eta_{c,l} = 1 - (1 - \eta_c) \cdot \frac{\sigma_{f,qp}}{f_{ftk,c}}$$

where, for glass FRP bars $\eta_c = 0.50$ (Table 4-2), so $f_{ftk,c} = \eta_c \cdot f_{ftk0} = 0.50 \cdot 850 = 425$ MPa and $\sigma_{f,qp}$ is the stress in the FRP bars under the quasi-permanent load combination, calculated as follows.

The design value of the load under the quasi-permanent condition is:

$$q_{d,qp} = g_1 + g_2 + 0.3 q_k = 17.35 \text{ kN /m}$$

The corresponding maximum bending moment is:

$$M_{max,qp} = \frac{q_{d,qp} \cdot L^2}{8} = \frac{17.35 \cdot 5^2}{8} = 54.22 \text{ kN m}$$

which is greater than the cracking moment of the section, calculated (neglecting the FRP contribution) as $M_{cr} = \frac{b \cdot h^2}{6} f_{ctm} = 52.14$ kN m.

Assuming 4 bars of $d_b = 14$ mm (total area $A_f = 615$ mm^2), the tension $\sigma_{f,qp}$ is given by:

$$\sigma_{f,qp} = \frac{M_{max,qp}}{0.9 A_f \cdot d} = \frac{54.22 \cdot 10^6}{0.9 \cdot 615 \cdot 560} = 175 \text{ MPa.}$$

Hence:

$$\eta_{c,l} = 1 - (1 - 0.5) \cdot \frac{175}{0.5 \cdot 850} = 0.79$$

Therefore, the design tensile strength of the FRP bars is $f_{ftd} = 0.85 \cdot 0.9 \cdot 0.79 \cdot \frac{850}{1.25} = 413$ MPa.

The design value of the distributed load under the ULS loading condition is $q_{d,SLU} = 1.3 g_1 + 1.5 g_2 + 1.5 q_k = 39.6$ kN /m and the corresponding maximum design bending moment is $M_{Ed} = 123.6$ kN m.

The design compressive strength of concrete is $f_{cd} = 0.85 \cdot \frac{30}{1.5} = 17.0$ MPa, where $f_{ck} = 30$ MPa.

Assuming failure by tensile rupture of FRP bars, the equilibrium of axial forces gives:

$$\psi f_{cd} \cdot b \cdot x = A_f \cdot f_{ftd} \rightarrow x = \frac{A_f \cdot f_{ftd}}{\psi f_{cd} \cdot b} = 84 \text{ mm}$$

with $\psi = 0.593$, obtained iteratively using the strain-based expressions (see Eq. (6.8) where $\overline{\varepsilon_c} = 1000 \varepsilon_c$):

$$\psi = \begin{cases} \overline{\varepsilon_c}\left(0.5 - \dfrac{\overline{\varepsilon_c}}{12}\right) \text{ per } \overline{\varepsilon_c} \le 2.0 \\ 1 - \dfrac{2}{3\overline{\varepsilon_c}} \qquad \text{per } 2.0 \le \overline{\varepsilon_c} \le 3.5 \end{cases} \tag{6.8}$$

and:

$$\varepsilon_c = \varepsilon_{ftd} \cdot \frac{x}{(d-x)} = \frac{413}{45000} \cdot \frac{84}{(560-84)} = 0.0016 < 0.0020.$$

The rotational equilibrium gives:

$$M_{Rd} = \psi \cdot b \cdot x \cdot f_{cd} \cdot (0.5h - \lambda \cdot x) + A_f \cdot f_{ftd} \cdot (0.5h - c) = 134.7 \text{ kN m} > M_{Ed} = 123.6 \text{ kN m}$$

where $\lambda = 0.364$ calculated from Eq. (6.10), where $\overline{\varepsilon_c} = 1000\varepsilon_c$:

$$\lambda = \begin{cases} \dfrac{8 - \overline{\varepsilon_c}}{4\left(6 - \overline{\varepsilon_c}\right)} \qquad \text{per } \overline{\varepsilon_c} \le 2.0 \\ \dfrac{\varepsilon_c\left(3\overline{\varepsilon_c} - 4\right) + 2}{2\overline{\varepsilon_c}\left(3\overline{\varepsilon_c} - 2\right)} \quad \text{per } 2.0 \le \overline{\varepsilon_c} \le 3.5 \end{cases} \tag{6.10}$$

The calculated neutral axis depth and concrete strain confirm that failure occurs by FRP rupture (failure mode 1).

The provided tensile reinforcement (4 bars with d_b = 14 mm, $A_f = 615$ mm^2) exceeds the minimum required value, given by the following expression:

$$A_{f,min} = 0.34 \cdot \frac{b \cdot d \cdot f_{ctm}}{f_{ftd}} = A_{f,min} = 0.34 \cdot \frac{300 \cdot 560 \cdot 2.9}{413} = 401 \text{ mm}^2.$$

Anchorage length calculation

It is assumed $\sigma_{fd} = f_{ftd} = 413$ MPa.

For Class 1 bond quality, with k_{cp} =1, neglecting $\left(\dfrac{1.5d_b}{c_d}\right)^{1/2} < 1$, and using Eq. (5.2a):

$$\ell_a = k_{cp} \cdot k_\ell \cdot d_b \cdot \left(\frac{\sigma_{fd}}{500}\right)^2 \cdot \left(\frac{25}{f_{ck}}\right)^{4/5} \cdot \left(\frac{d_b}{20}\right)^{2/5} \cdot \left(\frac{1.5d_b}{c_d}\right)^{1/2} \text{ being } k_\ell = 30$$

$$\ell_a = 30 \cdot 14 \cdot \left(\frac{413}{500}\right)^2 \cdot \left(\frac{25}{30}\right)^{4/5} \cdot \left(\frac{14}{20}\right)^{2/5} = 215 \text{ mm } (\approx 15\ d_b)$$

For Class 2 bond quality, with k_{cp} =1, neglecting $\left(\frac{1.5d_b}{c_d}\right)^{1/2} < 1$, and using Eq. (5.2b):

$$\ell_a = k_{cp} \cdot k_\ell \cdot d_b \cdot \left(\frac{\sigma_{fd}}{500}\right)^{3/2} \cdot \left(\frac{25}{f_{ck}}\right)^{3/5} \cdot \left(\frac{d_b}{20}\right)^{3/10} \cdot \left(\frac{1.5d_b}{c_d}\right)^{1/2} \text{ being } k_\ell = 65$$

$$\ell_a = 65 \cdot 14 \cdot \left(\frac{413}{500}\right)^{3/2} \cdot \left(\frac{25}{30}\right)^{3/5} \cdot \left(\frac{14}{20}\right)^{3/10} = 550 \text{ mm} = (\approx 39\ d_b)$$

For FRP bars in Bond class 1: $\ell_a = 215\,\text{mm} < 300\,\text{mm}$ and 20 d_b = 280 mm → adopt $\ell_{ad} = 300\,\text{mm}$.

For FRP bars in Bond class 2: $\ell_a = 550\,\text{mm} > 300\,\text{mm}$ and 20 d_b = 280 mm → adopt $\ell_{ad} = 550\,\text{mm}$.

Given that exposure condition 2 applies, no environmental reduction factor is required.

Since the moment capacity obtained with 4 bars of d_b = 14 mm exceeds the design moment by about 10%, it is possible, in case of using FRP bars falling in Bond class 2, to reduce the anchorage length by recalculating the working stress in the bars as a function of the adopted anchorage length (using Eq. (5.5b)), and then updating the axial and rotational equilibrium equations accordingly.

16.1.2 Serviceability Limit State (SLS) Checks

16.1.2.1 Stress Verification

For the quasi-permanent load combination, the stress in the FRP bars shall satisfy the following limit (as per Eq. (7.1)):

$$\sigma_f \le \eta_T \cdot \eta_a \cdot \eta_c \cdot \frac{f_{ftk0}}{\gamma_f} = 325 \text{ MPa}$$

where:

f_{ftk0} = 850, η_T = 0.90, η_a = 0.85, η_c = 0.50, γ_f =1.0.

The design value of the distributed load under the quasi-permanent loading condition:

$$q_{d,qp} = g_1 + g_2 + 0.3q_k = 17.35 \text{ kN /m}$$

The corresponding maximum bending moment is $M_{max,qp} = \frac{q_{d,qp} \cdot L^2}{8} = \frac{17.35 \cdot 5^2}{8} = 54.22$ kN m. This moment exceeds the cracking moment of the section, calculated (neglecting the FRP contribution) as $M_{cr} = \frac{b \cdot h^2}{6} f_{ctm} = 52.14$ kN m. Therefore, the section under the maximum moment is cracked.

To account for creep effects in the compressed concrete, the effective modulus is used (§7.2) $E_{c,eff} = \frac{E_c}{1 + \varphi(t, t_0)} = \frac{32837}{1+2} = 10946$ MPa, assuming a creep coefficient $\varphi(t, t_0) = 2$.

Considering the four bars of d_b = 14 mm (total area $A_f = 615$ mm^2) defined based on the ULS verification, the stress in the FRP bars is computed (assuming linear-elastic behavior of materials, Eq.

(7.4)) as:

$$\sigma_f = \alpha_f \cdot \frac{M_{max,qp}}{I_2} \cdot (d - x_2)$$

where:

- $\alpha_f = \frac{E_f}{E_{c,eff}} = \frac{45000}{10946} = 4.1$ is the modular ratio between FRP and concrete;
- x_2 and I_2 are, respectively, the neutral axis depth and the moment of inertia of the cracked transformed section, where only the tensile FRP bars are included and transformed into equivalent concrete through the coefficient α_f.

The neutral axis is determined by setting the static moment of the cracked transformed section equal to zero:

$$S_n = 0 \quad \rightarrow \quad \frac{b \cdot x_2^2}{2} - \alpha_f \cdot A_f \cdot (d - x_2) = 0 \Rightarrow x_2 = 89.1 \text{ mm}$$

The corresponding moment of inertia is:

$$I_2 = \frac{b \cdot x_2^3}{3} + \alpha_f \cdot A_f \cdot (d - x_2)^2 = 631.8 \cdot 10^6 \text{ mm}^4$$

Hence, the tensile stress in the FRP bars is:

$$\sigma_f = \alpha_f \cdot \frac{M_{max,qp}}{I_2} \cdot (d - x_2) = 4.1 \cdot \frac{54.22 \cdot 10^6}{631.8 \cdot 10^6} \cdot (560 - 89.1) = 166 \text{ MPa} < 325 \text{ MPa}.$$

The compressive stress in concrete is calculated as follows and shall also satisfy the limits prescribed by current Standards under the quasi-permanent combination of actions:

$$\sigma_c = \frac{M_{max,qp}}{I_2} \cdot x_2 = \frac{54.22 \cdot 10^6}{631.8 \cdot 10^6} \cdot 89.1 = 7.6 \text{ MPa} < 0.45 f_{ck} = 13.5 \text{ MPa}.$$

Both checks are satisfied.

It can be noted that the minimum number of bars required to meet both stress limits is three; in fact, using three bars of d_b = 14 mm (total area $A_f = 462$ mm^2) yields $\sigma_f = 220$ MPa < 325 MPa and $\sigma_c =$ 8.7 MPa < 13.5 MPa.

For the characteristic (rare) load combination, the stress in the FRP bars shall satisfy Eq. (7.2):

$$\sigma_f \le \eta_T \cdot \eta_a \cdot 0.8 \cdot \frac{f_{ftk0}}{\gamma_f} = 520 \text{ MPa}$$

Where f_{fk} = 850 MPa, $\eta_a = 0.85$, $\eta_T = 0.9$, $\gamma_f = 1.0$.

The corresponding load and moment are $q_{d,rare} = g_1 + g_2 + q_k = 27.5$ kN /m and $M_{max,rara} = \frac{q_{d,rara} \cdot L^2}{8} = \frac{27.5 \cdot 5^2}{8} = 85.94$ kN m.

For this combination, the short-term modulus of concrete (not affected by creep) is used, $E_c = 32837$ MPa, and, hence, the modular ratio is $\alpha_f = \frac{E_f}{E_c} = \frac{45000}{32837} = 1.37$.

Using 4 bars of d_b = 14 mm ($A_f = 615$ mm^2), with $\alpha_f = 1.37$, the following results are obtained:

- x_2 = 53.4 mm, $I_2 = 231.7 \cdot 10^6$ mm^4,
- $\sigma_f = \alpha_f \cdot \frac{M_{max,rare}}{I_2} \cdot (d - x_2) = 1.37 \cdot \frac{85.94 \cdot 10^6}{231.7 \cdot 10^6} \cdot (560 - 53.4) = 257.5$ MPa < 520 MPa.
- $\sigma_c = \frac{M_{max,rare}}{I_2} \cdot x_2 = \frac{85.94 \cdot 10^6}{231.7 \cdot 10^6} 53.4 = 19.8$ MPa > 0.60 f_{ck} = 18.0 MPa

Thus, to satisfy the maximum compressive stress limit in the concrete, the number of FRP bars must be increased to 5 (with d_b = 14 mm). However, to satisfy the tensile stress limit in the FRP bars, only 2 bars (with d_b = 14 mm) would be sufficient, since in this case σ_f = 510 MPa < 520 MPa.

16.1.2.2 Crack Width Verification

For the quasi-permanent load combination under exposure condition 2, the maximum crack width (Eq. (7.6)) shall satisfy:

$w_k = k_{1/r} \cdot s_{r,max} \cdot (\varepsilon_{fm} - \varepsilon_{cm}) \leq 0.6$ mm

It is assumed the same modular ratio adopted for the quasi-permanent stress checks:

$\alpha_f = \frac{E_f}{E_{c,eff}} = \frac{45000}{10946} = 4.11$ with $\varphi(t, t_0) = 2$.

Using 5 bars with d_b = 14 mm (total area $A_f = 769.3$ mm^2), as defined by the rare combination stress check, the neutral axis and moment of inertia of the cracked section, where the only FRP bars in tension are transformed by α_f, are:

$x_2 = 98.6$ mm, $I_2 = 772.1 \cdot 10^6$ mm^4

hence: $k_{1/r} = \frac{h - x_2}{d - x_2} = \frac{600 - 98.6}{560 - 98.6} = 1.087$.

The maximum crack spacing, $s_{r,max}$, is obtained using equation (7.7):

$$s_{r,max} = \beta_w \cdot \left(k_c \cdot c_{geom} + k_{\phi/r} \cdot k_{fl} \cdot k_b \frac{f_{ctm} \cdot d_b}{\tau_{bfm} \cdot \rho_{l,ef}} \right)$$

where:

- β_w = 1.7;
- k_c = 1.5;
- $c_{geom} = c - 0.5 d_b = =$ 33 mm (distance of the bar axis from the tensile face, net of radius);
- $k_{\phi/r}$ = 0.25;

- $k_{fl} = \dfrac{h - h_{c,ef}}{h}$, where $h_{c,ef}$ is the effective tension zone height (Eq. (7.11):

$h_{c,ef} = \min\{c + 5d_b; 10d_b; 3.5c; h - x_2; h/2\} = \min\{40 + 5 \cdot 14; 140; 3.5 \cdot 40; 600 - 99; 300\} = 110$ mm,

so $k_{fl} = \dfrac{h - h_{c,ef}}{h} = \dfrac{600 - 110}{600} = 0.82$.

- $k_b = 0.9$ (bottom casting position);
- $\tau_{mf} = 1.25 \cdot f_{ctm}$ for Bond class 1 FRP, or $\tau_{mf} = 1.50 \cdot f_{ctm}$ for Bond class 2.
- $\rho_{l,ef} = \dfrac{A_f}{A_{c,ef}} = \dfrac{A_f}{b \cdot h_{c,ef}} = \dfrac{769.3}{300 \cdot 110} = 0.0233$

The maximum crack spacing is therefore:

$s_{r,max} = 209$ mm (Bond class 1)

$s_{r,max} = 234$ mm (Bond class 2)

Next, compute the mean strain difference between FRP and concrete in the cracked tensile zone:

$$\varepsilon_{fm} - \varepsilon_{cm} = \left(\frac{\sigma_f}{E_f} - k_t \frac{f_{ctm}}{E_f \cdot \rho_{l,ef}} + k_t \frac{f_{ctm}}{E_c} \right) \geq \frac{\sigma_f}{E_f}(1 - k_t)$$

The FRP stress for the quasi-permanent combination is:

$$\sigma_f = \alpha_f \cdot \frac{M_{max,qp}}{I_2} \cdot (d - x_2) = 4.11 \cdot \frac{54.20 \cdot 10^6}{769.2 \cdot 10^6} \cdot (560 - 99) = 133.2 \text{ MPa}$$

with $M_{max,qp} = 54.20$ kN m.

Assuming:

- $k_t = 0.4$ (long-duration or repeated load),
- $f_{ctm} = 2.9$ MPa
- $E_c = = 32837$ MPa
- $E_f = = 45000$ MPa

Then:

$$\varepsilon_{fm} - \varepsilon_{cm} = 0.00182 \geq 0.6 \frac{\sigma_f}{E_f} = 0.00178$$

The maximum crack width is, thus:

- for FPR bars with Bond class 1:

$w_k = 1.087 \cdot 209 \cdot 0.00182 = 0.414 \text{ mm} < 0.60 \text{ mm}$

- for FPR bars with Bond class 2:

$w_k = 1.087 \cdot 234 \cdot 0.00182 = 0.463 \text{ mm} < 0.60 \text{ mm}$

Thus, the check is satisfied with 5 bars with d_b = 14 mm for both bond classes.

It is worth noting that for Bond class 1, 4 bars with d_b = 14 mm satisfy the quasi-permanent crack-width limit, since $w_k = 1.085 \cdot 240 \cdot 0.00228 = 0.594 \text{ mm} < 0.60 \text{ mm}$.

For the frequent loading combination, the limit is (Eq. (7.6) and Table 7-1):

$w_k = k_{1/r} \cdot s_{r,max} \cdot (\varepsilon_{fm} - \varepsilon_{cm}) \leq 0.7 \text{ mm}$

Assuming $\varphi(t,t_0) = 1$, representing an intermediate time between t = 0 and $t = \infty$ (for steel RC $\varphi(t,t_0) = 1$ corresponds to a modular ratio of about 15). Then:

$$E_{c,eff} = \frac{E_c}{1+\varphi(t,t_0)} = \frac{32837}{2} = 16418 \text{ and } \alpha_f = \frac{E_f}{E_{c,eff}} = \frac{45000}{16418} = 2.74.$$

Assuming 5 bars with d_b = 14 mm ($A_f = 769.3$ mm^2) and α_f = 2.74, the cracked transformed section gives:

x_2= 82 mm, $I_2 = 536.9 \cdot 10^6$ mm^4, $k_{1/r} = \frac{h - x_2}{d - x_2} = \frac{600 - 82}{560 - 82} = 1.08$

With the same parameters as before (β_w = 1.7, k_c = 1.5, $c_{geom} = 33$ mm, $k_{\phi/r} = 0.25$; $k_{fl} = \frac{h - h_{c,ef}}{h}$=0.82, $h_{c,ef}$ = 110 mm, k_b = 0.9, $\rho_{l,ef} = 0.023$), the example keeps:

$s_{r,max} = 209$ mm (for FRP bars with Bond class 1)

$s_{r,max} = 234$ mm (for FRP bars with Bond class 2)

The FRP stress for the frequent combination:

$$\sigma_f = \alpha_f \cdot \frac{M_{max,fr}}{I_2} \cdot (d - x_2) = 2.74 \cdot \frac{63.3 \cdot 10^6}{536.9 \cdot 10^6} \cdot (560 - 82) = 154.4 \text{ MPa}$$

with:

$$M_{max,fr} = \frac{q_{d,fr} \cdot L^2}{8} = \frac{20.0 \cdot 5^2}{8} = 63.3 \text{ kNm and } q_{d,fr} = g_1 + g_2 + 0.5 q_k = 20.25 \text{ kN/m}.$$

Again, assuming:

- $k_t = 0.4$
- $f_{ctm} = 2.9$ MPa
- $E_c = = 32837$ MPa
- $E_f = = 45000$ MPa

$$\varepsilon_{fm} - \varepsilon_{cm} = 0.00292 \geq 0.6\frac{\sigma_f}{E_f} = 0.00206$$

The maximum crack width is, thus:

- For FRP bars with Bond class 1:

  $w_k = 1.084 \cdot 209 \cdot 0.00292 = 0.52$ mm < 0.7 mm

- For FRP bars with Bond class 1

  $w_k = 1.084 \cdot 234 \cdot 0.00292 = 0.58$ mm < 0.7 mm

Thus, the check is satisfied with 5 bars with d_b = 14 mm for both bond classes.

16.1.2.3 Deflection verification

The check under the rare load combination is done assuming 5 bars with d_b = 14 mm (A_f = 769.3 mm^2), as defined in the previous checks, and adopting the limit $f/L \leq 1/250$.

The maximum bending moment for the rare combination (already computed) is $M_{max,rare} = \frac{q_{d,rare} \cdot L^2}{8} = \frac{27.5 \cdot 5^2}{8} = 85.9$ kN m.

For the rare combination, we use the instantaneous concrete modulus, $E_c = 32837$, hence the modular ratio for FRP bars is $\alpha_f = \frac{E_f}{E_c} = \frac{45000}{32837} = 1.37$.

For this α_f and for $A_f = 769.3$ mm^2, the neutral axis and cracked-section inertia (from the rare-combo stress check) are x_2 = 59.3 mm and $I_2 = 285.2 \cdot 10^6$ mm^4.

The deflection calculated assuming the cracked (partially transformed) section is:

$$f_2 = \frac{5}{384}\frac{q_{d,rare} \cdot L^4}{E_c \cdot I_2} = \frac{5}{384}\frac{27.5 \cdot 5000^4}{32837 \cdot 285.2 \cdot 10^6} = 23.90 \text{ mm}$$

The calculation of deflection considering the gross (State 1) section can be done neglecting any FRP in compression and using α_f=1.37 and $A_f = 769.3$ mm^2, as follows:

$$x_1 = \frac{0.5b \cdot h^2 + \alpha_f \cdot A_f \cdot d}{b \cdot h + \alpha_f \cdot A_f} = 301.5 \text{ mm}$$

$$I_1 = \frac{b \cdot h^3}{12} + b \cdot h \cdot (0.5h - x_1)^2 + \alpha_f \cdot A_f \cdot (d - x_1)^2 = 5470.9 \cdot 10^6 \text{ mm}^4$$

$$f_1 = \frac{5}{384}\frac{q_{d,rare} \cdot L^4}{E_c \cdot I_1} = \frac{5}{384}\frac{27.5 \cdot 5000^4}{32837 \cdot 5470.9 \cdot 10^6} = 1.25 \text{ mm}$$

The combined deflection (Eq. (7.5)), is given by:

$$f = f_1 \cdot (1-\gamma) + f_2 \cdot \gamma$$

$$\gamma = 1 - \beta_1 \cdot \beta_2 \left(\frac{M_{cr}}{M_{max}} \right)^2$$

with:

- $\beta_1 = 0.85$ for Bond class 1, and 0.70 for Bond class 2**.**
- $\beta_2 = 1.0$ (short-term loads).
- $M_{max} = M_{max,rare} = 85.94$ kN m.
- M_{cr} is the cracking moment calculated as $M_{cr} = \frac{f_{ctm} \cdot I_1}{(h - x_1)} = 53.10$ kN, which is very close to the simplified one calculated neglecting the FRP contribution ($M_{cr} = \frac{b \cdot h^2}{6} f_{ctm} = 52.14$ kN m).

For bending-dominated members, Eurocode 2 also allows calculating the tensile strength as:

$f_{ctm,fl} = \max\left\{ \left(1.6 - \frac{h}{1000} \right) \cdot f_{ctm}; f_{ctm} \right\}$ which here equals $f_{ctm} = 2.9$ MPa.

Thus, the total deflections result:

- For FRP bars with Bond class 2 ($\beta_1 = 0.70$, $m = 2$)

$$\gamma = 1 - \beta_1 \cdot \beta_2 \left(\frac{M_{cr}}{M_{max}} \right)^2 = 1 - 1.0 \cdot 0.7 \cdot \left(\frac{52.14}{85.94} \right)^2 = 0.74$$

$$f = f_1 \cdot (1-\gamma) + f_2 \cdot \gamma = 1.25 \cdot 0.26 + 23.9 \cdot 0.74 = 18.1 \text{ mm} \rightarrow \frac{f}{L} = \frac{18.1}{5000} = 0.0036 < \frac{1}{250} = 0.004$$

- For FRP bars with Bond class 1 ($\beta_1 = 0.85$, $m = 2$)

$$\gamma = 1 - \beta_1 \cdot \beta_2 \left(\frac{M_{cr}}{M_{max}} \right)^2 = 1 - 1.0 \cdot 0.85 \cdot \left(\frac{52.14}{85.94} \right)^2 = 0.69$$

$$f = f_1 \cdot (1-\gamma) + f_2 \cdot \gamma = 1.25 \cdot 0.31 + 23.9 \cdot 0.69 = 16.8 \text{ mm} \rightarrow \frac{f}{L} = \frac{16.8}{5000} = 0.0034 < \frac{1}{250} = 0.004$$

Assuming 5 bars with $d_b = 14$ mm ($A_f = 769.3$ mm^2), the deflection check is easily satisfied for the $f/L \leq 1/250$. For completeness, we also report results for a reduced reinforcement of 4 bars with $d_b = 14$ mm ($A_f = 615.4$ mm^2).

The maximum bending moment (already computed) is:

$$M_{max,qp} = \frac{q_{d,qp} \cdot L^2}{8} = \frac{17.35 \cdot 5^2}{8} = 54.2 \text{ kN m}$$

For quasi-permanent loading, the effective concrete modulus $E_{c,eff} = \frac{E_c}{1+\varphi(t,t_0)} = \frac{32837}{3} = 10946$ MPa is used and $\alpha_f = \frac{E_f}{E_{c,eff}} = \frac{45000}{10946} = 4.11$ with $A_f = 615.4$ mm^2.

The cracked-section properties were already calculated in the tension checks and are x_2= 89.1 mm and $I_2 = 631.8 \cdot 10^6$ mm^4.

The deflection associated to the cracked section (State 2)is:

$$f_2 = \frac{5}{384}\frac{q_{d,qp} \cdot L^4}{E_c \cdot I_2} = \frac{5}{384} \cdot \frac{17.35 \cdot 5000^4}{10946 \cdot 631.8 \cdot 10^6} = 20.4 \text{ mm}$$

The deflection of the uncracked section (State 1) has to be calculated with α_f=4.11 and $A_f = 615.4$ mm^2, as follows:

$$x_1 = \frac{0.5b \cdot h^2 + \alpha_f \cdot A_f \cdot d}{b \cdot h + \alpha_f \cdot A_f} = 303.6 \text{ mm}$$

$$I_1 = \frac{b \cdot h^3}{12} + b \cdot h \cdot (0.5h - x_1)^2 + \alpha_f \cdot A_f \cdot (d - x_1)^2 = 5568.7 \cdot 10^6 \text{ mm}^4$$

$$f_1 = \frac{5}{384}\frac{q_{d,qp} \cdot L^4}{E_c \cdot I_1} = \frac{5}{384} \cdot \frac{17.35 \cdot 5000^4}{10946 \cdot 5568.7 \cdot 10^6} = 2.3 \text{ mm}$$

The total deflection combining f_1 and f_2 (using Eq. (7.5)):

$$f = f_1 \cdot (1 - \gamma) + f_2 \cdot \gamma$$

$$\gamma = 1 - \beta_1 \cdot \beta_2 \left(\frac{M_{cr}}{M_{max}}\right)^2$$

with:

- β_1 = 0.85, for Bond class 1, and 0.70 for Bond class 2
- β_2 = 0.5 (long-term loads)
- $M_{max} = M_{max,rara}$ = = 85.94 kN m (per §7.3(4))
- $M_{cr} = \frac{f_{ctm} \cdot I_1}{(h - x_1)} = 52.90$ kN m that is very similar to the simplified value previously calculated neglecting the FRP contribute ($M_{cr} = \frac{b \cdot h^2}{6} f_{ctm} = 52.14$ kN m)

The following results are obtained (4 bars with d_b = 14 mm):

- For FRP bars with Bond class 2 (β_1 = 0.70, m = 2)

$$\gamma = 1 - \beta_1 \cdot \beta_2 \left(\frac{M_{cr}}{M_{max}}\right)^2 = 1 - 0.5 \cdot 0.7 \cdot \left(\frac{52.14}{85.94}\right)^2 = 0.87$$

$$f = f_1 \cdot (1-\gamma) + f_2 \cdot \gamma = 0.13 \cdot 2.3 + 0.87 \cdot 20.4 = 18.05 \text{ mm}$$

- For FRP bars with Bond class 1 ($\beta_1 = 0.85$, $m = 2$)

$$\gamma = 1 - \beta_1 \cdot \beta_2 \left(\frac{M_{cr}}{M_{max}} \right)^2 = 1 - 0.5 \cdot 0.85 \cdot \left(\frac{52.14}{85.94} \right)^2 = 0.84$$

$$f = f_1 \cdot (1-\gamma) + f_2 \cdot \gamma = 0.16 \cdot 2.3 + 0.84 \cdot 20.4 = 17.56 \text{ mm}$$

The contribution of shrinkage to the deflection in the quasi-permanent load combination is:

$$f_{sh} = \frac{1}{8} \cdot \frac{M_{sh}}{E_c I_2} \cdot L^2 = \varepsilon_{sh} \cdot \frac{S_c \cdot L^2}{8 \cdot I_2} = \varepsilon_{sh} \cdot \frac{b \cdot x_2^2}{2} \cdot \frac{L^2}{8 \cdot I_2} = 2.06 \text{ mm}$$

with $\varepsilon_{sr} = 0.00035$, $I_2 = 631.8 \cdot 10^6 \text{ mm}^4$, $S_c = \frac{b \cdot x_2^2}{2}$ e x_2= 89.1 mm.

Total deflection:

- For FRP bars with Bond class 2:

$$f_{tot} = f + f_{sr} = 18.05 \text{ mm} + 2.06 \text{ mm} = 20.11 \text{ mm} \rightarrow \frac{f}{L} = \frac{20.11}{5000} = 0.0040 = \frac{1}{250} = 0.004$$

- For FRP bars with Bond class 1:

$$f_{tot} = f + f_{rit} = 17.56 \text{ mm} + 2.06 \text{ mm} = 19.65 \text{ mm} \rightarrow \frac{f}{L} = \frac{19.05}{5000} = 0.0039 < \frac{1}{250} = 0.004$$

16.1.3 Summary of verifications for flexural design

Table 16-1 summarizes the results of the serviceability (SLS) and ultimate limit state (ULS) verifications in terms of the minimum number of bars with nominal diameter d_b = 14 mm required to satisfy each check.

Table 16-1 - Summary of results for SLE and SLU: minimum number of bars d_b = 14 mm needing for satisfying each check

Load combination	SLS Crack Width Control	SLS Stress Limitation	SLS Deflection Control	ULS
ULS				4 bars d_b =14 mm
Quasi-permanent	$w_k \leq 0.6$ mm Bond class 1: 4 bars d_b =14 mm Bond class 2: 5 bars d_b =14 mm	3 bars d_b =14 mm	$f \leq$ L/250 Bond class 1: 4 bars d_b =14 mm* Bond class 2: 4 bars d_b =14 mm*	
Frequent	$w_k \leq 0.7$ mm Bond class 1: 5 bars d_b =14 mm Bond class 2: 5 bars d_b =14 mm			
Rare		5 bars d_b =14 mm	$f \leq$ L/250 Bond class 1: 5 bars d_b =14 mm Bond class 2: 5 bars d_b =14 mm	

*Including the effects of shrinkage

16.2 SHEAR DESIGN OF RC BEAMS WITH FRP STIRRUPS

The following example illustrates the design of shear reinforcement at the Ultimate Limit State (ULS) for a RC beam with GFRP bars. The rectangular cross-section has the following geometry:

- Width: b = 300 mm
- Height: h = 500 mm
- Concrete cover (to the center line of the tensile reinforcement): c = 40 mm
- Effective depth: $d = h\text{-}c$= 460 mm

The beam has a span of L = 5 m and is simply supported at both ends.

The concrete has a strength class C30/37 and, thus, the characteristic strength is f_{ck} = 30 MPa.

The design load combination at the Ultimate Limit State is $q_{d,ULS}$ = 52 kN/m.

The flexural reinforcement is made of GFRP bars with nominal diameter d_b = 16 mm, Class E45/850 (characteristic tensile strength f_{ftk0} = 850 MPa, mean modulus of elasticity E_f = 45 GPa) and the longitudinal reinforcement ratio is ρ = 0.6%.

The shear reinforcement is made of GFRP stirrups falling in the same Class (E45/850) and having a nominal diameter d_b = 8 mm.

For the ULS load combination, the characteristic tensile strength of the GFRP stirrups, in the absence of dedicated experimental data, is assumed to be:

$f_{ubk} = 0.4\, f_{ftk0} = 340$ MPa

and the design value:

$$f_{ubd} = \eta_a \cdot \eta_T \cdot \frac{f_{ubk}}{\gamma_f} = 186 \text{ MPa}$$

where f_{ftk0} = 850 MPa, $\eta_a = 0.85$, $\eta_T = 0.9$, $\gamma_f = 1.40$.

As indicated in Eq. (6.14), no additional reduction coefficient is applied to account for the effects of creep in the bars due to sustained tensile stresses.

The maximum bending moment corresponding to the design load is $M_{Ed,max}$ = 162.5 kN m, while the maximum design shear at the supports is $V_{Ed,max}$ = 130 kN.

The minimum amounts of transverse reinforcement are first evaluated according to §6.8.3 and §6.8.3.1. Adopting GFRP stirrups of nominal diameter d_b = 8 mm, the maximum spacing is calculated as 115 mm at the support section and 330 mm along the span. In addition, it shall be satisfied that ρ_{smin} = 0.1%.

Therefore, the minimum transverse reinforcement is provided as GFRP stirrups with diameter d_b = 8 mm spaced of 100 mm near supports (up to 1 m from each support) and of 300 mm in the remaining portion of the beam (until midspan)

16.2.1 Check at the supports (stirrups spacing 100 mm)

The design shear at the support is $V_{Ed,max}$ = 130 kN. Assuming GFRP stirrups with d_b = 8 mm spaced at s = 100 mm, the design shear resistance is given by Eq. (6.12):

$$V_{Rd} = \min(V_{Rd,f} + V_{Rd,ct}; V_{Rd,c}) \tag{6.12}$$

where $V_{Rd,c}$ is 527.8 kN and is evaluated using Eq. (6.15) assuming $\cot(\theta)$=1:

$$V_{Rd,c} = 0.9b \cdot d \cdot \alpha_c \cdot \nu \cdot f_{cd} \cdot 0.5 \quad (6.15)$$

taking f_{cd} = 17 MPa, ν = 0.5, and α_c = 1 (uncompressed member).

The shear resistance of cracked concrete, $V_{Rd,ct}$ is evaluated using Eqs. (6.11a–c) as follows:

$$V_{Rd,ct} = \frac{k_s}{\gamma_V} \cdot k \cdot \left(100\rho_l \cdot \frac{E_f}{210} \cdot f_{ck} \right)^{1/3} \cdot b_w \cdot d \geq V_{Rd,ct,min} \quad \text{with } \gamma_V = 1.5 \quad (6.11a)$$

$$V_{Rd,ct,min} = 0.035 \cdot k^{3/2} \cdot \sqrt{f_{ck}} \cdot b_w \cdot d \quad (6.11b)$$

$$V_{Rd,ct} = \frac{k'_s}{\gamma_V} \cdot \left(100\rho_l \cdot \frac{E_f}{210} \cdot f_{ck} \cdot \frac{d_{dg}}{d} \right)^{1/3} \cdot b_w \cdot d \geq V_{Rd,ct,min} \quad \text{with } \gamma_V = 1.4 \quad (6.11c)$$

where:

- b_w = 300 mm;
- d = 460 mm;
- k_s = 0.2 (factor empirically assessed);
- $\rho_l = A_f/(b \cdot d) = 0.006 \leq 0.02$ is the tensile reinforcement percentage;
- $k = 1 + \sqrt{\frac{200}{d}} = 1.66 \leq 2$;
- E_f = 45 GPa, then E_f / E_s =0.21;
- k'_s = 0.82 (factor empirically assessed);
- d_{dg} depends on the concrete roughness and can be calculated as:
  d_{dg} = 16 mm + $D_{min} \leq$ 40 mm for concrete with $f_{ck} \leq$ 60 MPa

Assuming that the maximum diameter of aggregate is 20 mm, it can be used in place of D_{min} (the smallest value of the upper sieve size) and, thus, d_{dg} = 16 mm + 20 mm = 36 mm.

The resulting shear capacities provided by Eq. (6.11) are summarized in Table 17-2, which evidences that both values of $V_{Rd,ct}$ = provided by Eq. (6.11a) and (6.11b) are lower than $V_{Rd,ct\ min}$. Thus, it can be assumed: $V_{Rd,ct} = V_{Rd,ct\ min}$ = 56.5 kN.

Table 17-2 - Values of shear capacities provided by Eq. (6.11)

$V_{Rd,ct}$ Approach 1 - Eq. (6.11a)	$V_{Rd,ct}$ Approach 2 - Eq. (6.11c)	$V_{Rd,ct,min}$ Minimum value - Eq. (6.11b)
47.4 kN	53.7 kN	56.5 kN

The stirrup contribution, $V_{Rd,f}$, is calculated using Eq. (6.13):

$$V_{Rd,f} = 0.9d \frac{A_{fw}}{s} f_{ubd} \cot\theta = 76.9 \text{ kN} \quad (6.13)$$

The total shear resistance is:

$V_{Rd} = 56.5 + 76.9 = 133.4$ kN > $V_{Ed} = 130$ kN

being $V_{Rd}/V_{Ed} = 1.03$

Hence, the assumed stirrups with d_b = 8 mm and spacing of 300 mm are adequate to satisfy the verifcations at the supports.

16.2.2 Check at section at 1.0 m from the support (stirrups spacing 300 mm)

In the remaining part of the beam, stirrups with a nominal diameter of d_b = 8 mm spaced at 300 mm on center are assumed. At a distance of one meter from the support, the applied shear force is:

$V_{Ed} = V_{Ed,max} - q_{dSLU}$ 1 m = 78 kN

The design shear resistance is given by: $V_{Rd} = V_{Rd,f} + V_{Rd,ct}$.

For $V_{Rd,ct}$, the same value calculated at the support (56.5 kN) is used.

For $V_{Rd,f}$ using Eq. (6.13) with A_{sw} / s = 100/300 mm^2/m, f_{ubd} = 186 MPa and cot(θ)=1, the following is obtained:

$$V_{Rd,f} = 0.9d \frac{A_{fw}}{s} f_{ubd} \cot\theta = 25.7 \text{ kN}$$

Thus, the total design shear resistance is:

$V_{Rd} = 56.5 + 25.7 = 82.2$ kN > $V_{Ed} = 78.0$ kN

being $V_{Rd} / V_{Ed} = 1.05$.

Hence, the assumed stirrups with d_b = 8 mm and spacing of 300 mm are adequate to satisfy the verification.

This Technical Document was prepared by the following Working Group:

Aiello, Prof. Maria A.	Università del Salento
Ascione, Prof. Luigi	Università di Salerno
Bilotta, Prof. Antonio	Università degli Studi di Napoli Federico II
Bonati, Eng. Antonio	Consiglio Nazionale delle Ricerche (CNR ITC)
Camata, Prof. Guido	Università di Chieti–Pescara
Ceroni, Prof. Francesca	Università degli Studi di Napoli "Parthenope"
D'Antino, Prof. Tommaso	Politecnico di Milano
Di Ludovico, Prof. Marco	Università degli Studi di Napoli Federico II
Ferretti, Eng. Francesca	Università di Bologna, Alma Mater Studiorum
Focacci, Prof. Francesco	Università e-Campus
Franco, Eng. Annalisa	Consiglio Nazionale delle Ricerche (CNR ITC)
Frassine, Prof. Roberto	Politecnico di Milano
Galati, Dr. E. Nessa	Structural Technologies, Columbia, Maryland, USA
Leone, Prof. Marianovella	Università del Salento
Lignola, Prof. Gian Piero	Università degli Studi di Napoli Federico II
Magliulo, Prof. Gennaro	Università degli Studi di Napoli Federico II
Mazzotti, Prof. Claudio	Università di Bologna, Alma Mater Studiorum
Monti, Prof. Giorgio	Università di Roma La Sapienza
Napoli, Prof. Annalisa	Università di Salerno
Nanni, Prof. Antonio	University of Miami, USA
Nigro, Prof. Emidio	Università degli Studi di Napoli Federico II
Occhiuzzi, Prof. Antonio	Università degli Studi di Napoli "Parthenope"
Pecce, Prof. Marisa	Università degli Studi di Napoli Federico II
Pisani, Prof. Marco A.	Politecnico di Milano
Poggi, Prof. Carlo	Politecnico di Milano
Prota, Prof. Andrea	Università degli Studi di Napoli Federico II
Puppio, Eng. Mario Lucio	Università di Cagliari
Realfonzo, Prof. Roberto	Università di Salerno
Saetta, Prof. Anna	IUAV Università di Venezia
Savoia, Prof. Marco	Università di Bologna, Alma Mater Studiorum

Industry Representatives

Balconi, Eng. Gabriele	Sireg Geotech S.r.l.
Casadei, Eng. Paolo	Owens Corning S.p.A.
Giamundo, Dr. Aniello	ATP S.r.l.
Morandini, Eng. Giulio	Mapei S.p.A.
Moroni, Mr. Federico	SIKA S.p.A.
Ussia, Eng. Gianluca	Fibrenet S.p.A.

Coordinators

Prof. Marco Savoia, Università di Bologna, Alma Mater Studiorum

Prof. Francesca Ceroni, Università degli Studi di Napoli "Parthenope"

This Techinical Document was approved in preliminary form on April 11, 2025 in order to be submitted to the public consultation, by "*Commissione di studio per la predisposizione e l'analisi di norme tecniche relative alle costruzioni*", composed as follows:

Angotti, Prof. Franco	Università di Firenze
Ascione, Prof. Luigi	Università di Salerno
Auricchio, Prof. Ferdinando	Università di Pavia
Aversa, Prof. Stefano	Università degli Studi di Napoli "Parthenope"
Baratta, Prof. Alessandro	Università degli Studi di Napoli Federico II
Bonati, Eng. Antonio	Consiglio Nazionale delle Ricerche (CNR ITC)
Cosenza, Prof. Edoardo	Università degli Studi di Napoli Federico II
Da Porto, Prof. Francesca	Università di Padova
Di Prisco, Prof. Marco	Politecnico di Milano
Iervolino, Prof. Iunio	Università degli Studi di Napoli Federico II
Lagomarsino, Prof. Sergio	Università di Genova
Mancini, Prof. Giuseppe	Politecnico di Torino
Mazzolani, Prof. Federico Massimo	Università degli Studi di Napoli Federico II
Occhiuzzi, Prof. Antonio (Chair)	Università degli Studi di Napoli "Parthenope" e CNR ITC
Pecce, Prof. Maria Rosaria	Università degli Studi di Napoli Federico II
Pinto, Prof. Paolo Emilio	Università "La Sapienza" di Roma
Poggi, Prof. Carlo	Politecnico di Milano
Prota, Prof. Andrea	Università degli Studi di Napoli Federico II
Renzi, Eng. Emanuele	ANSFISA
Royer Carfagni, Prof. Gianni	Università di Parma
Saetta, Prof. Anna	Università IUAV di Venezia
Savoia, Prof. Marco	Università di Bologna, Alma Mater Studiorum
Urbano, Prof. Carlo	Politecnico di Milano
Zanon, Prof. Paolo	Università di Trento

This Technical Document was approved on 03/02/2026 in its final version—incorporating the amendments and suggestions resulting from the public consultation—by the "*Commissione di studio per la predisposizione e l'analisi di norme tecniche relative alle costruzioni*", composed as follows:

Angotti, Prof. Franco	Università di Firenze
Ascione, Prof. Luigi	Università di Salerno
Auricchio, Prof. Ferdinando	Università di Pavia
Aversa, Prof. Stefano	Università degli Studi di Napoli "Parthenope"
Baratta, Prof. Alessandro	Università degli Studi di Napoli Federico II
Bonati, Ing. Antonio	Consiglio Nazionale delle Ricerche (CNR ITC)
Cosenza, Prof. Edoardo	Università degli Studi di Napoli Federico II
Da Porto, Prof.ssa Francesca	Università di Padova
Di Prisco, Prof. Marco	Politecnico di Milano
Iervolino, Prof. Iunio	Università degli Studi di Napoli Federico II
Lagomarsino, Prof. Sergio	Università di Genova
Landolfo, Prof. Raffaele	Università degli Studi di Napoli Federico II
Mancini, Prof. Giuseppe	Politecnico di Torino
Magenes, Prof. Guido	Università degli Studi di Pavia
Mazzolani, Prof. Federico Massimo	Università degli Studi di Napoli Federico II
Occhiuzzi, Prof. Antonio (Presidente)	Università degli Studi di Napoli "Parthenope" e CNR ITC
Pecce, Prof.ssa Maria Rosaria	Università degli Studi di Napoli Federico II
Poggi, Prof. Carlo	Politecnico di Milano
Prota, Prof. Andrea	Università degli Studi di Napoli Federico II
Royer Carfagni, Prof. Gianni	Università di Parma
Saetta, Prof.ssa Anna	Università IUAV di Venezia
Savoia, Prof. Marco	Università di Bologna, Alma Mater Studiorum
Urbano, Prof. Carlo	Politecnico di Milano

The Commission acknowledges Assocompositi (info@assocompositi.it) for the support provided for the English translation of this Technical Document.